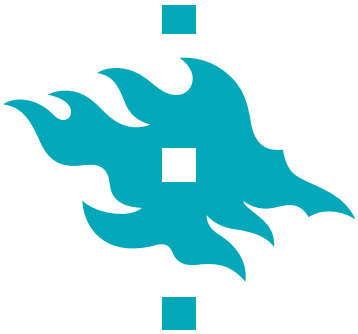

DISSERTATIONES SCHOLAE DOCTORALIS AD SANITATEM INVESTIGANDAM
UNIVERSITATIS HELSINKIENSIS

PRAVEEN KUMAR DHANDAPANI

EXPRESSING ALTERNATIVE OXIDASE (AOX) IN MICE: A VALUABLE TOOL TO STUDY MITOCHONDRIAL RESPIRATORY CHAIN DEFECTS

FACULTY OF MEDICINE
DOCTORAL PROGRAM IN BIOMEDICINE
UNIVERSITY OF HELSINKI

Doctoral Programme in Biomedicine
Faculty of Medicine
University of Helsinki
Finland

Expressing alternative oxidase (AOX) in mice:

A valuable tool to study mitochondrial respiratory chain defects

Praveen Kumar Dhandapani

ACADEMIC DISSERTATION

To be presented, with the permission of Faculty of Medicine of the University of Helsinki, for public examination in room P674, Porthania, Yliopistonkatu 3, Helsinki, on 05.06.2020, at noon.

Helsinki 2020

Supervised by

Marten Szibor, MD
Clinic for Heart and Thorax Surgery
Jena University Hospital
Friedrich-Schiller University of Jena

Prof. Howard T. Jacobs, PhD
Faculty of Medicine and Health Technology
Tampere University

Thesis committee

Prof. Katriina Aalto-Setälä, MD, PhD
Faculty of Medicine and Health Technology
Tampere University

Prof. Klaus-Dieter Schlüter, PhD
Physiological Institute
Faculty of Medicine
Justus-Liebig University of Giessen

Reviewed by

Jaakko Pohjoismäki, PhD
Department of Environmental and Biological Sciences
University of Eastern Finland

Prof. Roberta A. Gottlieb, MD
Department of Medicine; Department of Biomedical Sciences
Smidt Heart Institute
Cedars-Sinai Medical Center

Opponent

Prof. Anthony Moore, PhD
Biochemistry and Biomedicine
School of Life Sciences
University of Sussex

ISBN 978-951-51-5998-4 (paperback)
ISBN 978-951-51-5999-1 (PDF)
ISSN 2342-3161 (print)
ISSN 2342-317X (online)

Painosalama Oy
Turku 2020

To my mom, dad and mentors

We are all born with a divine fire in us. Our efforts should be to give wings to this fire and fill the world with the glow of its goodness.

- *APJ Abdul Kalam*

Abstract

Mitochondria are vital cellular organelles that produce the majority of the energy required by cells and are therefore represented as "the power house of the cell". Cellular energy, in the form of adenosine triphosphate (ATP), is generated through oxidative phosphorylation (OXPHOS), which is energized by the redox reactions of the electron transport chain (ETC) in mitochondria. Mitochondria are essential for maintaining metabolic homeostasis, fatty-acid metabolism, nucleotide synthesis and cellular redox balance, in addition to producing ATP.

Given the multitude of mitochondrial functions, failure of any of them can lead to mitochondrial dysfunction that can have drastic consequences. It can lead to cell loss, organ failure and even death. Mitochondrial disorders are commonly associated with debilitating childhood onset diseases with no known cure. Current therapeutic approaches are largey symptomatic, such as dietary modification for diabetes, anti-convulsant drugs to control seizures, physical exercise for hypotonia, pacemaker implants for cardiac rhythm abnormalities and cochlear implants for sensorineural deafness. However, these are not a permanent solution or cure for severe disorders caused by genetic mutations or irreversible physical damage.

Cardiomyopathy, failure of the heart muscle, is one of the most common symptoms of mitochondrial disorders, while cardiomyopathies almost always are associated with mitochondrial dysfunction. In severe forms of cardiomyopathy, the ultimate treatment option of heart transplantation is invasive and carries high risk, and the waiting list for a functional healthy heart is increasingly outstripping availability.

I have investigated the use of a mitochondrial enzyme, the alternative oxidase (AOX), which is found in plants and lower eukaryotes, as well as in primitive metazoans but not in mammals as a new approach to better understand the underlying molecular mechanisms of diseases involving mitochondrial dysfunction. On a broader perspective, this would also aid in the development of a possible treatment for diseases associated with mitochondrial dysfunction. If catalytically engaged, AOX branches the mitochondrial ETC by oxidizing ubiquinol, which accumulates in the reduced form if the cytochrome pathway is impaired. By doing so it reduces oxygen directly to water, which is typically carried out by cytochrome oxidase, and thus maintains redox balance by recycling NADH and $FADH_2$, two by-products of the Krebs cycle and upstream metabolism.

Focusing on different types of cardiomyopathy, my strategy has been to introduce the AOX gene from the tunicate *Ciona intestinalis*, a close relative of vertebrates, into mouse models of disease, using genomic manipulation. I have studied and characterized two transgenic mouse models expressing *C. intestinalis* AOX. The first was designed to express AOX constitutively and ubiquitously. I verified this at the RNA and protein level revealing high-level expression in all tissues tested, including the heart, with the exception of the adult brain. The mice did not show any observable phenotype, making them nearly indistinguishable from their wild-type littermates under non-stressed conditions. Heart function, as measured by ejection fraction and left ventricular mass, treadmill performance and grip strength were all normal in one-year-old AOX-expressing mice. Weight was indistinguishable from that of wild-type littermates on chow or high-fat diet; although on ketogenic diet AOX-expressing mice showed a slightly mitigated weight gain, at least when caged in same-sex groups.

A second AOX transgenic line was characterized, in which AOX expression was designed to be activatable by Cre-loxP-mediated removal of a STOP cassette (SNAP coding sequence, pA signal) located downstream of a CAG promoter and upstream of the AOX coding sequence. After verification of the transgenic insertion by PCR and Southern blotting, test activation by breeding to mice ubiquitously expressing Cre recombinase under the control of a β-actin promoter resulted in successful activation, based on ubiquitous expression of AOX and concomitant loss of SNAP expression. This allowed me to test the tissue-specificity of AOX-mediated modification of pathological phenotypes in mouse models of cardiomyopathy.

Two different mouse models of cardiomyopathy were investigated. In the first, inflammatory cardiomyopathy was induced by overexpressing monocyte chemo-attractant protein 1 (MCP1) in the cardiomyocytes, which leads to loss of cardiac function commencing during early adulthood (12 weeks of age). Previously published data showed mitochondrial structural damage, decrease in ATP levels; and suggested induced oxidative stress as a pathological mechanism. Although the majority of oxidative stress in the cardiomyocytes of Mcp1 mice is induced by the infiltrating monocytes, via NADPH oxidase pathway, the contribution of mitochondria to the production of reactive oxygen species (ROS) is not well understood. I hypothesized that mitochondrial ROS production, especially via a defective or overloaded cytochrome pathway in the mitochondrial respiratory chain, might play a key role in the underlying molecular mechanisms. Therefore we wanted to test whether AOX could mitigate it, as it has been shown to alleviate oxidative stress under

conditions where the cytochrome pathway is dysfunctional. I found that expressing AOX in this model preserved cardiac ejection fraction at 12 weeks of age but not at later time points. At the molecular level, I determined that mitochondrial complex I-linked respiration was severely affected in Mcp1-overexpressing mice irrespective of AOX expression. However, AOX preserved complex II mediated respiration. In theory, this should maintain mitochondrial redox homeostasis and limit oxidative stress and damage within mitochondria, but at the expense of ATP production and mitochondrial-ROS signaling. Ultrastructural analysis revealed mitochondrial damage in the cardiac tissue of 12 week-old Mcp1-overexpressing mice, which was alleviated by AOX expression. Despite this, AOX had no effect on the survival of Mcp1-overexpressing mice, whilst cardiomyocyte-specific AOX expression actually resulted in earlier death than Mcp1 alone. Autophagic markers were mildly elevated in all cases, and metabolic changes consistent with OXPHOS dysfunction were essentially unaffected by AOX expression in the Mcp1 mouse model. Overall, I conclude that AOX is insufficient to block lethal damage to mitochondria and/or other cellular components in this inflammatory cardiomyopathy model, despite transient beneficial effects. Previously, West et al (2011) and Mills et al (2016) reported on the significance of mitochondrial ROS in inducing macrophage activity in a LPS-induced inflammatory mouse model. Additionally, Mills et al (2016) also showed AOX expression prevented LPS-induced lethality in mice, where succinate-dependent ROS production in the ETC was reported to be the underlying cause for the observed severe phenotype. However, since AOX was unable to prevent lethality in Mcp1 mice, it is indicative that the ROS production in this inflammatory model might not be dependent on the ETC.

The second model I studied was of Cox-deficient mitochondrial cardiomyopathy, induced by cardiomyocyte-specific knockout of Cox10, an essential enzyme of heme *a* biosynthesis. Cox10 knockout in the heart was lethal within the first days or weeks of life, and concomitant AOX expression had hardly any effect on this. Mice with heterozygous knockout of Cox10 survived for months but eventually succumbed to heart failure. However, this phenotype was produced by the cardiomyocyte-specific Cre expression alone, and was again exacerbated by AOX activation, despite transient improvements in cardiac performance in young mice.

In conclusion, AOX can serve as a valuable tool to study disease mechanisms where mitochondrial dysfunction is proposed to play a key role in the pathophysiology. Although AOX did not rescue the disease models I studied, it did shed light on

underlying molecular mechanisms. Considering the fact that AOX showed a partial, if transient, functional rescue in both of the heart failure models investigated, it might yet be relevant as a potential therapeutic option. Further research is necessary to fully understand the therapeutic potential of AOX, either by itself or in combination with other treatments that address different pathological processes, as well as the apparently negative effects of AOX itself during disease progression.

Tiivistelmä

Mitokondriot ovat elintärkeitä soluorganelleja, jotka tuottavat suurimman osan solujen tarvitsemasta energiasta ja ovat välttämättömiä ylläpitämään useita aineenvaihduntareittejä. Siten mitokondrioiden toimintahäiriöt voivat usein johtaa solujen menetykseen, elinten vajaatoimintaan ja jopa kuolemaan. Mitokondriaaliset sairaudet liittyvät yleensä vakaviin lapsuuden aikaisiin sairauksiin, joille ei ole tunnettuja parannuskeinoja. Kardiomyopatia, sydänlihaksen vajaatoiminta, on yksi yleisimmistä mitokondriohäiriöiden oireista, ja se on yksi suurimmista kuolinsyistä maailmassa. Ymmärtääkseni paremmin sellaisten sairauksien taustalla olevia molekyylimekanismeja, joihin liittyy mitokondrioiden toimintahäiriöitä, etenkin hengityskompleksien III ja / tai IV aiheuttamia toimintahäiriöitä, olen tutkinut mitokondriaalista entsyymiä, vaihtoehtoista oksidaasia (AOX), joka löytyy kasveista ja alemmista eukaryooteista, mutta ei nisäkkäistä. Katalyyttisesti aktivoituneena AOX haaroittaa mitokondriaalisen hengitysketjun ohittaen hengityskompleksit III ja IV ja redusoiden hapen suoraan vedeksi, minkä tyypillisesti suorittaa hengityskompleksi IV.

Keskityin tutkimaan AOX-ilmentymisen vaikutusta erityyppisissä kardiomyopatioissa. Tätä varten strategiani on ollut siirtää AOX-geeni *Ciona intestinalis* -vaippaeläimestä kardiomyopatiahiirimalleihin geenimanipulaatiolla. Olen tutkinut ja karakterisoinut kahta siirtogeenistä hiirimallia, jotka ekspressoivat *C. intestinalis* AOX-geeniä. Ensimmäinen malli oli suunniteltu ekspressoimaan AOX:ia jatkuvasti ja kaikkialla, ja toinen AOX-siirtogeeninen linja suunniteltiin aktivoitavaksi tietyissä kudoksissa Cre-loxP-välitteisellä geenimanipulaatiolla. Molemmissa hiirimalleissa AOX-ekspressio varmistettiin RNA- ja proteiinitasoilla. Hiirillä ei ollut havaittavaa fenotyyppiä, mikä teki niiden erottamisen villityyppistä poikuetovereistaan lähes mahdottomaksi stressittömissä olosuhteissa. Ensimmäisessä mallissa normaali tai korkearasvainen ruokavalio ei erottanut siirtogeenisiä eläimiä villityyppisistä eläimistä, tosin ketogeenisellä ruokavaliolla AOX:ia ekspressoivat hiiret osoittivat hieman lievempää painonnousua kuin villityyppiset eläimet, ainakin ollessaan samaa sukupuolta olevien joukossa.

Kahta erilaista kardiomyopatiahiirimallia tutkittiin. Ensimmäisessä indusoitiin tulehduksellinen kardiomyopatia MCP1 (monocyte chemo-attractant protein 1)

yliekspression avulla sydänlihassoluissa, mikä johtaa sydämen toiminnan menettämiseen, joka alkaa varhaisessa aikuisiässä (12 viikon ikäisenä). Aikaisempien julkaisujen tutkimustulokset ovat osoittaneet mitokondrioiden rakennevaurioita, ATP-tasojen laskua, ja viittaavat indusoituun oksidatiiviseen stressiin patologisena mekanismina. Hypoteesin mukaan mitokondriaalisten reaktiivisten happiradikaalien (ROS) tuotannolla voisi olla avainrooli taustalla olevissa molekyylimekanismeissa. Siksi halusin testata, voisiko AOX lieventää sitä, koska sen on osoitettu lievittävän oksidatiivista stressiä olosuhteissa, joissa hengityskomplekseissa III ja / tai IV on toimintahäiriöitä. Havaitsin, että AOX:n ilmentäminen tässä mallissa säilytti sydämen ejektiofraktion 12 viikon iässä, mutta ei myöhemmin. Molekyylitasolla määrittelin, että mitokondriaalisen kompleksin I-linkittynyt hengitys vaikutti voimakkaasti MCP1:tä yliekspressoivissa hiirissä riippumatta AOX-ekspressiosta. AOX kuitenkin säilytti kompleksin II välittämän hengityksen. Teoriassa tämän pitäisi ylläpitää mitokondrioiden redox-homeostaasia ja rajoittaa oksidatiivista stressiä ja vaurioita mitokondrioissa, mutta ATP-tuotannon ja mitokondrion ROS-signaloinnin kustannuksella. Tästä huolimatta AOX:lla ei ollut vaikutusta MCP1:tä yliekspressoivien hiirten selviytymiseen, kun taas sydänsolujen spesifinen AOX-ekspressio johti tosiasiallisesti aikaisempaan kuolemaan kuin pelkkä MCP1. Kaiken kaikkiaan päättelen, että AOX ei riitä estämään mitokondrioiden ja/tai muiden solukomponenttien tappavia vaurioita tässä tulehduksellisessa kardiomyopatian mallissa, huolimatta ohimenevistä hyödyllisistä vaikutuksista. Nämä havainnot osoittavat, että ROS-tuotanto tässä tulehduksellisessa mallissa ei ehkä ole riippuvainen ETC:stä.

Toinen tutkimani malli oli Cox-vajaatoimintainen mitokondriaalinen kardiomyopatia, jonka aiheuttaa kardiomyosyyttispesifinen Cox10:n puute, hemibiosynteesin välttämätön entsyymi. Cox10:n geenin poisto sydämestä oli tappavaa elämän ensimmäisinä päivinä tai viikkoina, ja samanaikaisella AOX-ekspressiolla ei ollut juuri mitään vaikutusta tähän. Hiiret, joilla oli heterotsygoottinen Cox10-geenin poisto, selvisivät kuukausia, mutta lopulta menehtyivät sydämen vajaatoimintaan. Tämä fenotyyppi tuotettiin kuitenkin pelkästään kardiomyosyyttispesifisellä Cre-ilmentymällä, ja AOX-aktivaatio pahensi sitä uudelleen, huolimatta sydämen suorituskyvyn ohimenevistä parannuksista nuorilla hiirillä.

Yhteenvetona voidaan todeta, että AOX voi toimia arvokkaana välineenä tutkittaessa sairauden mekanismeja, joissa mitokondrioiden toimintahäiriöiden uskotaan olevan avainasemassa patofysiologiassa. Vaikka AOX ei toiminut pelastuskeinona tutkimissani sairausmalleissa, se valotti taustalla olevia molekyylimekanismeja. Kun otetaan huomioon, että AOX osoitti olevansa osittainen, joskin ohimenevä, toiminnallinen pelastuskeino molemmissa tutkituissa sydämen vajaatoimintamalleissa, se saattaa vielä tulevaisuudessa olla potentiaalinen terapeuttinen vaihtoehto. Jatkotutkimukset ovat välttämättömiä, jotta voidaan täysin ymmärtää AOX:n terapeuttinen potentiaali, joko itsenäisesti tai yhdessä muiden patologisiin prosesseihin kohdistuvien hoitomenetelmien kanssa, mutta yhtä lailla myös AOX:n nähtävästi negatiiviset vaikutukset sairauden etenemisen aikana.

Table of contents

List of original publications

This thesis is based on the following publications

I. Szibor M*, **Dhandapani PK***, Dufour E, Holmström KM, Zhuang Y, Salwig I, Wittig I, Heidler J, Gizatullina Z, Gainutdinov T; German Mouse Clinic Consortium, Fuchs H, Gailus-Durner V, de Angelis MH, Nandania J, Velagapudi V, Wietelmann A, Rustin P, Gellerich FN, Jacobs HT, Braun T. Broad AOX expression in a genetically tractable mouse model does not disturb normal physiology. Dis. Model. Mech. 2017, 10(2): 163-171. *Equal contribution
DOI: 10.1242/dmm.027839.

II. **Dhandapani PK**, Lyyski AM, Paulin L, Khan NA, Suomalainen A, Auvinen P, Dufour E, Szibor M, Jacobs HT. Phenotypic effects of dietary stress in combination with a respiratory chain bypass in mice. Physiol. Rep. 2019, 7(13): e14159.
DOI: 10.14814/phy2.14159.

III. **Dhandapani PK**, Begines-Moreno IM, Brea-Calvo G, Gärtner U, Graeber TG, Javier Sanchez G, Morty RE, Schönig K, Hoeve JT, Wietelmann A, Braun T, Jacobs HT, Szibor M. Hyperoxia but not AOX expression mitigates pathological cardiac remodeling in a mouse model of inflammatory cardiomyopathy. Sci. Rep. 2019, 9(1): 12741.
DOI: 10.1038/s41598-019-49231-9.

The publications are referred to in the text by their roman numerals.

Abbreviations

ADP	Adenosine diphosphate
AOX	Alternative oxidase
ATP	Adenosine triphosphate
cDNA	Complementary DNA
cI	NADH:ubiquinone oxidoreductase; complex I
cII	Succinate:ubiquinone oxidoreductase; complex II
cIII	Ubiquinol-cytochrome c oxidoreductase; complex III
cIV	Cytochrome *c* oxidase; complex IV
CoQ	Coenzyme Q; ubiquinone
$CoQH_2$	Coenzyme Q (reduced); ubiquinol
COX	Cytochrome oxidase
COX10	Cytochrome oxidase 10
COX15	Cytochrome oxidase 15
cV	F0-F1-ATPase; complex V
DNA	Deoxyribonucleic acid
EF %	Cardiac ejection fraction
ETC	Electron transport chain
FAD	Flavin adenine dinucleotide
$FADH_2$	Flavin adenine dinucleotide (reduced)
GMC	German Mouse Clinic
IL	Interleukin
IMM	Inner mitochondrial membrane
IMS	Intermembrane space
IMS	Intermembrane space
I/R	Ischemia/reperfusion
KO	Knockout
LV vol	Left ventricular volume of blood
MCP1	Monocyte chemoattractant protein-1
mRNA	Messenger RNA
mtDNA	Mitochondrial DNA
Myh6	Myosin, heavy polypeptide 6, cardiac muscle, alpha; α myosin heavy chain
Myh7	Myosin, heavy polypeptide 7, cardiac muscle, beta; β myosin heavy chain

NAD^+	Nicotinamide adenine dinucleotide (oxidized)
NADH	Nicotinamide adenine dinucleotide (reduced)
nDNA	Nuclear DNA
OMM	Outer mitochondrial membrane
OXPHOS	Oxidative phosphorylation
pA	Poly-A tail
RNA	Ribonucleic acid
ROS	Reactive oxygen species
rRNA	Ribosomal RNA
SAM	Sorting and assembly machinery
TCA	Tricarboxylic cycle
TIM	Translocase of inner membrane
TOM	Translocase of outer membrane
tRNA	Transfer RNA
VDAC	Voltage-dependent anion channels
WHO	World Health Organization
β-oxidation	Beta oxidation; fatty acid oxidation
$\Delta\Psi$	Membrane potential

1. Introduction

The mammalian heart is composed of several different cell types of which cardiomyocytes comprise about 30 - 50% in number (Banerjee *et al.,* 2007, Pinto *et al.,* 2016), and about 70 – 85% by volume (cited in Zhou *et al.,* 2016), while the rest is composed of endothelial cells, fibroblasts, macrophages and perivascular cells (Pinto *et al.,* 2016, reviewed by Gray *et al.,* 2018). A properly functioning healthy heart muscle is dependent on effective communication within and function of the complex cellular network in the muscle. Thus, malfunction of even one cell type, whether a myocyte or a non-myocyte, could compromise the function of the whole organ, resulting in heart failure (Aoki *et al.,* 2011, Acharya *et al.,* 2012; reviewed by Tian *et al.,* 2013, Moore-Morris *et al.,* 2015, Gray *et al.,* 2018, Segers *et al.,* 2018).

According to the WHO, cardiovascular diseases are the major cause of death, accounting for over 17 million every year globally, of which 85% were due to heart failure or stroke. Heart failure is clinically characterized as the reduced ability of the heart muscle to effectively pump blood. The New York Heart Association (NYHA) has classified 4 different stages of heart failure based on the severity of their impact on physical activity (Inamdar, *et al.,* 2016). There are several possible causes of heart failure, including behavioral and genetic (Inamdar, *et al.,* 2016). Irrespective of the nature of cause, it brings a huge personal and socio-economic burden, considering the fact that over three quarters of the reported heart failure cases are from low- and middle-income countries (source: WHO, 2017).

Primary treatment options for early-stage heart failure symptoms address the issue by controlling behavioral factors like use of alcohol and tobacco, unhealthy diet and physical inactivity. Secondary treatment options for patients with established heart failure include administration of medications like beta-blockers and statins, along with changes in diet and improved physical activity. For patients in critical stages, the only option is an invasive surgery that sometimes requires a heart transplantation. According to WHO, thus far the availability of a healthy heart never satisfied the demand, making heart failure a complex and serious issue world-wide .

To address this issue from the molecular perspective, I have used tools to study and better understand the biology of cardiomyocytes in conditions of mitochondrial respiratory dysfunction. Cardiomyocytes make up for the majority of the volume in the heart muscle. Effective function of the cardiomyocytes demands a high and constant supply of cellular energy, adenosine triphosphate (ATP), the majority of which is

supplied by mitochondria. Thus cardiomyocytes are among the few cell types known to contain a large mitochondrial mass. When and if mitochondria fail to produce enough ATP or maintain the metabolic homeostasis of the cell, the normal cellular functioning is severely affected even leading to cardiomyocyte death (Nakayama *et al.,* 2007). On a larger scale, loss of cardiomyocytes results in several severe forms of cardiomyopathy, such as hypertrophic cardiomyopathy (Kavantzas *et al.,* 2000), idiopathic dilated cardiomyopathy (Narula *et al.,* 1999, Kavantzas *et al.,* 2000) and arrhythmogenic right ventricular cardiomyopathy (Valente *et al.,* 1998, Kavantzas *et al.,* 2000). This ultimately leads to critical stages of heart failure (Nakayama *et al.,* 2007; reviewed by Ingwall *et al.,* 2004, Neubauer, 2007, Chiong *et al.,* 2011, Chen *et al.,* 2010).

Although mitochondrial dysfunction can occur due to several different reasons, I have addressed whether disturbed mitochondrial respiration, can potentially be the primary cause of mitochondrial dysfunction and the pathophysiology in the two heart failure models I have studied. The mitochondrial respiratory chain is the central component needed for OXPHOS, i.e. the process by which mitochondria generate ATP while reducing the inhaled oxygen to water. It is a complex process by itself involving several protein complexes and by-products of a larger metabolic cycle that serve as substrates. When the respiratory chain is defective, ATP generation is affected, oxygen is converted in to a highly reactive molecular species (ROS) and connected metabolic pathways are stalled due to the lack of reoxidation of NADH and $FADH_2$. This eventually leads to a cascade of events that could potentially result in cell death (reviewed by Adams *et al.,* 1996, Martin, 2010).

To address mitochondrial dysfunction due to ETC defects, especially in the cytochrome pathway, I have used AOX, a naturally occurring enzyme that can branch the electron flow to the cytochrome pathway and reduce oxygen to water directly but at the cost of ATP production. This should decrease excessive ROS production and maintain the interlinked metabolic pathways (reviewed by Valerberghe, 2013).

Since AOX is not naurally expressed in mammals (McDonald *et al.*, 2004), I first characterized a mouse model where AOX is expressed constitutively, as a result of genetic manipulation. I used basic and advanced scientific methods to profile behavior, heart function and physical performance of the mice including an extensive characterization at the molecular level by studying the mitochondrial respiration, protein expression and overall metabolism of different tissues. I have also characterized a second mouse model where expression of AOX can be targeted to a

specific cell type using Cre-loxP recombination. After validating AOX expression in both of these mouse models, I have combined them with two established models of heart failure. In the first model, heart failure is induced by excessive inflammation which is proposed to be triggered by excessive ROS production and in the second model, heart failure is induced by disrupting the cytochrome pathway, especially complex IV, of mitochondrial OXPHOS.

In the following chapter I discuss the scientific background to my thesis work by referring to the findings from decades of research in this field

2. Literature Review

2.1. Mitochondria

Mitochondria are widely recognized as the 'power plant' of the cell as they are the major source of adenosine triphosphate (ATP), the energy molecule that drives fundamental cellular functions. Richard Altmann (1890) reported the ubiquitous occurrence of these organelles and termed them 'bioblasts'. A few years later, Carl Benda (1898) coined the term 'mitochondrion' based on the Greek words 'mitos' (thread) and 'chondros' (granule), from his observations of these structures during spermatogenesis (also see review by Ernster *et al.*, 1981). In addition to ATP production, mitochondria play key roles in modulating Ca^{2+} homeostasis (reviewed by Vandecasteele *et al.,* 2001; Clapham, 2007; Giorgi *et al.,* 2012; Paupe *et al.,* 2018), maintaining redox balance (Pelicano *et al.,* 2006; reviewed by Trachootham *et al.,* 2008; Handy *et al.,* 2012), influencing cellular growth and cell death (Shimizu *et al.,* 1999, reviewed by Green *et al.,* 1998; Kroemer *et al.*, 2000; Antico Arciuch *et al.,* 2012), maintaining metabolic homeostasis (reviewed by Cheng *et al.,* 2013) and signaling (reviewed by Chandel, 2014 and 2015). In eukaryotic cells, mitochondria and chloroplasts (in plants and photosynthetic algae) are the only organelles that contain their own DNA, apart from the nucleus (Lodish *et al.,* 2000).

2.2. Evolutionary origins of mitochondria

A widely accepted theory for the origin of mitochondria in eukaryotic cells is the endosymbiotic theory. It postulates that an event occurred during or after the appearance of molecular oxygen in the Earth's atmosphere, wherein aerobic proteobacteria were engulfed by host microbes, believed to be related to present-day archaea, that could ferment glucose, resulting in a symbiotic relationship (Margulis, 1981; Gray *et al.,* 1999).

2.3. Mitochondrial structure and biogenesis

Palade (1952) first reported the fine structure of mitochondria. In albino rat tissues, mitochondria were observed as either circular or oval-shaped organelles with a diameter varying between 0.2 to 1 µm, depending on the cell type. The first

observations of mitochondria in rat tissues and human blood leucocytes showed that mitochondria are a double-membraned structure, where the outer membrane is separate from the inner membrane, which surrounds an internal matrix (Palade, 1952; Low, 1956; schematic shown in figure 1). The mitochondrial membranes consist of phospholipid bilayers with many protein complexes embedded in them. Such complexes facilitate various functions, ranging from transportation of molecules between mitochondria and the cytosol of the cell, to the generation of ATP through OXPHOS (reviewed by Neupert *et al.*, 2007; see section 2.3.1 below).

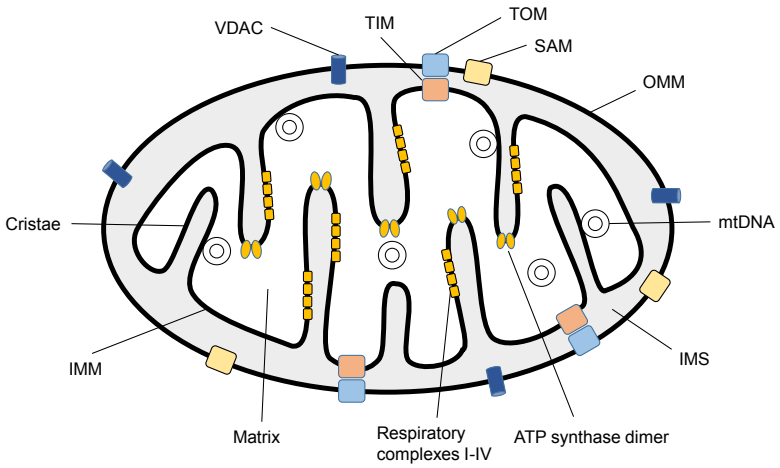

Figure 1: Schematic representation of a cross-sectioned mammalian mitochondrion. ATP synthase (complex V, F1-Fo-ATPase), IMM – inner mitochondrial membrane, IMS – intermembrane space, mtDNA – mitochondrial DNA, OMM – outer mitochondrial membrane, Respiratory complexes: complex I (NADH:ubiquinone oxidoreductase); complex II (succinate:ubiquinone oxidoreductase); complex III (ubiquinol-cytochrome c oxidoreductase) and complex IV (cytochrome *c* oxidase), SAM - the sorting and assembly machinery, TIM - the translocases of the inner membrane, TOM - the translocase of the outer membrane, VDAC - voltage-dependent anion channels.

2.3.1. Outer membrane

The outer mitochondrial membrane (OMM) contains two major protein complexes; the translocase of the outer membrane (TOM) and the sorting and assembly machinery (SAM), as well as voltage-dependent anion channels (VDAC, porin). These membrane protein complexes facilitate the transport of all relevant molecules, including precursor proteins and ions. Smaller molecules, that are less than 5 kDa, are able to diffuse through VDAC but protein molecules larger than 5 kDa can only be transported via the TOM and SAM complexes (Wiedemann *et al.,* 2003; Bayrhuber *et al.,* 2008; also see review by Neupert, 1997).

2.3.2. Inner membrane

The first electron-microscopic images of mitochondria revealed invaginations of the inner mitochondrial membrane (IMM), termed cristae (Palade, 1952; Low, 1956). The cristae increase the surface area of the IMM and their number varies according to the functional activity of mitochondria (reviewed by Cogliati, 2016). Like the OMM, protein transfer through the IMM is mediated by protein complexes denoted as the translocases of the inner membrane (TIM) (reviewed by Neupert *et al.*, 2007). Unlike the OMM, the transfer of molecules across the IMM requires an electrical membrane potential ($\Delta\Psi$). The cristae of the IMM contain the assembled respiratory chain complexes, as well as ATP synthase.

2.3.3. Intermembrane space and matrix

The space between the OMM and IMM is denoted as the intermembrane space (IMS). The IMS is an aqueous compartment that acts as a bridge between the cytoplasm of the cell and the mitochondrial matrix. The IMS contains protein molecules and metabolites in transit between the IMM and OMM, and has a lower pH than the innermost compartment of mitochondria, the matrix. The mitochondrial matrix, which is also an aqueous compartment, contains mitochondrial DNA (mtDNA), enzymes for the citric acid cycle (TCA cycle) and beta-oxidation of fatty acids, as well as proteases, ribosomes and ions. The mitochondrial matrix generally has a high pH, 7.9 to 8.0 (Llopis *et al.,* 1998), which generates the electrochemical gradient for ATP synthesis. The mitochondrial matrix is the site of numerous enzymatic reactions, including several major metabolic pathways, such as those already mentioned above, as well as the urea cycle (in liver), plus the molecular machineries for mtDNA replication and transcription and protein synthesis.

2.3.4. Mitochondrial biogenesis and distribution

Mitochondrial biogenesis is the process of growth and/or division of existing mitochondria. The mitochondrial mass (Robin and Wong, 1988), and their dynamics and spatial arrangement, i.e. networks *vs* fragment (reviewed by Kuznetsov *et al.,* 2009), varies between cell types but are generally consistent within a given cell type. Mitochondrial proteins are encoded in both mtDNA and nuclear DNA (nDNA), although the latter comprises the vast majority. Mitochondrial DNA is circular and

double stranded in most species, with the exception of a few unicellular eukaryotes which contain linear mtDNA, e.g. *Tetrahymena, Paramecium* (Borst, 1977), *Chlamydomonas, Pandorina, Polytomella, Sphaerellopis, Candida, Theileria* and *Lobochlamys* (reviewed by Nosek *et al.,* 1998; Smith *et al.,* 2010). The human mitochondrial genome is 16.6 kb long and encodes 37 genes in total, namely 22 tRNAs (transfer RNAs), 13 proteins (all of them being subunits of OXPHOS complexes) and 2 rRNAs (ribosomal RNAs) (figure 2). However, the majority of proteins required for mitochondrial biogenesis and function, approximately 1500 (Lopez *et al.,* 2000), including all other subunits of the OXPHOS complexes, are encoded in the nDNA, synthesized in the cytosol and imported into the mitochondria.

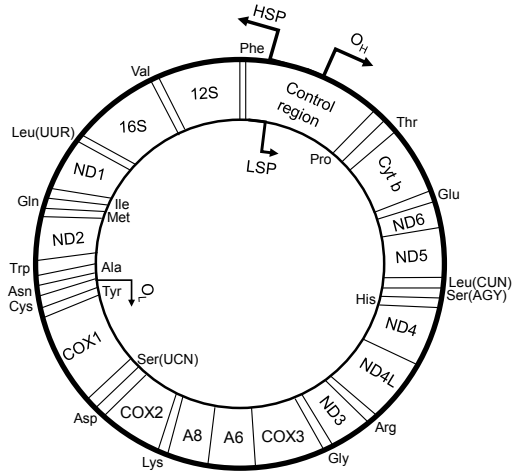

Figure 2: Schematic representation of human mitochondrial DNA. Genes encoding proteins, rRNA and tRNA are indicated along with their respective positions (segments are not to actual scale). The genes encoding specific tRNAs are represented by their cognate amino acid (e.g. Ser – Serine) and, where appropriate, the specific codon group decoded. O_H and O_L are the origins of heavy- and light-strand replication, respectively. HSP and LSP are the transcription promoters for the heavy- and light-strand, respectively. Note – strand assignments not shown for protein coding genes, of which ND6 is opposite to all the others.

Unlike nDNA, mtDNA does not contain introns and the non-coding sequences are present in a single region, referred to as the control region. The control region is approximately 1.1 kb, located between the coding sequences of tRNA(Pro) and tRNA(Phe), and contains the origin of replication of the heavy strand (O_H), the displacement-loop (D-loop) region, and the transcriptional start sites of both strands, conventionally denoted as heavy and light, based on their buoyant densities. Since mitochondria are the major source of ATP, especially in muscle and heart, increased physical exercise has been shown to increase mitochondrial biogenesis (Holloszy, 1967). Apart from physiological stress, many other factors influence mitochondrial

biogenesis, such as, reactive oxygen species (ROS), hypoxia, Ca^{2+} homeostasis, inflammation and thermogenesis (reviewed by Nisoli *et al.,* 2006, Jornayvaz *et al.,* 2010, Dominy *et al.,* 2013, Wenz, 2013, Suliman *et al.,* 2015, Cherry *et al.,* 2015).

Within the cell, mitochondria are generally observed as interconnected organelles that form a network (Lewis & Lewis, 1914). However, mitochondria are also highly dynamic and constantly change their shape and network connections depending on the physiological needs of the cell (reviewed by Westermann, 2010). Mitochondrial network formation and granulation is facilitated by fusion and fission reactions, respectively. In mammals, mitochondrial fusion is mediated by mitofusin I (MFN1), mitofusin II (MFN2) and optic atrophy I (OPA1) proteins, where MFN1 and 2 mediate outer membrane fusion and OPA1 mediates inner membrane fusion. Mitochondrial fission is mediated by dynamin-1-like protein (DMN1L, also commonly known as DRP1) (reviewed by Westermann, 2010; Lackner, 2014). A balance between mitochondrial fission and fusion is essential to maintain the cell in a healthy state and a shift towards either direction may affect metabolic and energy homeostasis, unless such a shift is dictated by the state of the cellular activity (reviewed by Westermann, 2010).

2.4. Mitochondrial functions

One of the most widely studied functions of mitochondria is ATP production *via* OXPHOS, energized by the electron transport chain (ETC). Since my project has largely involved studying ETC defects in disease conditions, I will primarily focus on OXPHOS and the ETC, and only briefly describe other important functions of mitochondria.

2.4.1. OXPHOS

OXPHOS is the biochemical process involving the re-oxidation of the primary electron carriers of metabolism, NADH and $FADH_2$, which drives the phosphorylation of ADP to ATP in the mitochondria. The protein complexes involved in this pathway are all located in the IMM. Mitchell (1961) first proposed a model for the process of ATP formation in mitochondria, known as the chemiosmotic hypothesis. The reduced electron carriers, NADH and $FADH_2$, which are produced by the major metabolic pathways in mitochondria, are oxidized by the first two ETC complexes.

NADH:ubiquinone oxidoreductase (complex I, cI) oxidizes NADH, whilst $FADH_2$ is an intermediate in the reactions catalyzed by succinate:ubiquinone oxidoreductase (succinate dehydrogenase, complex II, cII) and other mitochondrial dehydrogenases. The protons released in these oxidation reactions are pumped from the mitochondrial matrix into the IMS, whilst the electrons are shuttled through subsequent steps of the ETC, ultimately reducing oxygen to water through a series of protein complexes. The flow of electrons and subsequent proton pumping creates an electrical potential and a pH gradient across the IMM that is used to drive ATP synthesis *via* the F_1-F_o-ATPase (ATP synthase, complex V, cV). A schematic diagram of the OXPHOS pathway is shown in figure 3.

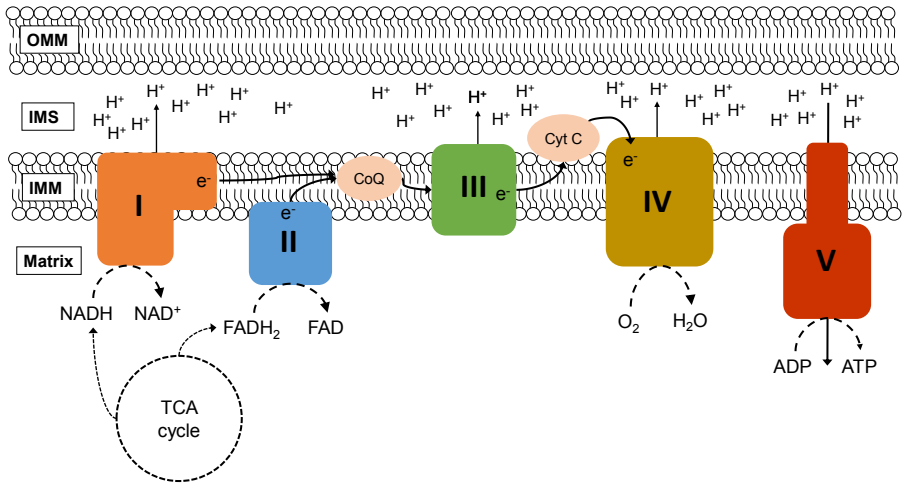

Figure 3: Schematic representation of the OXPHOS pathway. Electrons obtained from the oxidation of NADH and $FADH_2$ by cI and cII, respectively, are transferred to cIII via ubiquinone (CoQ), which is then transferred to cIV via cytochrome *c*. cIV transfers the electrons to molecular oxygen to convert it into water. In this process, cI, cIII and cIV pump protons to the IMS. The resulting proton motive force is utilized by cV to convert ADP to ATP. TCA cycle is shown as an example for the source of NADH and $FADH_2$.

2.4.2. Electron transport chain (ETC)

As well as cI and cII, the mitochondrial ETC includes two additional multi-subunit enzyme complexes, namely ubiquinol-cytochrome *c* oxidoreductase (complex III, cIII) and cytochrome *c* oxidase (complex IV, cIV), as well as 2 mobile intermediate electron carriers – ubiquinone, also known as coenzyme Q (CoQ) and cytochrome *c*. These 'standard' ETC components are prevalent in the majority of eukaryotes. However, many species, including most plants and fungi, also contain alternative enzymes to

oxidize NADH and reduce O_2 to water, which I will describe later in this chapter (2.4.2.8). For a comprehensive review of the structure and organization of mitochondrial respiratory complexes, see review by Lenaz and Genova (2010).

2.4.2.1. Complex I

Complex I is the largest of the respiratory chain complexes containing 45 subunits, with a combined molecular mass of approximately 1000 kDa in mammals (Hirst *et al.,* 2003, Caroll *et al.,* 2006). Only 7 of the 45 subunits are encoded in the mtDNA, with the remainder encoded by nDNA. The nuclear-coded cI polypeptides are imported into the mitochondria for cI assembly. The fully assembled protein complex is L-shaped (Guenebaut *et al.,* 1997; Radermacher *et al.,* 2006), with one arm embedded in the inner membrane and the other protruding into the mitochondrial matrix. Oxidation of NADH to NAD^+ results in the transfer of electrons to ubiquinone and 4 protons to the IMS, as represented by the following reaction scheme.

$$NADH + H^+ + Q + 4H^+_{matrix} \rightarrow NAD^+ + QH_2 + 4H^+_{IMS}$$

In the above equation, Q is ubiquinone and QH_2 is ubiquinol, the reduced form of ubiquinone. Several compounds can inhibit the activity of cI: for example, the classical inhibitor rotenone. The majority of known cI inhibitors target the NADH-Q reductase activity (reviewed by Esposti, 1997).

2.4.2.2. Complex II

Mitochondrial cII is the only protein complex of the ETC whose subunits are all nuclear-coded. It consists of 4 subunits: SDHA, SDHB, SDHC and SDHD. SDHA and SDHB protrude out into the matrix whereas SDHC and SDHD are embedded in the IMM. cII catalyzes the conversion of succinate to fumarate, one of the reactions of the TCA cycle, resulting in the reduction of FAD to $FADH_2$ in the flavoprotein subunit SDHA. The electrons obtained from this step are passed to ubiquinone via three iron-sulfur (Fe-S) clusters, reducing it to ubiquinol. The biochemical reaction catalyzed by cII is therefore described by the following scheme:

$$\text{Succinate} + \text{FAD} \rightarrow \text{Fumarate} + \text{FADH}_2 + 2e^-$$

$$Q + 2e^- + 2H^+ \rightarrow QH_2$$

Unlike cI, the reduction of quinone by cII does not involve proton translocation into the IMS. There are several inhibitors for cII that target the quinone-binding site, such as 2-thenoyltrifluoroacetone (TTFA), 3-methyl-carboxin and 2-n-heptyl-4-hydroxyquinoline-N-oxide (HQNO) (reviewed by Hägerhäll, 1997). Malonate is also a competitive inhibitor of cII (Thorn, 1953) as it binds to the active site of SDHA, preventing succinate binding.

2.4.2.3. Ubiquinone

Ubiquinone (CoQ) is a naturally synthesized, lipid-soluble coenzyme that interacts with three mitochondrial respiratory complexes, cI, cII and cIII. It also contributes to the regulation of the NADH/NAD^+ ratio and to antioxidant activity, as well as influencing cell growth and proliferation (reviewed in Bentinger *et al.,* 2010). The polyprenilated sidechain of CoQ differs depending on the species, for example, rodents have predominantly CoQ_9 (9-carbon side chains) whereas humans have almost exclusively CoQ_{10} (10-carbon side chain, reviewed by Fabra *et al.,* 2016).

2.4.2.4. Complex III

Mitochondrial cIII consists of 11 subunits of which only one is encoded in the mtDNA (reviewed by Lenaz and Genova, 2010). The enzyme catalyzes the transfer of electrons from ubiquinol to oxidized cytochrome *c* (Cyt c), and pumps 4 protons to the IMS in a reaction that may be summarized thus:

$$QH_2 + 2\text{Cyt } c_{\text{ oxidized}} + 2\ H^+_{\text{matrix}} \rightarrow Q + 2\text{Cyt } c_{\text{ reduced}} + 4H^+_{\text{IMS}}$$

The molecular mechanism of electron transport from ubiquinol to cytochrome *c* by cIII is termed the *Q* cycle, described in detail by Berg *et al*. (2002). Mitochondrial cIII is also known as the cytochrome bc_1 complex since it contains a total of three heme

groups, heme b_L (low affinity heme), heme b_H (high affinity heme) and a *c*-type heme. In addition, cIII contains the Rieske iron-sulfur protein, which stabilizes the complex in the reduced state (reviewed by Berg *et al.,* 2002). The majority of cIII inhibitors target Q cycle function, including the commonly used agent antimycin A (reviewed by Lenaz and Genova, 2010).

2.4.2.5. Cytochrome *c*

Cytochrome *c* carries electrons from cIII to cIV by bridging the cytochrome c_1 moiety and the Cu_A centre of cIV (Berg *et al.,* 2002). It is a small, nuclear encoded, water-soluble hemoprotein (approx. 12.5 kDa), loosely bound to the IMM on the IMS side. Apart from its function in the ETC, the protein also participates in several other processes, including modulating ROS levels, apoptosis and cardiolipin peroxidation (reviewed by Ow *et al.,* 2008; Huttemann *et al.,* 2011).

2.4.2.6. Complex IV

Cytochrome *c* oxidase is the terminal enzyme of the respiratory pathway that catalyzes the conversion of molecular oxygen to water. The enzyme complex consists of 13 subunits of which 3 are encoded in the mtDNA. The enzyme includes 2 heme groups, heme *a* and heme a_3, and 2 copper centers, Cu_A and Cu_B. The oxygen molecule binds to heme a_3 where, with the addition of 4 protons, it is converted to 2 water molecules, in the process pumping 4 protons to the IMS (Berg, 2002) as summarized by the following scheme:

$$4\text{Cyt } c_{\text{reduced}} + O_2 + 8H^+_{\text{matrix}} \rightarrow 4\text{Cyt } c_{\text{oxidised}} + 2H_2O + 4H^+_{\text{IMS}}$$

The intermediate steps in the conversion of oxygen to water theoretically involve the generation of highly reactive superoxide anions (O_2^-) and/or peroxides (O_2^{2-}), which might escape the enzymatic complex and induce oxidative damage. However, the reaction mechanism effectively prevents their release, although inhibition of cIV could still lead to excess ROS production at upstream sites in the ETC, for which ROS detoxifying systems are required. cIV can be inhibited by cyanide, carbon monoxide

(CO) and azide, all of which target the oxygen binding site of the enzyme (reviewed by Lenaz and Genova, 2010).

2.4.2.7. Complex V

The ETC ends with the transfer of electrons to molecular oxygen via cIV. However, the protons pumped into the IMS by cI, cIII and cIV form a proton gradient that drives the generation of ATP from ADP, catalyzed by cV (Mitchell, 1961). cV can therefore be considered as the terminal enzyme of the OXPHOS system. It consists of two major sub-complexes, F_o (the 'oligomycin fraction'), which conducts protons from the IMS to the matrix, and the soluble F_1 ('fraction 1'), which protrudes into the matrix and is the catalytic moiety that converts ADP to ATP using the energy generated from the proton gradient (Stock *et al.,* 1999; Watt *et al.,* 2010). The proton gradient drives the rotation of the motor units of cV, which are the c ring of the F_o and the central stalk, comprising F_1 subunits ɣ, ε and δ (reviewed by Stewart *et al.,* 2014). Briefly, the catalytic reaction of cV can be described as follows:

$$\sim 3\text{-}5H^+_{IMS} + ADP + P_i \rightarrow ATP + \sim 3\text{-}5H^+_{matrix}$$

In the above equation, ADP is adenosine diphosphate and P_i is inorganic phosphate. The number of protons required to generate one molecule of ATP depends on the size of the F_o region (the number of subunits in the c ring) and for every 360° rotation of the motor elements, 3 molecules of ATP are generated (Watt *et al.,* 2010). Complex V can be inhibited using oligomycin (A), which targets the F_o segment (reviewed by Nicholls *et al.*, 2013).

2.4.2.8. Alternative respiratory enzymes

Apart from the standard ETC protein complexes, many species, including most plants, protists and fungi, but not mammals, contain alternative enzymes capable of replacing cI and cIII plus cIV, namely alternative NADH dehydrogenases (NDH) and alternative oxidases (AOX), respectively. These alternative enzymes perform catalytic reactions similar to the standard ETC enzymes but do not translocate protons from the matrix to IMS and thus result in decreased ATP production when

active (reviewed by Lenaz *et al.*, 2010). The alternative enzymes are also resistant to the common inhibitors of cI, cIII and cIV. Since my thesis focuses on studying the effect of AOX expression in mammals,the biology of AOX is described in greater detail in the following section.

2.4.2.9. Alternative oxidase

As mentioned, AOX is an alternative terminal oxidase that can bypass the catalytic activity of cIII and cIV by transferring electrons directly from ubiquinol to oxygen, reducing it to water (figure 4).

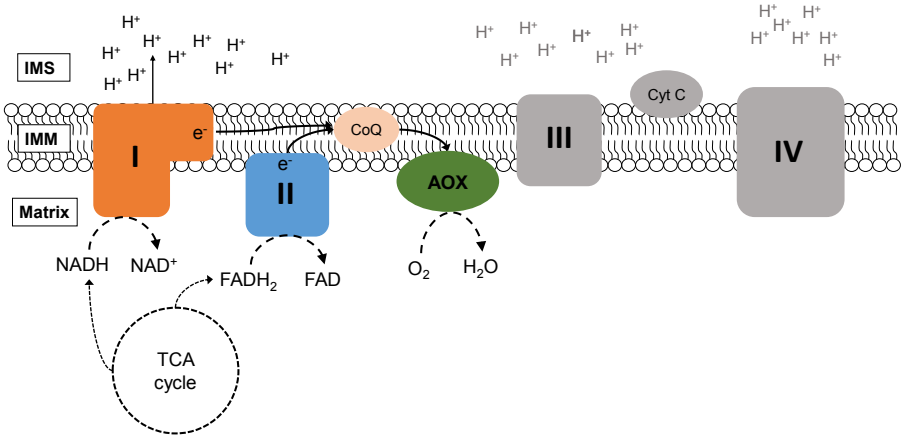

Figure 4: Schematic representation of the ETC showing AOX activity. AOX is activated under conditions of cytochrome pathway dysfunction of the ETC or increased accumulation of reduced CoQ. When active, AOX catalyzes the reduction of oxygen to water in a non-proton-motive reaction. Thus, cI is the only proton pump when AOX is fully active in place of cIII and cIV.

Genes for AOX are present in plants, and are widely distributed in fungi, protists and invertebrates (McDonald *et al.*, 2004). AOX is a nuclear-coded, diiron carboxylate enzyme with a molecular weight of approximately 35 kDa, that is bound to the IMM facing the matrix side (Moore *et al.,* 1995, Siedow *et al.,* 1995, reviewed by Berthold *et al.*, 2003). The catalytic activity of AOX is resistant to respiratory inhibitors such as cyanide, antimycin A, and azide. Unlike cIII and cIV, electron transport by AOX does not involve proton translocation and the energy is rather dissipated as heat in a thermogenic process. Organisms harboring AOX benefit from branched respiration under conditions where cIV is either slowed down or defective, and when ADP levels are low in mitochondria, for example, during photosynthesis in plants. AOX activity has also been shown, in plants, to lower ROS production in mitochondria (Maxwell *et*

al., 1999), to induce thermogenesis (Wagner *et al.,* 2008), and prevent over-reduction of quinones (Yoshida *et al.,* 2010). Several independent observations, in plants, fungi and protists have indicated that AOX can maintain respiration under conditions of cytochrome pathway impairment due to genetic or environmental causes (Albury *et al.,* 1996, reviewed by McDonald & Gospodaryov, 2019). Although beneficial effects and widespread presence of the enzyme have been described in sessile animals, AOX is not present in vertebrates, as a consequence of evolutionary loss of the AOX gene. Since cIII has a higher affinity for ubiquinol than AOX, the AOX-mediated alternative respiratory pathway does not compete with the traditional ETC pathway under steady-state conditions (Bahr *et al.*, 1973). Therefore, AOX is enzymatically active and contributes to electron flow in the ETC only when the concentration of ubiquinol is abnormally high, indicating a respiratory chain defect downstream of ubiquinol. This unique property of AOX made it a suitable candidate to be transgenically expressed in mammals with a functional cytochrome pathway, yet minimizing any detrimental effects that might result from by-passing the OXPHOS system under standard physiological conditions.

2.4.2.10. ROS production in the ETC

Since the majority of the inhaled oxygen is metabolized in the ETC, the ETC is also a major source of ROS production. In the ETC, single electron reduction of oxygen results in the formation of oxygen radicals, such as the superoxide anion ($O_2^{\bullet -}$) and the hydroxyl radical ($OH^{\bullet}$), as well as the nonradical molecules like hydrogen peroxide (H_2O_2), which are derived from superoxide anions. The catalytic reactions of ROS production can be described as following:

$$O_2 + e^- \rightleftharpoons O_2^{\bullet -}$$

$$2O_2^{\bullet -} + 2H^+ \rightarrow H_2O_2 + O_2$$

$$O_2^{\bullet -} + H_2O_2 \longrightarrow OH^{\bullet} + OH^- + O_2$$

$$H_2O_2 + Fe^{2+} \rightarrow OH^{\bullet} + OH^- + Fe^{3+}$$

The superoxide anion and hydrogen peroxide are the two major ROS products of the ETC. Under physiological conditions about 0.2 - 2% of the electrons deviate from the

normal electron transfer pathway and result in ROS formation (reviewed by Zhao *et al.,* 2019). In the ETC, cI and cIII are the major sites of ROS production (Brand, 2010).

In cI, superoxides can be generated and passed into the matrix during both forward and reverse electron transfer via I_F (FMN site) and the I_Q (CoQ binding site), respectively (Treberg *et al.*, 2011). However, ROS production via site I_Q is of a higher magnitude than via site I_F (Brand, 2010). Blocking the I_Q site with rotenone results in a several-fold increase in ROS production from the site I_F (reviewed by Murphy, 2009; Brand, 2010). Likewise, reverse electron flow through cI, arising from an over-reduced Q-pool, results in electron leak via site I_Q, and blocking this site with rotenone significantly diminishes the superoxide production (Brand *et al.,* 2016).

In cIII, superoxide is mainly generated via the $III Q_o$ site (semiquinone at center *o*). When exposed to the cIII inhibitor, antimycin A, electron transfer from heme b_L to the quinone at center *i* is blocked, leading to a buildup of semiquinone at center *o* that can readily reduce O_2 to superoxide (Cape *et al.,* 2007; Brand, 2010). Unlike cI, cIII can release superoxide into both the matrix and the IMS (Brand, 2010).

Other sites of ROS production in mitochondria are glycerol 3-phosphate dehydrogenase, the electron transferring flavoprotein: Q oxidoreductase (ETFQOR) of fatty acid beta oxidation, pyruvate and 2-oxoglutarate dehydrogenases, as well as negligible amounts from cII (Brand, 2010).

Although mitochondria are a major source of ROS production in the cell, paradoxically, they are also a major target of ROS-mediated damage, which can affect mtDNA, proteins and lipids. Such deleterious effects of ROS can be prevented by various antioxidant systems. For instance, superoxides are converted into a more stable H_2O_2 by a family of metalloenzymes called superoxide dismutases (SOD, Fridovich, 1995). Superoxides produced in the matrix are processed by manganese-superoxide dismutase (Mn-SOD; SOD2) and those produced in the IMS are processed by copper-zinc-superoxide dismutase (CuZnSOD; SOD1, Fridovich, 1995). Other relevant antioxidants in the cell are glutathione peroxidases (GPXs), peroxiredoxins (PRXs) and catalases, which convert H_2O_2 to H_2O.

2.4.3. Metabolic pathways

As mentioned above, major metabolic pathways in mitochondria are the tricarboxylic acid (TCA, Krebs, citric acid) cycle, fatty acid oxidation (β-oxidation) and the urea

cycle. The TCA cycle is an oxidative aerobic pathway, which results in the oxidation of acetyl-CoA to carbon dioxide and water, with the concomitant production of ATP via the OXPHOS system. Acetyl-CoA is synthesized mostly via three pathways; a) at the terminal step in carbohydrate metabolism, which begins with the translocation of pyruvate, a product of glycolysis, from the cytosol to the mitochondrial matrix, where it is oxidized to acetyl-CoA by the pyruvate dehydrogenase complex; b) fatty acid oxidation, which takes place in the mitochondrial matrix and c) catabolism of some specific amino acids, for example, tryptophan, leucine and isoleucine. Acetyl-CoA is the substrate for the TCA cycle. After a series of enzymatic reactions it finally gives rise to oxaloacetate, which is required for the incorporation of the next molecule of acetyl-CoA to form citrate, the first step in the TCA cycle. Oxaloacetate is therefore regenerated by the cycle. Two major rate-limiting factors of the TCA cycle are a) the concentration of substrates - acetyl-CoA and oxaloacetate, which participate in the first step of the TCA cycle, and b) the activity of citrate synthase, which can be regulated by the concentration of ATP (Krebs, 1970). The TCA cycle produces ATP mainly through OXPHOS, via the generation of NADH and $FADH_2$. For every acetyl-CoA molecule metabolized, three molecules of NADH and one molecule of $FADH_2$ are produced in the TCA cycle.

Fatty acid oxidation breaks down fatty acids to generate acetyl-CoA. Fatty acids are first activated in the cytosol by the enzyme acyl-CoA synthetase to form fatty acyl-CoA, which can then be imported into the mitochondrial matrix indirectly, through the carnitine shuttle. This transport involves intermediate steps catalyzed by the carnitine palmitoyltransferases CPT-I and CPT-II. Fatty acyl-CoA then undergoes a cyclical four-step reaction producing acetyl-CoA, NADH and $FADH_2$ in each cycle. The pathway is also called β-oxidation because it involves the removal of two carbon units at the beta position of the fatty acid in each cycle (reviewed by Schulz, 1991). Fatty acid oxidation also occurs in peroxisomes, which handle the first steps in the degradation of very long chain fatty acids.

Amino acid breakdown produces large quantities of ammonia (NH_3), which is a toxic metabolite, and is primarily processed in mammals in the liver into a non-toxic form, urea. Urea is released into the bloodstream, which is excreted by the kidneys as urine. The metabolic pathway of conversion of ammonia into urea is termed the urea cycle, which was first proposed by Krebs (1932). The urea cycle involves five enzymatic steps of which the first two occur in the mitochondria. Briefly, ammonia derived from the mitochondrial matrix is converted to carbamoyl phosphate, which reacts with

ornithine to produce citrulline. Citrulline is translocated to the cytosol where it undergoes 3 more enzymatic reactions producing urea and ornithine as end products. Ornithine re-enters the mitochondrial matrix to initiate another cycle (Nelson *et al.*, 2017).

All the above-mentioned metabolic pathways can function on their own, yet they are also closely interconnected (figure 5). For example, the end product of fatty acid breakdown, acetyl-CoA, feeds into the TCA cycle as a substrate and the by-products from these two pathways, NADH and $FADH_2$ enter the OXPHOS pathway to generate ATP. Transamination of oxaloacetate, an intermediate product of the TCA cycle, produces aspartate, which feeds into the urea cycle. Likewise, an intermediate product of the urea cycle, fumarate, produced from arginosuccinate, feeds into the TCA cycle where it is converted to malate. Therefore, dysfunction in any one of these pathways might, theoretically, affect metabolic homeostasis within mitochondria, ultimately affecting net ATP production and other important mitochondrial functions.

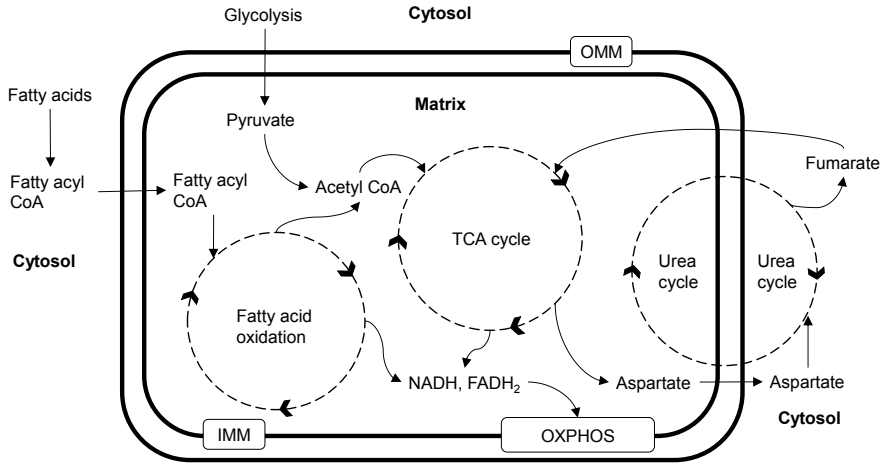

Figure 5: A simplified schematic diagram representing the interconnected metabolic pathways in the mitochondria highlighting the TCA cycle, fatty acid oxidation and urea cycle. Due to the interconnected nature of the metabolic pathways, dysfunction in one might disturb metabolic homeostasis within the entire mitochondrion. As a consequence, mitochondrial function is affected, including net ATP production via the OXPHOS pathway.

2.5. Mitochondrial diseases

Since ATP production is considered the major biological activity of mitochondria, the term mitochondrial disease is usually applied to cases with defective OXPHOS.

These diseases are further classified into primary and secondary mitochondrial diseases, based on the underlying cause of the dysfunction. Primary mitochondrial diseases are caused by mutations in mtDNA or in nDNA genes that directly encode OXPHOS proteins, mitochondrial tRNA or rRNA, or other proteins that affect the OXPHOS pathway. Such mutations may be inherited from either one or both parents. In contrast, secondary mitochondrial diseases include pathological conditions that either arise due to germline mutations of non-OXPHOS genes or adverse environmental effects, for example, oxidative stress in the course of aging or associated with inflammatory response, that affect mitochondrial function. Thus, secondary mitochondrial diseases can be either inherited or acquired, whereas primary mitochondrial diseases are most commonly inherited (reviewed by Niyazov *et al.,* 2016).

Current estimates for the prevalence of mitochondrial disease mutations, including both mtDNA and nDNA genes encoding mitochondrial proteins, are 1 in 4300 in the UK, including non-symptomatic mutations (Gorman *et al.,* 2015). Mitochondria contain thousands of copies of mtDNA per somatic cell, ranging from 1000 to 10000 depending on the cell type. This may lead to the co-existence of both a normal and mutated mtDNA population within the same cell, referred to as heteroplasmy, which was first reported in patients suffering from mitochondrial myopathy (Holt *et al.,* 1988). However, symptoms leading to disease generally occur only when the mutation load exceeds a particular threshold in the cell, which varies for different mutations and cell types. Conversely, the term 'homoplasmy' describes the condition where cells harbor identical mtDNA copies. Due to variations in the extent of heteroplasmy, mitochondrial diseases differ widely in age of onset, ranging from early childhood to late adulthood. They can affect a single organ (e.g. LHON) or multiple organs (e.g. GRACILE syndrome) (reviewed by Khan *et al.,* 2015).

In the heart muscle, the majority of ATP is produced by mitochondria. Thus mitochondrial diseases often present with cardiac involvement, especially cardiomyopathy, estimated to occur in 20 to 40% of children with mitochondrial diseases (Holmgren *et al.,* 2003, Scaglia *et al.,* 2004, reviewed by El-Hattab *et al.,* 2016). Mitochondrial disease patients with cardiomyopathy exhibit a higher rate of mortality (71%) at a very young age, compared to patients without (Holmgren *et al.,* 2003, Scaglia *et al.,* 2004). Cardiomyopathies may also occur in patients with mtDNA mutations with no previously known connection to mitochondrial diseases. In such cases, cardiomyopathy may be the first or the sole clinical manifestation (reviewed

by Brunel-Guitton *et al.,* 2015). On the other hand, due to the heterogeneous nature of mitochondrial diseases, the severity of symptoms and age of onset can vary between individuals. Therefore, cardiac involvement cannot, on its own, present a comprehensive picture of a mitochondrial disease (Catteruccia *et al.,* 2015).

2.5.1. Defective OXPHOS pathway

Defective OXPHOS can have a wide range of adverse effects on the cell, including ATP deficiency, metabolic imbalance and excessive production of reactive oxygen species (ROS). Mutations in genes encoding subunits of OXPHOS protein complexes and/or its assembly factors account for several diseases. These can present either as a defect in a single multisubunit complex (e.g. GRACILE syndrome) or as a combined dysfunction of many complexes (e.g. most cases of mitochondrial cardiomyopathy), in either case giving rise to diverse clinical features. A list of some widely known mitochondrial diseases caused by defective OXPHOS complexes and/or their assembly factors are provided in table 1.

Apart from mutations in genes encoding OXPHOS subunits mitochondrial dysfunction can also be due to:

a) deletions in mtDNA – e.g. Kearns-Sayre syndrome (KSS, Zeviani *et al.,* 1998), mitochondrial recessive ataxia syndrome (MIRAS, Hakonen *et al.,* 2008),
b) dysfunction of the mitochondrial protein synthesis machinery – e.g. mitochondrial myopathy, lactic acidosis and sideroblastic anemia (MILASA), due to a mutation in the *YARS2* gene (Riley *et al.,* 2010), which encodes for the mitochondrial protein that catalyzes the aminoacylation of tyrosyl tRNA,
c) disrupted mitochondrial dynamics – e.g. Charcot-Marie-Tooth diseases type 2A (CMT2A) due to mutations in the mitofusin 2 gene (*MFN2*, Nicholson *et al.,* 2008), which regulates mitochondrial fusion; or
d) external factors like aging, diet, inflammation and many pharmacologic agents, such as statins, valporic acid, metformin and barbiturates (reviewed by Niyazov *et al.,* 2016; Neustadt *et al.,* 2008).

Table 1: List of widely known mitochondrial diseases and the dysfunctional OXPHOS complex associated with them. Online Mendelian Inheritance in Man (OMIM) IDs are provided for further information. For cardiomyopathy and encephalopathy, OMIM IDs of mitochondrial complexes are provided.

Disease	Dysfunctional OXPHOS complex(es)	Mutated Gene(s)	OMIM
Björnstad syndrome	cIII	*BSC1L*	262000
Cardiomyopathy	cI	*NDUFS2, NDUFV2*	252010
	cIII	*CYTB*	516020
	cIV	*COX10, COX15, SCO1, SCO2*	220110
	cV	*ATP8*	614052
Encephalopathy	cI	*NDUFS2, NDUFV2, NDUFA2*	252010
	cIII	*BCS1L*	516020
	cIV	*SCO1, COX10*	220110
	cV	*ATPAF2*	614052
Growth Retardation, Amino aciduria, Cholestasis, Iron overload, Lactic acidosis, and Early death syndrome (GRACILE)	cIII	*BCS1L*	603358
Leber's Hereditary Optic Neuropathy (LHON)	cI	*ND1, ND2, ND4, ND5, ND6*	535000
	cIII	*CYTB*	
Leigh syndrome (LS)	cI	*ND2, ND3, ND5, ND6, NDUFS1, NDUFS3, NDUFS4, NDUFS7, NDUFS8, NDUFA2, NDUFA9, NDUFA10, NDUFA12, NDUFAF6, NDUFAF5*	256000
	cII	*SDHA*	
	cIII	*BCS1L*	
	cIV	*COX3, COX10, COX15, SCO2, SURF1*	
	cV	*ATP6*	
Mitochondrial Encephalopathy, Lactic acidosis, Stroke-like episodes (MELAS)	cI	*ND1, ND5, ND6*	540000
	cIV	*COX1, COX3*	
Neuropathy, Ataxia, Retinitis and Pigmentosa syndrome (NARP)	cV	*ATP6*	551500

2.5.2. Diagnosis of mitochondrial diseases

Early diagnosis of mitochondrial diseases is very challenging due to; a) overlapping clinical presentations for a specific genotype, for example, the A3243G point mutation in mtDNA, which can lead to maternally inherited diabetes and deafness (MIDD), or MELAS, or chronic progressive external ophthalmoplegia (CPEO) and b) wide variations in the onset of symptoms, like in case of MELAS (reviewed by El-Hattab *et al.,* 2015).

A general roadmap for diagnosing mitochondrial diseases involves a series of evaluations, including biochemical assessment of blood, cerebrospinal fluid and urine samples, histological assessment of muscle biopsy, evaluation of heart function by echocardiography and of pathological signs in the brain by magnetic resonance imaging (MRI), genetic screening (whole exome sequencing) and investigation of family history for pathological symptoms and routine follow-up of clinical symptoms (Parikh *et al.,* 2014; reviewed by Dimmock *et al.*, 2018).

Despite advances in diagnostic tools and methods, challenges remain in providing accurate diagnoses of mitochondrial diseases. These are either due to limitations in testing methods, including challenges with tissue processing and variability of methods between labs, or due to a lack of in-depth understanding of the genotype-phenotype variations (reviewed by Parikh *et al.,* 2019).

2.5.3. Current therapeutic options for mitochondrial diseases

No cure is currently available for any mitochondrial disease. Existing therapeutic strategies aim to control specific symptoms and disease progression. These therapies include increasing aerobic exercise (Jeppesen *et al.,* 2006), diet interventions (Ahola *et al.,* 2010; Joshi *et al.,* 2009), supplementation of vitamins such as riboflavin (Bugiani *et al.,* 2006) or other organic compounds, e.g. creatine monohydrate (Tarnopolsky *et al.,* 1997), carnitine (Gimenes *et al.,* 2015) and idebenone (Rudolph *et al.,* 2013), and redox agents such as lipoic acid and glutathione (reviewed by El-Hattab *et al.,* 2017). For comprehensive recent reviews see Parikh *et al.* (2009), Suomalainen (2011) and El-Hattab *et al.* (2017).

A lack of accurate pathophysiological knowledge about the majority of mitochondrial diseases is another major reason for the absence of available treatments. However, over recent decades, mitochondrial diseases have been studied extensively, leading

to the generation of many research models in order to gain deeper understanding of the underlying molecular mechanisms, to identify accurate biomarkers and/or potential drug targets for these diseases.

2.6. The mammalian heart

The heart is the first functioning organ to develop during embryogenesis (reviewed by Keller *et al.,* 2007; Wittig *et al.,* 2016). The mammalian adult heart is a complex muscle system made up of several different cell types. Its main purpose is to pump blood throughout the body, which is done by a continuous coordinated movement of the muscle referred to as heartbeats, or the cardiac cycle. In every cycle, the muscle contracts, referred to as the systolic phase of the cycle, so as to eject blood, followed by relaxation of the muscle, referred to as the diastolic phase of the cycle, to readmit blood into the heart. The contraction and relaxation of the muscle is carried out by the coordinated activity of cardiomyocytes, which account for approximately 30% of total cells, and occupy 70-85% of the total volume in the mammalian heart (Pinto *et al.,* 2016: cited in Zhou *et al.,* 2016). Apart from cardiomyocytes, the heart comprises conduction cells, fibroblasts, endothelial cells, smooth muscle cells and resident macrophages.

2.6.1. Cardiomyocytes

Adult cardiomyocytes can have 1-16 nuclei depending on the species (reviewed by Botting *et al.,* 2012) and, in most mammals, they do not proliferate. Cardiomyocyte division occurs during embryogenesis until a few days after birth. For instance, in mice, cardiomyocyte proliferation continues until 7 days after birth, after which the majority of cardiomyocytes are terminally differentiated and the heart loses its potential to regenerate (Soonpaa *et al.,* 1996, Porrello *et al.,* 2011). In rodents, terminal differentiation is marked by binucleation of the cells, whereas in humans, the majority of terminally differentiated adult cardiomyocytes (74%) are mononucleated while only 25% are binucleated cells (Olivetti *et al.,* 1996; reviewed by Bottling *et al.,* 2012). DNA synthesis in the cardiomyocytes occurs in two distinct phases, one during embryogenesis resulting in cell division and the other after birth, resulting in nuclear but not cell division (Soonpaa *et al.,* 1996). Cardiac regeneration has been observed in amphibians and fish following mechanical incisions of the ventricular apex region

(Oberpriller *et al.*, 1974; Becker *et al.,* 1974; Poss *et al.,* 2002), but this is very limited or absent in most mammals, including humans, under healthy conditions. However, under pathological conditions such as ischemia and chronic hypoxia, the adult heart switches to a 'fetal-like' condition indicated by triggered expression of specific transcription factors and their target genes, which normally are highly expressed during embryonic development, as well as metabolic adaptations such as the upregulation of glycolysis (reviewed by Taegtmeyer, 2010). This can be viewed as an alternative intracellular tissue renewal strategy operating after birth, as opposed to proliferation at the cellular level.

2.6.2. Metabolism in the healthy heart

The fetal heart is predominantly dependent on glucose and lactate for energy production, but after birth, a metabolic switch to fatty acid oxidation occurs in mammals (Bartelds *et al.,* 2000). The metabolic switch is a result of metabolite availability and a rapid increase in myocardial energy demand. The switch from a relatively hypoxic environment during fetal development to oxygen-rich conditions after birth has been shown to increase mitochondrial biogenesis and alter mitochondrial morphology (Neary *et al.,* 2014). The post-natal increase in mitochondrial volume is accompanied by an increase in the expression of about one-third of all mitochondrial proteins (Pohjoismäki *et al.,* 2012). Investigation of rat hearts at different stages showed evidence for an upregulation of mitoribosomal proteins and other components of the mitochondrial translation machinery at 10 days post-natal (P10), whereas the expression of OXPHOS and fatty-acid oxidation proteins was triggered only at later stages (Pohjoismäki *et al.,* 2012). The increase in mitochondrial biogenesis, at P10 also results in increased oxidative stress, leading to mtDNA damage, and concomitant upregulation of DNA repair proteins (Pohjoismäki *et al.,* 2012). In human cardiomyocytes, the fetal to adult transition is accompanied by an approximately 2 fold increase in mitochondrial mass, although mtDNA copy number is relatively similar between the two developmental stages (Pohjoismäki *et al.,* 2013). Additionally, proteins involved in mitochondrial transcription and translation are abundant in fetal cardiomyocytes, whereas proteins involved in the ETC and fatty-acid oxidation are more abundant in adult cardiomyocytes (Pohjoismäki *et al.,* 2013). The energy pool in adult heart consists of ATP and phosphocreatine (PCr). PCr is generated by the transfer of a phosphate group from ATP to creatine, catalyzed by creatine kinase inside mitochondria (mtCK). PCr readily moves through the

mitochondrial membranes and can be rapidly metabolized to regenerate ATP from ADP in the cytosol, catalyzed by cytosolic creatine kinase. The majority of cardiac ATP is generated from fatty acid oxidation, although glucose, lactate, amino acids and ketone bodies can serve as alternate fuels (reviewed by Doenst, *et al.,* 2013). The heart has a high rate of ATP hydrolysis resulting in complete turnover of the ATP pool every 10 seconds under normal conditions. Most of the ATP in cardiomyocytes (approx. 60 to 70%) is used to power contraction, whilst the remainder primarily facilitates ion exchange through the sarcoplasmic reticulum (reviewed by Stanley *et al.,* 2005).

2.6.3. Heart mitochondria

In adult heart, mitochondria provide about 90% of the ATP and constitute about 20 to 40% of cellular volume in cardiomyocytes (Barth *et al.,* 1992). Proper mitochondrial function, including ATP production and maintenance of Ca^{2+} homeostasis, is essential for contraction and relaxation of cardiomyocytes. In adult cardiomyocytes, mitochondria are segregated into three main locations, namely underlying the sarcolemma (sub-sarcolemmal mitochondria, SSM), between myofibrils (interfibrillar mitochondria, IFM) and around the nucleus (perinuclear mitochondria). The IFM are tightly packed, arranged in rows and in close contact with myofibrils and the sarcoplasmic reticulum. On the other hand, the SSM are distributed below the sarcolemma and are relatively loosely packed. Due to their close proximity to the sarcoplasmic reticulum and T-tubule, and tight contact with myofibrils, IFM are important for buffering Ca^{2+} and providing ATP for the contractile system. In contrast, SSM are important for active transport of metabolites and electrolytes across the sarcolemma (Palmer *et al.,* 1977; Hollander *et al.,* 2014). The IFM and SSM are both morphologically and biochemically different. For instance, the oxidative rate of IFM is 1.4 to 1.7 times higher than that of SSM in rat cardiomyocytes (Palmer *et al.,* 1977; reviewed by Pohjoismäki *et al.,* 2017).

2.6.4. Heart failure

Heart failure can occur when the heart muscle weakens and fails to pump blood effectively (systolic failure) or stiffens and fails to relax, thereby affecting filling blood re-entry (diastolic failure). Heart failure can be classified into three main types, based

on ejection fraction; heart failure with reduced ejection fraction (HFrEF), heart failure with preserved ejection fraction (HFpEF) and heart failure with mid-range ejection fraction (HFmrEF). Ejection fraction is measured using echocardiography or MRI and refers to the amount of blood ejected out of the left ventricle during each contraction. According to the American Heart Association (AHA), the ejection fraction of healthy individuals is in the range of 50 – 70%, whilst 41 – 49% is considered borderline and less than 40% is classified as reduced ejection fraction, which may lead to symptoms becoming noticeable. In conditions of HFpEF, the ejection fraction may still be normal (preserved) even though patients are diagnosed with heart failure. Symptoms of heart failure include fatigue, shortness of breath (dyspnea), retention of fluid in body tissues and altered heartbeat rates. In addition, heart failure is considered a cumulative disorder, where the initial stages are usually asymptomatic due to physiological compensatory mechanisms, for example, cardiac hypertrophy (enlargement of ventricles). However, under prolonged cardiac stress, the same mechanisms could lead to ventricular remodeling and compromised heart function (reviewed by Stanley *et al.,* 2005 and Rosca *et al.,* 2013).

Cardiomyopathy is a disorder of the heart muscle, and is one of the many causes of heart failure. Four major kinds of cardiomyopathies have been described: a) dilated cardiomyopathy, a condition where the heart walls are stretched; b) hypertrophic cardiomyopathy, a condition arising due to thickening of the ventricular walls; c) restrictive cardiomyopathy, a condition where the walls become rigid and d) arrhythmogenic right ventricular cardiomyopathy, caused by the replacement of muscle cells with fibrous and fatty tissue. Hypertrophic cardiomyopathy is the most common form of cardiomyopathy reported in patients with mitochondrial diseases (approximately 50%). Dilated cardiomyopathy can occur as a primary or secondary clinical manifestation following hypertrophic cardiomyopathy, whereas restrictive cardiomyopathy is rarely reported in patients with mitochondrial diseases (Bates *et al.,* 2012, Scaglia *et al.,* 2004, reviewed by Brunel-Guitton *et al.,* 2015; El-Hattab and Scaglia 2016). Inflammatory cardiomyopathy or myocarditis is a condition caused by inflammation of the cardiac tissue, predominantly due to viral infections or, in some cases, autoimmunity, and is marked by excessive infiltration of monocytes into the myocardium.

2.6.5. Metabolic adaptation of failing heart

Metabolic adaptation as a response to heart failure is a complex process. As indicated above, fatty acids are the predominant fuel for a healthy adult heart. However, under conditions of hypertrophy, glycolysis is upregulated and fatty acid oxidation is downregulated (Allard *et al.,* 1994). Such a change in the metabolic fuel preference resembles the fetal period of cardiac development, where glucose oxidation is the major source of energy (figure 6).

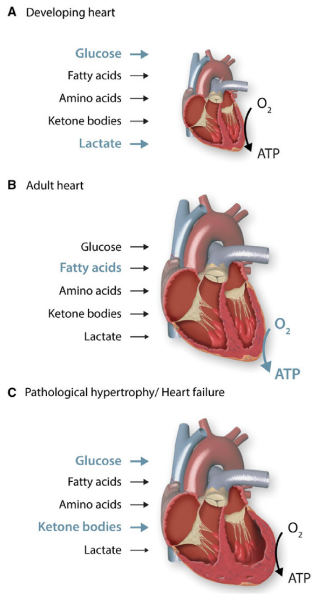

Figure 6: Changes in substrate utilization by the heart at different stages of growth and under pathological conditions. Although the heart is capable of utilizing several different substrates for ATP production, the substrate preference changes with age, physiological and pathological conditions. The developing heart has a strong preference for glycolysis and lactate oxidation for energy production, while only minimal contribution is provided by fatty acid oxidation. In the adult heart, ATP is mainly produced via OXPHOS, fueled by fatty acids. The increased dependency on OXPHOS is also reflected by the increase in mitochondrial mass in the cardiomyocytes. Under pathological conditions, the heart switches to a fetal metabolic profile with increased reliance on glycolysis for energy production. Figure reprinted with permission (Ritterhoff et al., 2017).

The accompanying changes in the gene expression pattern are referred to as the fetal gene program (Taegtmeyer *et al.,* 2010). Studies on volume-overloaded heart showed decreased fatty acid oxidation along with marked drop in tissue carnitine levels (El Alaoui-Talibi *et al.,* 1992). Since carnitine is required for the transport of long-chain fatty acids, such as palmitate, into mitochondria, a decrease in its level

directly affects fatty acid oxidation in mitochondria. However, whether it is appropriate to consider this as metabolic adaptation or maladaptation depends on the stage and cause of heart failure. For example, in conditions of ischemia/reperfusion (Liu *et al.,* 2002) or diabetic cardiomyopathy, fatty acid oxidation is upregulated and glucose oxidation is decreased (reviewed by Fillmore *et al.,* 2014). Although fatty acid oxidation is the primary fuel for ATP production in adult cardiomyocytes, an imbalance in the use of metabolic pathways results in decreased cardiac efficiency (reviewed by Fillmore *et al.,* 2014).

Oxygen concentration is another important factor in the progression of heart failure. The mammalian heart cannot generate sufficient energy under anaerobic conditions and thus requires a constant supply of oxygen of about 8-15 ml of oxygen per minute per 100 g of tissue at rest. Under conditions of ischemia, where tissues suffer diminished blood flow, or hypoxia, where oxygen supply is decreased, hypoxic-inducible factor 1 alpha (HIF-1α) is stabilized as a consequence of metabolic maladaptation: for example, accumulation of succinate. HIF-1α regulates the expression of several genes, including genes involved in vascular remodeling, inflammation, angiogenesis, cell death and antioxidant mechanisms (reviewed by Giordano, 2005 and Howell *et al.,* 2014). In addition, partial reduction of oxygen, i.e. transfer of only one or two electrons, results in the generation of ROS, which are generally considered as by-products of aerobic metabolism (figure 7; also see section 2.3.2.10). However, when accumulated in larger amounts, ROS can induce irreversible cellular damage, which is often observed in cardiac diseases, including ischemia-reperfusion (Gottlieb *et al.,* 1994), inflammation and cardiac hypertrophy (reviewed by Giordano, 2005; Zhou *et al.,* 2018).

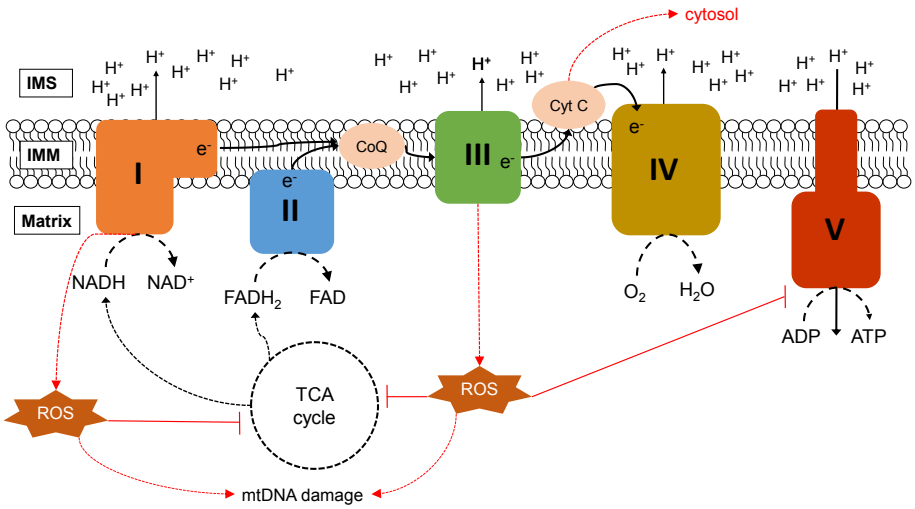

Figure 7: ROS production in the OXPHOS pathway. ROS is produced both as a consequence of normal electron transport and due to dysfunctional OXPHOS. Electron leak from cI and cIII, which are the major sites of ROS production in the OXPHOS pathway, leads to one-electron reduction of oxygen into ROS. Excessive ROS production contributes to mitochondrial dysfunction causing several irreversible types of damage, including that to mtDNA and enzymes of the TCA cycle, further affecting the OXPHOS pathway and resulting in less ATP production. Severe oxidative damage can also lead to the release of cytochrome *c* from the IMS to the cytosol, which in turn signals the induction of cell death. Note, ROS is also produced in several other sites in the mitochondria, which are not shown here.

2.6.6. Mitochondrial dysfunction in heart failure

Due to the constant demand of energy by the cardiac muscle, defects in mitochondrial ATP production severely affect its function, potentially leading to cardiac failure and death. Decreased mitochondrial oxidative metabolism and phosphocreatine levels (Conway *et al.,* 1991; Neubauer *et al.,* 1997), genetic defects arising from nDNA and mtDNA mutations (Antonicka *et al.,* 2003, Brecht *et al.,* 2015; Andreu *et al.,* 2000; Abdulhag *et al.,* 2014) and conditions causing mitochondrial dysfunction as a secondary effect, such as in cases of ischemic injury (Piper *et al.,* 1985; reviewed by Chen *et al.,* 2007), have been observed in several forms of heart failure. In addition, IFM serve as a sink for Ca^{2+} from the sarcoplasm, and disturbed calcium homeostasis has widespread effects on mitochondrial metabolism (Otto *et al.,* 1977, Wan *et al.,* 1989; reviewed by Pohjoismäki *et al.,* 2017), as well as affecting antioxidant mechanisms. Thus, mitochondrial dysfunction and metabolic adaptation or maladaptation of the myocardium are closely connected. Alternatively, mitophagy, which is selective degradation of mitochondria by autophagy, has been shown to be essential for cardioprotection under conditions of ischemic stress (Huang *et al.,*

2011). These observations make mitochondrial dysfunction and homeostasic responses to it a complex yet critical parameter in the progression of heart failure.

In order to better understand the impact of mitochondrial dysfunction in conditions of heart failure, I studied two genetically modified mouse models, which I now describe.

2.7. Mcp1 mouse model

Monocyte chemoattractant protein (MCP1) is a chemokine (chemotactic cytokine) that regulates the migration and infiltration of monocytes, natural killer (NK) cells and memory T-cell lymphocytes. MCP1 is expressed and secreted by many cells, including fibroblasts, inflammatory, endothelial, smooth muscle, astrocytic and microglial cells, in response to a proinflammatory stimuli and tissue injury (reviewed by Deshmane *et al.,* 2009, Niu *et al.,* 2009). When secreted, chemokines bind to specific receptors on the surface of immune cells, inducing migration towards the chemokine source, mediated by the chemokine concentration gradient. MCP1 was also shown to regulate the expression of monocyte cell surface adhesion molecules, induce the secretion of interleukins IL-6 and IL-1 (Jiang *et al.,* 1992) and regulate the expression of NADPH oxidase family proteins following ischemia/reperfusion injury (Morimoto *et al.,* 2008), as well as that of matrix metalloproteinases (MMPs), TGF-β and TGF-β1 (Niu *et al.,* 2009). These observations indicate that MCP1 can function as a chemokine and regulate gene expression in the heart to mediate proinflammatory responses through interleukins, cardiac remodeling via MMPs and oxidative stress response via NADPH oxidase family proteins. Addition of external MCP1 showed significant protection against apoptosis in cardiomyocytes exposed to hypoxic conditions followed by reoxygenation, while untreated cardiomyocytes showed induced apoptosis (Morimoto *et al.,* 2008). In a knockout mouse model for CCR2, the primary receptor for MCP1, experimentally induced myocardial infarction resulted in a decreased infiltration of macrophages and subsequent gene expression of MMPs and TNFα in the infarcted region, compared with control mice, and was beneficial for left ventricular remodeling (Kaikita *et al.,* 2004). Serum MCP1 levels were found to be elevated in patients suffering from ischemic stroke and myocardial infarction (Arakelyan *et al.,* 2005) and an ischemia/reperfusion experiment on rat kidney showed elevated MCP1 expression mediated by activation of NF-κB and oxidative stress (Sung *et al.,* 2002). These studies provide a potential link between oxidative stress, MCP1-mediated inflammatory responses and pathogenesis in

ischemic conditions. MCP1 is one of the most studied chemokines and its involvement has been documented in several diseases, including HIV-1 pathogenesis, atherosclerosis, cardiac ischemia, coronary artery disease, multiple sclerosis and some tumors (reviewed by Deshmane *et al.,* 2009, Niu *et al.,* 2009).

In order to understand the underlying mechanism by which MCP1 triggers the progression of cardiovascular diseases involving inflammation, a mouse model was generated showing constitutive expression of mouse MCP1 in adult cardiomyocytes (Kolattukudy *et al.,* 1998, hereafter referred to as Mcp1 mice). Mcp1 mice developed lethal cardiac failure. The severity of the phenotype was transgene-dose dependent: mice homozygous for overexpressed MCP1 suffered early lethality, at about 6 months of age, whereas heterozygous overexpressing mice survived to about 1 year of age. Echocardiographic analysis of one-year-old Mcp1 mice revealed poor cardiac contractility and increased left ventricular mass compared to wild-type mice (Kolattukudy *et al.,* 1998). Conversely, under conditions of ischemia/reperfusion, Mcp1 mice showed better LV diastolic function and decreased ROS generation, accompanied by increased CuZn-SOD activity in the myocardium, compared to wild-type mice (Morimoto *et al.,* 2008). Further studies on Mcp1 mice have revealed mitochondrial abnormalities, including swelling and dense deposits, decreased creatine phosphate/ATP ratio and increased ROS or inducible nitric oxide synthase (iNOS; Niu *et al.,* 2009). Administration to Mcp1 mice of cerium oxide (CeO_2) nanoparticles, shown to exhibit antioxidant properties (reviewed by Dhall *et al.*, 2018), attenuated left ventricular dysfunction, diminished monocyte/macrophage infiltration and myocardial oxidative stress, and decreased the expression of proinflammatory cytokines, ER-stress markers and heat shock proteins (HSPs; Niu *et al.,* 2007). Additionally, MCP1 binding to CCR2 results in the expression of MCP1-induced protein (MCPIP), a zinc-finger protein that functions as a transcription factor. Chronic expression of MCPIP in cardiomyoblasts has been shown to induce oxidative and ER-stress and to activate autophagy (Younce *et al.*, 2010), suggesting that these processes are causally linked (Younce *et al.*, 2010; Kolattukudy *et al.*, 2012). However, the source of oxidative stress is yet to be clearly understood. Since mitochondria are a major source of ROS production in the cell, mainly due to electron leak via respiratory complexes I and III under conditions of respiratory chain overload or dysfunction, mitochondrial ETC dysfunction could play a critical role in MCP1-mediated cardiac failure. Although macrophages themselves produce ROS (Tieu *et al.,* 2009), previous observations of mitochondrial structural abnormalities and

decreased ATP production in the heart of Mcp1 mice (Niu *et al.,* 2009) suggested a potential involvement of mitochondrial-ROS production in the pathophysiology. In order to understand if the observed mitochondrial dysfunction is either the cause or the consequence of the induced oxidative stress, I expressed AOX in Mcp1 mice. Assuming ROS production *via* a defective or overloaded cytochrome pathway of the mitochondrial respiratory chain is a major contributor to the underlying molecular mechanism, AOX should be able to mitigate it and thereby reduce the symptoms.

2.8. Cox10 mouse model

COX10, also known as heme A:farnesyltransferase or Heme O synthase, is a nuclear-coded enzyme required for the assembly of mitochondrial cIV. It catalyzes the conversion of heme *b* to heme *o* in the heme biosynthetic pathway. Heme *o* is then rapidly converted by COX15 to heme *a*, which is essential for the function of cIV. Both COX10 and COX15 are embedded in the IMM, and the protein levels, in yeast, are in the ratio of 1:8, respectively (Wang *et al.,* 2008). *COX10* shares a high sequence similarity among yeast, human and bacteria, with the exception of an amino-terminal domain of approximately 150 residues that is absent in bacteria (Nobrega *et al.,* 1990, Glerum *et al.*, 1994). The human *COX10* gene is approximately 135 kb in length, comprises 7 exons and is ubiquitously expressed, with highest expression levels in the heart, skeletal muscle and testes (Murakami *et al.,* 1997). Mutations in COX10 have been reported in several patients with clinical manifestations of leukodystrophy and tubulopathy, fatal infantile hypertrophic cardiomyopathy, anemia, sensineural deafness and Leigh-like syndrome (Valnot *et al.,* 2000, Antonicka *et al.,* 2003, Coenen *et al.,* 2004). The patients exhibited rapid progression of clinical symptoms, isolated COX deficiency and decreased levels of heme A. Over-expression of COX10 using retroviral *COX10* cDNA in cultured patient fibroblasts normalized COX activity (Antonicka *et al.,* 2003, Coenen *et al.,* 2004) by replenishing heme A levels (Antonicka *et al.,* 2003), indicating that COX10 activity could be a rate-limiting step in the formation of heme *a*, and thus of the assembly of COX and its activity.

To study the molecular mechanisms involving COX deficiencies, a conditional KO mouse model for COX10 was generated by flanking exon 6 of Cox10 with loxP recognition sites (Diaz *et al.,* 2005). Cox10-floxed mice were reported to be indistinguishable from wild-type mice. Muscle-specific Cox10 KO achieved by

crossing the floxed mice with mice expressing a muscle-specific Cre driver (*mlc1f-Cre)* showed a late-onset phenotype of muscle weakness and inactivity leading to death by 7 months of age. Loss of COX holoenzyme and severe deficiency of its activity were accompanied by the accumulation of enlarged mitochondria and loss of muscle tissue (Diaz *et al.,* 2005).

Liver-specific KO of Cox10, achieved by crossing Cox10 floxed mice with mice expressing Cre under the control of the rat albumin reporter, exhibited a liver phenotype, with severity correlating in a dose-dependent manner with Cre expression levels (Diaz *et al.,* 2009). Phenotypic abnormalities included loss of total body weight, increased lipid accumulation, severe decrease in COX activity, prominent mitochondrial proliferation and a mild decrease in ATP levels in younger mice. Interestingly, loss of cIV activity was complemented by an increase in activity of other respiratory chain complexes. However, as the steady-state levels of Cre decreased with age, COX activity and the number of COX-positive cells almost normalized to the levels of control mice (Diaz *et al.,* 2009).

These studies highlight the potential use of Cox10 floxed mice to study COX deficiency in specific tissues, thus mimicking diseases with both tissue-specific and multi-organ manifestation. I used this mouse model to study COX deficiency in heart tissue, as described in section 4.4.

Aiming to reveal the role of respiratory chain defects leading to mitochondrial dysfunction in the above models, I combined them with mice expressing AOX, as described in the next section. Before describing the AOX-expressing mouse models, I provide background information relating to the expression of AOX from *Ciona intestinalis* in human cells and *Drosophila*.

2.9. AOX models

a. Human cell-culture models

Xenotopic expression of AOX from *Ciona intestinalis*, in cultured human embryonic kidney (HEK) cells showed no detrimental effect under normal conditions (Hakkaart *et al.,* 2006), providing initial evidence for the safe expression of AOX in a mammalian context. When expressed, AOX localized to mitochondria and conferred enzymatic activity only in the presence of cyanide or antimycin A, which affects the standard

ETC by blocking cIII or cIV activity, respectively. Additionally, AOX also conferred protection against antimycin-induced superoxide production (Hakkaart *et al.,* 2006). Similarly, AOX expression complemented defects in respiration, in cell growth on low-glucose media, as well as antimycin-induced cell death and superoxide production, in human cells depleted of either COX10 or COX15 (Dassa *et al.,* 2009).

b. *Drosophila* models

Observations of such beneficial effects of *Ciona* AOX in human cells inspired the generation of transgenic *Drosophila* models expressing *Ciona* AOX (Fernandez-Ayala *et al.,* 2009, Kemppainen *et al.,* 2014). *Drosophila* ubiquitously expressing AOX were viable and fertile. However, they exhibited a minor delay in development and minor weight loss in younger flies; otherwise, the flies did not show any major phenotypic difference from wild-type animals. Like in the case of transgenic HEK cells, AOX flies exhibited resistance to cyanide and antimycin A *in vivo*, as well as cyanide resistance when respiration was analyzed in isolated mitochondria. Additionally, AOX expression in flies also prevented lethality caused by partial knockdown of cytochrome oxidase, and complemented the detrimental phenotype in a fly model of Parkinson's disease, dj-1β mutant (Fernandez-Ayala *et al.,* 2009).

c. Mouse models

Following the successful expression of AOX in human cells and *Drosophila*, three different lines of mice expressing AOX were generated. The first mouse model (hereafter referred to as MitAOX mice) harbored the coding sequence of *Ciona* AOX, codon-optimized for enhanced expression, introduced into the germline by lentiviral transduction (El-Khoury *et al.,* 2013). MitAOX mice were viable, exhibited no observable phenotypic differences from wild-type mice and showed widespread expression of AOX protein, which localized to mitochondria. Additionally, stable AOX expression did not affect the expression levels of endogenous respiratory complex subunits or the amount of ETC supercomplexes. However, the use of lentiviral transduction to create the model resulted in multiple integrations of the AOX transgene, such that ubiquitous, high-level expression could not be stably transmitted. This made the MitAOX model unsuitable for long-term maintenance or for combination with disease models of disease.

In order to create a genetically tractable AOX mouse line, the second mouse model (AOX^{Rosa26}) was generated by site-directed integration of *Ciona* AOX into the mouse *Rosa26* locus (I). In this model, the AOX transgene was inserted downstream of synthetic CAG promoter (figure 8A), so as to achieve strong and ubiquitous expression. These mice were the starting point for the study, and their detailed phenotypic analysis is described below, in section 4.1, and published papers (I) and (II). AOX^{Rosa26} mice were subsequently demonstrated to rescue the lethality and confer protection against detrimental phenotypes when combined with a mouse model for GRACILE syndrome, *Bcs1l* mutant mice (Rajendran *et al.,* 2019), or in a mouse model for sepsis, induced by administration of LPS (Mills *et al.,* 2016). Conversely, when combined with a mouse model for skeletal muscle-specific COX deficiency, via muscle-specific Cox15 KO, AOX expression was found to exacerbate the phenotype. It was inferred to blunt superoxide production, thereby affecting ROS-mediated response pathways, which were necessary for cellular regeneration (Dogan *et al.,* 2018).

Aiming to study the effect of tissue-specific AOX expression, and its ability to modify the phenotype of disease models that exhibit tissue-specific metabolic defects, a mouse model conditionally expressing AOX (SNAP-AOX^{Rosa26}) was also generated (III). The characterization of this model also forms part of my thesis, as described in (III). The difference between ubiquitous and conditional AOX models is the addition, upstream of AOX, of the coding sequence of the SNAP-tag (derived from human O6-alkylguanine-DNA-alkyltransferase (AGT), Keppler *et al.,* 2004), followed by an SV40 pA sequence for 3' RNA processing (figure 8). The additional sequence was surrounded by loxP sites to enable Cre-mediated excision. In this system, the CAG promoter naturally drives the expression of SNAP unless the SNAP cassette is removed by Cre-mediated recombination between the loxP sites, thus enabling the CAG promoter to drive the expression of AOX. Further details on this mouse model are provided in section 4.1 and paper (III).

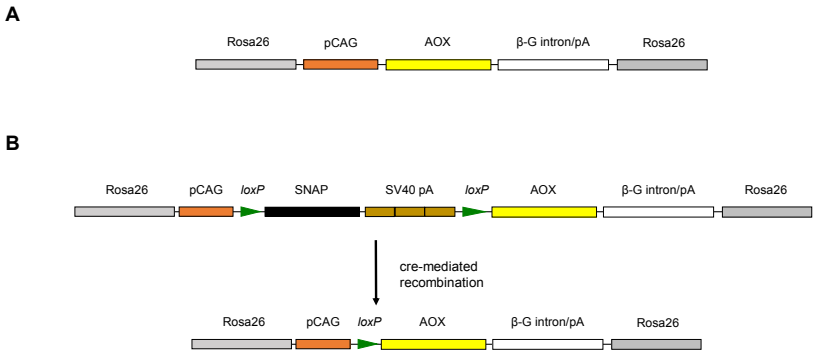

Figure 8: Schematic diagram of the AOX expression constructs of the AOX^{Rosa26} and SNAP-AOX^{Rosa26} mouse model. A) Single copy of *Ciona* AOX coding sequence integrated into the Rosa26 locus of mouse chromosome. AOX expression is driven by synthetic CAG promoter, and transcription termination by beta globin poly A signal. B) Expression construct of SNAP-AOX^{Rosa26} mice has additional elements compared to the construct of AOX^{Rosa26} mice between the CAG promoter and the AOX transgene, in the following order: loxP site, SNAP coding sequence, SV40 poly A sequence and loxP site. Through Cre-mediated recombination, the loxP flanked STOP cassette is excised leaving one loxP site, and thus allowing for AOX expression. In the absence of Cre-mediated recombination, only SNAP is expressed. Figure reprinted from (III) under Creative Commons Attribution 4.0 International License (CC by 4.0).

3. Aims

The general aim of this thesis work was to study the consequences of mitochondrial respiratory chain defects in mouse cardiomyopathy models, using AOX as a tool.

The more specific aims of this work were:

1. To profile the effects of expressing AOX in the mouse under non-stressed conditions and dietary manipulation manipulation, as essential background information for the cardiomyopathy study.

2. To test the effects of AOX expression in a mouse model of inflammatory cardiomyopathy, proposed to be mediated by oxidative stress.-

3. To investigate whether AOX can mitigate the effects of severe mitochondrial dysfunction in a mouse model of COX-deficient cardiomyopathy.

4. Materials and Methods

4.1. Animal handling and ethical considerations

Wild-type mice (C57BL/6JOlaHsd) were purchased from Envigo. All transgenic mice used in (I), (II) and (III) were backcrossed into the C57BL6/JOlaHsd background for over 8 or more generations before the start of each experiment. Tissue-specific AOX expression was achieved by crossing SNAP-Aox mice with mice expressing ACTB-Cre (The Jackson Laboratory, Stock No: 019099), for ubiquitous expression, or with mice expressing Myh6-Cre (The Jackson Laboratory, Stock No: 011038), for adult cardiomyocyte-specific expression. All animals were treated according to regulations detailed by the Finnish animal welfare board (ELLA), and all the experiments performed were approved and run according to the ethical permits ESAVI/8766/04.10.07/2015 and ESAVI/2954/04.10.07/2015. Mice were housed in a humidity and temperature-regulated animal facility with food and water provided *ad libitum* and a 12-hour light/dark cycle. After completion of the experiments, mice were euthanized either by cervical dislocation or, in some cases, exposure to CO_2 followed by cervical dislocation. Humane end points were followed, as described in the ethical permit.

4.2. Echocardiography

Cardiac ejection fraction and left ventricular mass were determined by echocardiography (Vevo 2100 system, FujiFilm VisualSonics Inc.). Mice were anesthetized using 4% isoflurane and were placed on a warm platform, maintained at 37 °C during the entire measurement. The obtained images were used to measure ventricular parameters using Vevo Lab software.

4.3. Treadmill

Treadmill (Exer- 6M Treadmill, Columbus Instruments) running was performed to measure mouse exercise endurance. Mice were trained on the treadmill for 3 days before the experiment. On the experiment day, mice were placed on the treadmill and the instrument was set to gradually reach a speed of 6.5 m/min before the start of measurement. The speed was then raised in steps of 0.5 m/min every 3 min. Mice were removed from the treadmill chamber immediately following a stay of more than

5 s on the electrified motivation grid (0.5 mA current), which was considered as the end point of each test. Either run-time (I) or run distance (II) was evaluated as an indicator of mouse performance.

4.4. Grip Strength analysis

Grip strength of the mice was measured using the BIO-GS3 apparatus (Bioseb). Mice were placed on the metallic grid platform until all four limbs were completely engaged on the grid. Then mice were pulled gently, to measure the force generated. Every measurement was repeated three times and the mean value was normalized to body weight (g/g) for each animal tested. All animals were trained for three successive days before the actual experiment.

4.5. DEXA imaging

DEXA imaging (GE LUNAR PIXImus2 imager) was used to measure mouse body composition. Before imaging, animals were anesthetized with a 1:1 mixture of pentobarbital (Orion Pharma, 100 mg/kg of body weight) and lidocaine (Orion Pharma, 16 mg/kg of body weight). Once anesthetized, mice were placed in the instrument for imaging, taking approximately 15 min per measurement.

4.6. Blood metabolite measurements

Blood droplets were collected from the tail vein by making a small incision. Glucose, lactate, and ketone body concentrations were measured using Freestyle Precision (Abbot Laboratories, USA), Lactate Pro (Arkay, Kyoto, Japan), and Freestyle Precision metering instruments, respectively, according to manufacturer's instructions.

4.7. Diet manipulation

Male littermates were randomized into different diet groups and were either caged in littermate groups (2–5 per cage) or individually, which was done for a small group, as described in II. Special diets, sterilized by irradiation, were introduced 8 weeks after birth. This delay ensured that the mice were already accustomed to solid food. They

were maintained on the relevant diet for 40 weeks. Diets used were standard chow (Teklad 2918, Teklad Global 18% Protein Rodent Diet), high fat (HF-60; Teklad Custom Diet TD.06414) and ketogenic (Teklad Custom Diet TD.96355). Animals were weighed at regular intervals, twice weekly, and the change in body weight was recorded.

4.8. DNA extraction and genotyping

Total DNA was extracted from ear punches or tail cuts using either standard laboratory methods as described in (I) or with a commercially available extraction kit, Extracta^{TM} DNA prep for PCR (QuantaBio), in (II) and (III). PCR genotyping was carried out to verify the genotype of all mice at the manipulated loci, using primers listed in Table 2. PCR reactions contained 4 pmol of each primer, and either DMSO at 2%, 0.2 µl DyNazyme II (Thermo Fisher Scientific) in (I) or Accustart II PCR SuperMix (QuantaBio) in (II) and (III). The cycle parameters were as follows: Initial denaturation at 95 °C for 5 min, then 39 cycles of denaturation at 95 °C for 20 s, respective annealing temperature (Table 2) for 30 s and extension at 72 °C for 60 s, with a final extension step at 72 °C for 10 min. The PCR products were verified using agarose gel electrophoresis.

4.9. RNA extraction, Northern blotting and RT-qPCR

RNA was prepared from frozen mouse tissues by bead-homogenization (Precellys lysing kit, Bertin Instruments) in 700 µl (> 10 volumes) of Trizol reagent (Sigma). After incubation for 5 min at room temperature, 0.2 volume of chloroform was added followed by centrifugation at 12,000 g_{max} for 15 min at 4 °C. The upper (aqueous) phase, containing RNA, was transferred to a fresh tube and an equal volume of isopropanol was added, followed by centrifugation at maximum speed, 21,000 g_{max}, for 10 min at 4 °C. Isopropanol was then decanted and the RNA pellet was washed in 70% ethanol, with a further centrifugation at 21,000 g_{max} for 5 min at 4 °C. After decanting the ethanol, RNA pellets were air-dried followed by resuspension in 20 µl RNase-free water and quantification using NanoDrop spectrophotometry.

For Northern blotting, resuspended RNA pellets were fractionated on formaldehyde (20%)-agarose gels followed by blotting to Hybond N+ membrane (GE Healthcare).

The blot was hybridized with end-labelled (^{32}P labelling) DNA probes, as described in (I).

For RT-qPCR, 1 µg of RNA was treated with DNase enzyme and was reverse transcribed using the Maxima First Strand cDNA Synthesis Kit for RT-qPCR (ThermoFisher Scientific). The processed samples were then diluted to 1:10 with nuclease-free water and 5 µl of the dilution was used for RT-qPCR reactions using the SensiFAST SYBR® No-ROX Kit (Bioline) and primers listed in (III).

4.10. Protein extraction and Western blotting

Small pieces of fresh or frozen tissue were placed in 500 µl of lysis buffer (50 mM Tris/HCl, 150 mM NaCl, 1 mM EDTA, 1% Triton X-100, pH 7.4,) containing a dissolved protease inhibitor cocktail tablet (Pierce), in a 5 ml tube on ice. Homogenization was done using a POLYTRON® PT 1200 E Manual Disperser (Ecoline). Homogenates were transferred to fresh 2 ml tubes and were incubated on ice for 30 min followed by centrifugation at 14,000 g_{max} for 5 min at 4 °C. Supernatants were transferred to a fresh tube and protein concentration was measured using the Bradford reagent (Bio-Rad). After quantification, samples were diluted into SDS-PAGE sample buffer for electrophoresis on SDS-12% polyacrylamide gels (10 µg of protein per lane), followed by transfer to PROTRAN nitrocellulose membranes (PerkinElmer) by semi-dry transfer (I) or PVDF membranes using Trans-Blot® TurboTM PVDF Transfer pack (Bio-Rad; III). A complete list of antibodies used are presented in Table 3.

4.11. Mitochondrial isolation and respirometry

Organs harvested from mice were collected in 15 ml Falcon tubes containing ice-cold PBS. Soft tissues (brain, lung and liver) were fine-chopped (to ca. 1 mm^3) in ice-cold PBS and hand-homogenized in 3 ml extraction buffer (225 mM sucrose, 75 mM D-mannitol, 10 mM Tris/HCl, 1 mM EGTA, 1 mg/ml bovine serum albumin (BSA), pH 7.4) using a glass-teflon homogenizer. Hard tissues (heart, skeletal muscle and kidney), chopped to a similar size, were treated with 3 ml (approx. 10 volumes) ice-cold trypsin-EDTA (500 µg/ml trypsin (Difco), 0.5 mM EDTA, 10 µg/ml phenol red, pH 7.4) for 10 min followed by blocking with 300 µl fetal bovine serum (Gibco/Life Technologies). The treated tissue pieces were then homogenized using a glass-teflon

homogenizer. Homogenates were transferred to fresh 15 ml tubes and centrifuged at 1,300 g_{max} for 5 min at 4 °C. Supernatants were collected and re-centrifuged at 17,000 g_{max} for 15 min at 4 °C. The obtained pellet was resuspended, according to its size, in 75-250 µl of ice-cold MiR05 buffer (0.5 mM EGTA, 3 mM $MgCl_2$, 60 mM lactobionic acid (Aldrich, buffered to pH 7.0 with 5 M KOH), 20 mM taurine (Sigma), 10 mM KH_2PO_4, 20 mM HEPES/KOH, 110 mM sucrose and 1 g/l fatty-acid free BSA (Sigma), pH 7.2 at room temperature) and stored on ice until respirometry. Mitochondrial protein content was measured using the Bradford reagent (Bio-Rad).

Respirometry was performed on freshly resuspended mitochondria using an O2K oxygraph (Oroboros). 2 ml of MiR05 buffer was added to the 2 ml chamber, to which 50 or 100 µg of mitochondria was added, according to the tissue. Substrates and inhibitors were added in the following order: (i) 5 mM sodium pyruvate + 5 mM sodium glutamate + 5 mM sodium malate, (ii) 4 mM ADP, (iii) 150 nM rotenone (Sigma), (iv) 17 mM sodium succinate, (v) 22.5 ng/ml antimycin A (Sigma), (vi) 200 µM n-propyl gallate (nPG, Sigma) (vii) 0.5 mM N,N,N',N'-tetramethyl-p-phenylenediamine (TMPD, Sigma) + 2 mM sodium L-ascorbate (viii) 100 mM NaN_3 or 1 mM KCN. The flux values (pmol/s*ml) obtained from the trace were normalized to the amount of mitochondrial protein and final values of flux (pmol/s*µg) were used for evaluations.

4.12. Collaborative experiments

Detailed protocols for all collaborative experiments are provided in the respective publications. For gut microbiome analysis, animal droppings were collected from 48-week old mice and were stored at 20 °C until further processing. For electron microscopy, mice were sacrificed by cervical dislocation and a small piece of left ventricle was collected and stored in a buffer containing 1.5% glutaraldehyde, 1.5% formaldehyde, 0.15 M HEPES/KOH, pH adjusted to 7.4, until further processing. For metabolomics (I), food was withdrawn 4-6 hours before sacrifice, followed by collection of a small piece of left ventricle. Samples were kept frozen until further processing. For metabolomic flux analysis (III), food was withdrawn 4-6 hours prior to the experiment. Mice were anesthetized with 4% isoflurane and were injected with either U-13C6 labeled (CLM-1396, Larodan) or 12C6 (492167, Sigma-Aldrich) glucose solution (2 g/kg bodyweight). 15 min after the injection, mice were sacrificed by cervical dislocation and a small piece of left ventricle was collected, snap frozen in liquid nitrogen and stored at -80 °C until further processing. In both experiments,

water was provided *ad libitum*. For analysis of CoQ, mice were sacrificed by cervical dislocation and a small piece of the left ventricle was collected and frozen until further processing.

4.13. Statistics

All data are reported as mean±SD. Data groups were compared by one-way ANOVA with *post hoc* Tukey HSD (multiple comparisons) test or, where two factors were considered, by two-way ANOVA, followed by *post hoc* Tukey HSD (multiple comparisons) test where interaction was detected or where more than two levels were considered for a given significant factor.

In (II), all data, except gut microbiome analysis, were analyzed using GraphPad Prism software.

In (III), survival curves were compared by the log-rank (Mantel-Cox) and Gehan-Brewslow-Wilcoxon tests, all using GraphPad Prism software. Significant differences from expectation, of progeny numbers of different output genotypes from crosses, was assessed by chi-squared test with Yates' correction for continuity, implemented using online tool (http://www.quantpsy.org/chisq/chisq.htm).

Statistical analyses presented in Supplementary Tables give exact p-values, which are generally quoted in figures and legends using a conventional *, **, *** nomenclature to denote appropriate thresholds.

Table 2: List of primers used

Primer	Sequence	Product size (bp)	Annealing temperature (°C)	Purpose
Aox_F	GCGATGCAAGATGGAGGGTA	317	56	Genotyping by PCR
Aox_R	TGAATCCAACCGTGGTCTCG			
Rosa26_F	GACCTCCATCGCGCACTCCG	520	56	
Rosa26_R	CTCCGAGGCGGATCACAAGC			
Cag_F	GGGCAACGTGCTGGTTATTG	400	63	
SNAP_R	AAGCTCTCCTGCTGGAACAC			
Myh6-Cre_F	ATGACAGACAGATCCCTCCTATCTCC	300	58	
Myh6-Cre_R	CTCATCACTCGTTGCATCATCGAC			
Internal Cre ctrl_F	CAAATGTTGCTTGTCTGGTG	200	58	
Internal Cre ctrl_R	GTCAGTCGAGTGCACAGTTT			
ACTB-Cre_F	GCGGTCTGGCAGTAAAAACTATC	100	64	
ACTB-Cre_R	GTGAAACAGCATTGCTGTCACTT			
Mcp1_F	TTCTCTGCCCAGCTGCCC	500	58	
Mcp1_R	CCTTCCTTTTTATGCTCC			
Cox10_F	ACCCATTAGAAACTGCTGATGGCT	Cox10 wt - 700; Cox10 flox - 840	61	
Cox10_R	CACTGACGCAGCGCCAGCATCTT			
Myh6_F	CTACAAGCGCCAGGCTGAG	188	60	RT-qPCR
Myh6_R	GGAGAGGTTATTCCTCGTCGT			
Myh7_F	GCTGTTTCCTTACTTGCTACCC	198		
Myh7_R	GCCTCTCCTTCTCAGACTTCC			
GATA4_F	TTTTCTGGGAAACTGGAGCTGG	159		
GATA4_R	ATCACCCACCGGCTAAAGAAG			
Egln3_F	AATGGTGATGGCCGCTGTAT	173		
Egln3_R	TCATGTGGATTCCTGCGGTC			
Gpx3_F	CATCCTGCCTTCTGTCCCTG	126		
Gpx3_R	CGATGGTGAGGGCTCCATAC			
SOD2_F	CGTGAACAATCTCAACGCCA	172		
SOD2_R	TCCTTTGGGTTCTCCACCAC			
Mtor_F	CGCTACTGTGTCTTGGCATC	237		
Mtor_R	CTTGATTCTCCCAATGCCGC			
IL10_F	AGGCGCTGTCATCGATTT	91		
IL10_R	CACCTTGGTCTTGGAGCTTAT			
Mcp1_F	CTGCTGTTCACAGTTGCCG	218		
Mcp1_R	CATTCCTTCTTGGGGTCAGC			
FGF21_F	CTGGGGGTCTACCAAGCATA	220		
FGF21_R	CAC CCA GGA TTT GAA TGA CC			
RPS18_F	GTTCCAGCACATTTTGCGAGT	136		
RPS18_R	GGTGAGGTCGATGTCTGCTT			
GDF15_F	CAACCAGAGCCGAGAGGAC	156		
GDF15_R	TGCACGCGGTAGGCTTC			

Table 3: List of antibodies used

Antibody	Company	Catalog number	Species	Dilution	Detected size (KDa)
Porin	Abcam	ab15895	rabbit	1:1,000	37
OXPHOS cocktail	Abcam	ab110413	mouse	1:250	NDUFB8 - 20 SDHB - 25 UQCRC2 - 48 MTCO1 - 40 ATP5A - 55
NDUFS3	Mitosciences	ab14711	mouse	1:4,000	24
HSP60	Abcam	ab46798	rabbit	1:20,000	60
GAPDH	Cell Signalling	#2118	rabbit	1:1,000	37
LC3b	Novus	NB600-1384	rabbit	1:1,000	LC3-I - 10
					LC3-II - 15
AOX	Customized antibody, 21st Century Biochemicals		rabbit	1:40,000	37
Goat anti-mouse IgG	Jackson ImmunoResearch	Cat#115-035-146	goat	1:10,000	-
Goat anti-rabbit IgG	Jackson ImmunoResearch	Cat#111-035-144	goat	1:20,000	-

5. Results

5.1 Impact of AOX expression in mice under non-stressed conditions

I studied the consequences of AOX expression in mammals using two different mouse lines, one designed to express AOX ubiquitously (AOX^{Rosa26}), the other containing a tissue-specific, conditionally activatable AOX transgene (SNAP-AOX^{Rosa26}). These mouse models were generated (Dr. M. Szibor) by integrating the *Ciona intestinalis* AOX coding sequence into the *Rosa26* locus, as described in Chapter 2.

A broad initial assessment of general traits including size, color and general mobility of mice in cages showed no observable differences between wild-type and transgenic mice. Note, these were mere qualitative assessments and no quantitative measurements were made for the above-mentioned parameters. The mice were originally generated in the C57Bl6/J background and were backcrossed to the C57Bl6/JOlaHsd background in Helsinki due to their ready availability and wide use among local research groups. The major difference between these two strains is a deletion in the alpha synuclein (Snca) and multimerin-1 (Mmrn1) genes in C57Bl6/JOlaHsd mice. C57Bl6/JOlaHsd mice were reported to show some minor phenotypic differences including impaired platelet adhesion, impaired thrombus formation (Reheman *et al.,* 2010) and decreased motor impulsivity (Pena-Oliver *et al.,* 2014) when compared to C57Bl6/J mice. Except for these differences C57Bl6/JOlaHsd mice were not reported to show any obvious phenotype and are generally used as wild-type control (Specht & Schoepfer, 2004). However, in a recent study, C57Bl6/JOlaHsd mice were reported to exhibit a significant decrease in trabecular bone mass (Liron *et. al.,* 2018). In all experiments reported in this thesis, the mice were backcrossed over 8 or more generations before crosses for phenotyping of the model or its progeny were made. After backcrossing, the above-mentioned basic traits of the mice continued not to differ qualitatively.

In order to evaluate these mouse models in detail, I first profiled the expression of AOX in different tissues. In the case of the conditionally activatable SNAP-AOX^{Rosa26} line this was done both before and after Cre-mediated activation. Next, I assessed the physical performance of the mice in comparison with non-transgenic littermates. I then evaluated the impact of AOX expression on relevant molecular parameters and finally validated the functional activity of AOX in tissues where it was expressed.

5.1.1. Expression profiling in AOX transgenic mice

Ideally, to use AOX as both a research tool and as a model for therapy, expression should be strong and ubiquitous. Therefore, the CAG promoter was initially selected to drive the expression of AOX. In order to test the prediction of ubiquitous expression, I analyzed the expression of the AOX transgene at the RNA and protein level, in different tissues of AOX mice.

a) AOX^{Rosa26} mice: RNA expression analysis using Northern blotting was carried out on heart, lung, liver, brain, kidney, spleen, testis and skeletal muscle tissues from both wild-type and AOX^{Rosa26} mice. AOX mRNA, 1.1 kb, was detected in all the tissues tested from AOX-expressing mice but not in wild-type mice, as expected. The expression levels of AOX, however, differed between tissues, with the highest levels observed in heart and skeletal muscle and the lowest in the brain (figure 9A). Protein expression analysis performed by western blotting using total protein extracts from heart, thigh muscle, masseter muscle, pancreas, lung, liver, kidney, spleen, cerebrum cerebellum, salivary gland and testis showed AOX expression in all the tissues (figure 9B). The pattern of relative protein expression in different tissues was similar to that of the mRNA, with the highest expression in heart and muscle and the lowest in brain.

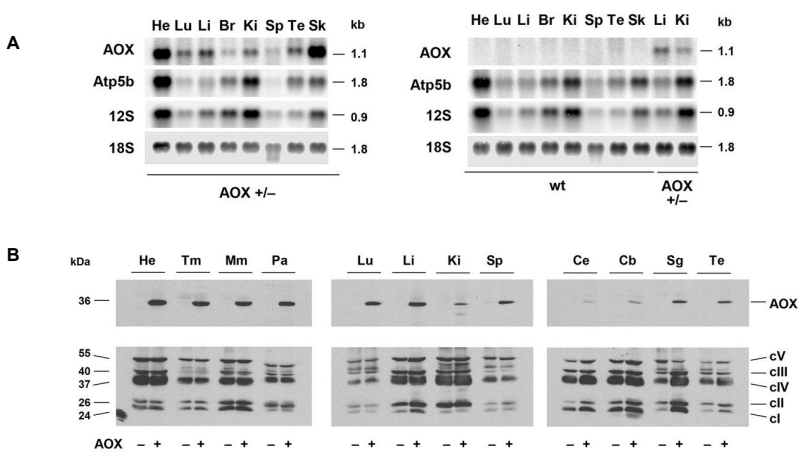

Figure 9: Expression analysis of AOX in mice. (A) Northern blotting showing RNA expression and (B) Western blotting showing protein expression from different tissues from 1-year-old male mice. He – heart, Lu – lung, Li – liver, Br – brain, Ki – kidney, Sp – spleen, Te – testes, Sk – skeletal muscle, Tm – thigh muscle, Mm – masseter muscle, Pa – pancreas, Ce – cerebrum, Cb – cerebellum, Sg – salivary gland. cI – cV shown in (B) were stained with OXPHOS cocktail antibody. Genotype and respective band sizes are as shown in the figure. Image reprinted from (I) under CC by 4.0 license.

In addition, based on experiments in brain tissue of one-month old mice (conducted by Dr. K. Holmström and Y. Zhuang), mice homozygous for AOX showed approximately two-fold higher expression of the protein compared to the heterozygous mice (figure S2D of paper (I)). The reason for different expression levels in different tissues is unknown but given that AOX is a mitochondrial protein, variation in the amount of mitochondria or respiratory capacity could be possible reasons. However, this does not explain the reason for very low AOX expression levels in the brain of AOX mice. This issue is discussed in depth in the next chapter.

b) SNAP-AOX^{Rosa26} mice: As described in Chapter 2, without recombination catalyzed by Cre, AOX expression cannot be activated in these mice. In order to verify that AOX expression can be activated in this manner, I analyzed protein expression using western blotting on different tissues from SNAP-AOX^{Rosa26} mice with and without *Cre* recombination. Without Cre recombination, all the tissues tested were expressing SNAP but not AOX protein. To check the activation of AOX expression, I crossed SNAP-AOX^{Rosa26} mice with mice expressing Cre ubiquitously, driven by the beta-Actin (ACTB) promoter, and, in a separate experiment, with mice expressing Cre only in adult cardiomyocytes, driven by the alpha-myosin heavy chain (*Myh6*) promoter. In both cases, I was able to activate AOX expression as predicted (figure 10). In general, expression of SNAP protein was not observed in tissues where AOX expression was activated using ACTB promoter; this is due to the removal of the SNAP sequence resulting from by Cre-mediated recombination. However, in the heart tissue from the progeny of SNAP-AOX^{Rosa26} combined with mice expressing *Cre* under the *Myh6* promoter, residual SNAP expression was observed, which could be from the non-myocytes, where *Cre* expression is not activated (bottom panel, figure 10).

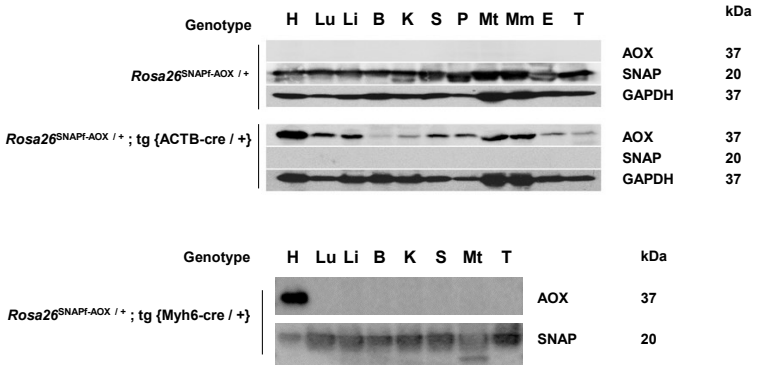

Figure 10: Tissue specific activation of AOX expression achieved by combining SNAP-AOX^{Rosa26} mice with two different *Cre* expressing mouse lines; ubiquitously expressing *Cre* under beta actin promoter (ACTB-Cre – top lane) and cardiomyocyte specific expression under *Myh6* promoter (Myh6-Cre – bottom lane). Genotype and band sizes are as indicated. H – heart, Lu – lung, Li – liver, B – brain, K – kidney, S – spleen, P – pancreas, Mt – thigh muscle, Mm – masseter muscle, E – eye, T – testes. Image reprinted from (III) under CC by 4.0 license.

5.1.2. Protein localization and association

In plants and other species where AOX is naturally expressed, it is present in the IMM. To verify that this was also the case for *Ciona* AOX expressed in mice, I separated membrane-bound proteins from soluble cytosolic proteins, from the liver tissue of AOX^{Rosa26} mice, using sodium carbonate extraction, and then performed western blotting to detect the protein (figure S2E of (I)). As expected, AOX protein was found in the membrane but not in the soluble fraction, validated by of its colocalization with subunit I of complex IV (MTCO1), indicating that AOX protein is membrane-associated when expressed in the mouse.

To test whether AOX protein is associated with other protein or protein complexes when expressed in mammals, Dr. I. Wittig performed Blue native PAGE on tissue lysates from heart, liver, lung, kidney, spleen, muscle testis and brain from AOX^{Rosa26} mice. In all the tissues tested AOX migrated predominantly as dimers and other multimers (figure S2F of paper (I)). Analysis of the heart mitochondria, also performed by Dr. I. Wittig, using Blue native PAGE confirmed that AOX was not associated with any endogenous respiratory chain complexes or supercomplexes (figure S2G of paper (I)).

5.1.3. Enzymatic activity of AOX

The enzymatic activity of expressed AOX was verified in different tissues using mitochondrial respirometry. External substrates and inhibitors were supplied to isolated mitochondria in the presence of ADP, i.e. the conditions for state-3 or coupled respiration, to measure oxygen consumption driven by different respiratory chain complexes as well as via AOX. In order to make a broad assessment of the respiratory capacity or enzymatic activity of AOX in mice, I studied mitochondrial respiration in heart, lung, liver, brain, kidney and skeletal muscle. In all the tissues tested, AOX expression did not modify the activity of any of the endogenous respiratory-chain complexes (figure 11A). However, with the exception of brain mitochondria, where AOX expression was much lower than in other tissues (figure 9), the presence of the AOX transgene overcame the respiratory blockade resulting from the presence of antimycin A, an inhibitor of cIII, and maintained mitochondrial respiration until AOX itself was inhibited with n-propyl-gallate, a known inhibitor of AOX (Moller *et al.,* 1988). Analysis from biological triplicates of samples from male AOX^{Rosa26} mice indicated AOX was able to maintain a respiratory capacity of up to 90 % of the uninhibited cII-mediated value in muscle (including heart), and about 50 – 70 % in other tissues tested, apart from brain (figure 11A). This antimycin-resistant respiration was consistent between biological replicates with no major variation, indicating that AOX enzymatic activity does not vary between individual mice.

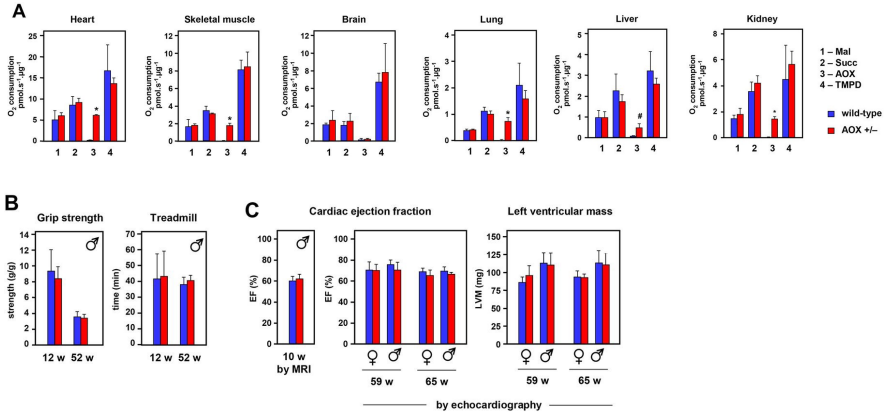

Figure 11: AOX is enzymatically functional and does not affect normal physiology of mice. (A) Enzymatic activity of AOX, measured by respirometry analysis on isolated mitochondria from different tissues as indicated. Oxygen consumption rate represented in pmol s^{-1} μg^{-1}. 1 (Mal) – rotenone-sensitive oxidation of malate in the presence of glutamate, pyruvate and ADP; 2 (Succ) – antimycin A- plus n-propyl gallate-sensitive succinate oxidation; 3 (AOX) – rate of n-propyl gallate-sensitive, antimycin A-insensitive succinate oxidation; 4 (TMPD) – rate of ascorbate-reduced TMPD oxidation. (B) Mouse muscle strength measured using grip strength analysis, and endurance measured by treadmill experiment. (C) Cardiac ejection fraction measured either by MRI, by Dr. A. Wietelmann or echocardiography, by me. Age, sex and genotype of mice as indicated in the figure. Figure reprinted from (I) under CC by 4.0 license.

Based on these results, the expression of AOX in mice was as expected, including its enzymatic activity that was measured by respirometry. This led me to assess the impact of AOX expression on biochemical and physiological parameters of the mice.

5.1.4. Effect of AOX expression on mice

Functionally active AOX contributing to mitochondrial respiration can compete with mitochondrial cIII and transfer electrons from the quinone (Q) pool. Since this electron transfer is non-proton motive, it can affect net ATP production. Although AOX is expected to become functionally active only under conditions where mitochondrial cIII and/or IV is dysfunctional, even a partial activation of AOX might nevertheless cause it to compete with cIII. This will eventually result in a decline in mitochondrial ATP production, and thus affecting the function of many organs, especially those that are highly dependent on mitochondrial ATP synthesis like the heart. To test if transgenic AOX expression induces such malfunction, a broad phenotyping of AOX^{Rosa26} mice was carried out under non-stressed conditions, to assess both physiological and behavioral parameters.

Basic morphological and physiological assessment, including measurements of body weight for both sexes (figure 4 of paper (I)), showed no difference between AOX^{Rosa26} mice and their wild-type littermates. This led me to assess more complex physiological parameters in mice, as described below.

A. Physical performance

To assess the physical performance of the AOX^{Rosa26} mice, I measured their endurance and muscle strength by treadmill and grip-strength analysis, respectively, at two different time points, 12 and 52 weeks of age, using wild-type littermates as controls. At both ages, AOX^{Rosa26} mice performed similarly to the controls (figure 11B). Both these analyses were also performed in an independent study, which was done in collaboration with the German Mouse Clinic (GMC) as described in section 4.1.5. The latter study, on both sexes, also found no difference in performance between AOX transgenic and wild-type mice.

B. Cardiac function

Cardiac function of AOX^{Rosa26} mice was analyzed by MRI (Dr. A. Wietelmann) at age 10 weeks on males, and by echocardiographic imaging, done by me, at ages 59 and 65 weeks on both sexes. Both experiments showed that the cardiac ejection fraction of transgenic mice was indistinguishable from that of their wild-type littermates (figure 11C).

I also performed echocardiographic imaging on SNAP-AOX^{Rosa26} mice with and without transgene activation via adult cardiomyocyte-specific Cre, to test whether cardiac function was affected by AOX expression in these mice. I performed the analysis on 5 or more male mice per group at ages 12 and 16 weeks. The results confirmed no difference in cardiac performance of SNAP-AOX^{Rosa26} and 'Cardio AOX' mice (mice expressing AOX only in the adult cardiomyocytes as shown in figure 2C of paper (III)) compared to control mice which, in this case, were wild-type mice, mice expressing only Cre in the adult cardiomyocytes, and AOX^{Rosa26} mice.

C. Molecular parameters

If AOX is functionally active, even at a low level, it could partially replace the activity of mitochondrial complexes III and IV, potentially affecting their expression levels as a secondary effect. To test this, I analyzed the protein expression levels of endogenous mitochondrial respiratory chain subunits using western blotting. In order to perform a broad analysis and also due to the ubiquitous AOX expression, I prepared total protein lysates from heart, lung, liver, cerebrum, cerebellum, kidney, spleen, thigh muscle, masseter muscle and testis of 54-week old male AOX^{Rosa26} mice for the westerns and probed the blot with an OXPHOS antibody cocktail. The expression levels of subunits representing all 5 OXPHOS complexes did not differ between AOX^{Rosa26} mice and wild-type littermates (figure 9B). Since there were no obvious differences, I did not quantify the intensity of the bands in this experiment.

To test if cardiac-specific expression of AOX affected the expression of endogenous mitochondrial respiratory complexes, I performed a similar analysis, but only on the heart tissue of Cardio AOX mice at ages 12 and 16

weeks old, with appropriate controls as mentioned in section 4.3.2. As expected, expression of AOX did not affect that of representative subunits of the endogenous mitochondrial OXPHOS complex (figure 5C and S3A of paper (III)).

Since AOX^{Rosa26} mice did not show any obvious phenotypic difference from wild-type, I hypothesized that any minor physiological modification caused by AOX expression might nevertheless be detectable at the metabolic level. To test this idea, I used metabolomic analysis, in collaboration with V. Velagapudi and J. Nandania, on heart and skeletal muscle tissues that were selected due to their dependence on mitochondrial energy compared with other tissues. Principal Component Analysis (PCA), performed by Dr. V. Velagapudi and J. Nandania, of total measured metabolites confirmed that AOX-expressing tissues, both skeletal muscle and heart, had a similar metabolite profile as wild-type tissues (figure 2C and S2H of paper (I)). The lack of any observable biochemical disturbance in AOX^{Rosa26} mice indicates that the expressed AOX is benign under steady-state (unstressed) conditions in transgenic mice. However, it is predicted to be activated under conditions where the concentration of ubiquinol rapidly increases or mitochondrial complex III and/or IV is impaired, as has been observed in a mouse sepsis model (Mills *et al*., 2016). Therefore, the heart metabolome was also analyzed in Cardio AOX mice: the relevant data are presented in a later section (5.3.4 - f), in the context of my studies of the effect of AOX on two cardiomyopathy models.

5.1.5. The Primary phenotyping screening at the German Mouse Clinic

To test whether any other metabolic or physiological abnormalities were evident in AOX^{Rosa26} mice, I collaborated with the German Mouse Clinic (Helmholtz Zentrum münchen, GMC) to perform a detailed phenotyping. My collaborators measured over 350 different parameters and extensively phenotyped the mice over a period of 14 weeks, as summarized in figure 12.

AOX^{Rosa26} mice showed only very small (and statistically non-significant) differences in physical performance from wild-type mice (complete GMC data is available online, link provided in I). They did not differ in measurements of physical activity, including rotarod and grip strength analysis, with only a minor trend towards decreased locomotor activity in the modified SHIRPA test.

AOX^{Rosa26} mice also showed a trend towards decreased hearing sensitivity, particularly at higher frequencies, but again this was not statistically significant. Other parameters where AOX^{Rosa26} mice showed subtle, but generally non-significant differences from wild-type mice were:

a) mild decrease in LV mass in both sexes, as measured by echocardiography;

b) decrease in eye size in males, as measured by laser interference biometry;

c) mild increase in plasma fructosamine levels in both sexes and

d) sex-dependent changes in immune cell populations, based on flow cytometry, where transgenic males had increased NK cells and a high representation of CD44 high and CD11b-expressing NK cells, whereas females had increased CD11c-expressing monocytes and B cells

Except for these parameters, AOX transgenic mice did not differ from wild-type mice in any other phenotypic measurements, including body weight, size and shape, cardiac function, rectal body temperature, metabolome and sensitivity to pain. A detailed report from the German Mouse Clinic is available online (see Materials and Methods, III).

In summary, from all the measurements made by myself and in collaboration with others, including the GMC, I found that AOX expression does not significantly affect the physiology and metabolism of mice under standard laboratory conditions, nor in an age- or sex-dependant manner. However, my analysis did not include all possible parameters that could be affected in mice over their lifetime, which would be much more laborious to execute and not practically feasible. However, specific issues may need to be addressed in the future if AOX is to be considered as a therapeutic agent.

In addition to the above, experiments done under contract by Luria Scientific Industries, Herzliya, Israel, showed that AOX^{Rosa26} mice were also resistant to cyanide, when administered via IP at a concentration of 8.5 mg/Kg weight of the mouse, whereas 50% of wild-type mice did not survive this dose of the poison (figure 5 of paper (I)).

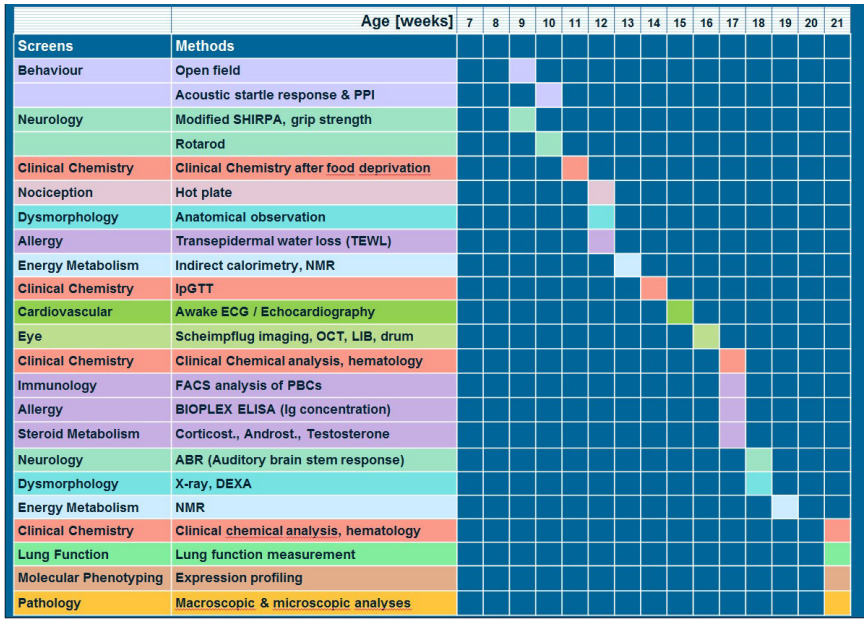

Figure 12: Schematic of experimental design followed in the German Mouse Clinic.

In conclusion, I report in (I) that AOX can be successfully expressed in the mouse and, when expressed, it does not alter the general physiology of the animal compared to wild-type littermates, even though the protein is enzymatically active and provides protection against cyanide. These initial studies were a crucial first step before using the AOX mice in combination with disease models and other stresses.

5.2 Impact of AOX expression in mice under dietary stress

Although I was unable to detect any phenotypic deviation from wildtype in AOX^{Rosa26} mice, *Drosophila melanogaster* transgenically expressing AOX were previously found to exhibit a very mild phenotypic difference from wild-type flies in the form of a slight developmental delay and slightly exaggerated weight loss of adult flies (Fernandez-Ayala *et al.,* 2009). This could imply that AOX might be partially active in the transgenic flies, resulting in a less efficient use of available nutritional sources compared to non-transgenic or wildtype files. A follow up study (Saari *et al*., 2019) where AOX flies were cultured in a nutrition-deprived medium, containing only 3.5% yeast and 5% glucose plus agar and antimicrobials, maintained at temperatures 25 °C or 26 °C, resulted in a dramatic loss (> 80%) of developing flies at the pupal stage, whereas control flies eclosed normally under the same conditions.

These data, indicating a potentially severe impact of nutritional modification on AOX-expressing animals, provided me with the motivation to study the impact of AOX on mice that were also subject to dietary stress. To this end, I subjected AOX^{Rosa26} mice to diets containing high fat and/or low carbohydrate content, and measured relevant physiological parameters.

To study how the combination of AOX expression and fat-rich diets affects phenotype, I administered two different kinds of fat-rich diet to AOX^{Rosa26} mice and wild-type littermates. These were: a) HF-60, where 60% of total calories come from fat and b) Ketogenic diet, where 90% of total calories come from fat with almost none (approximately 0.5%) derived from carbohydrates. Mice fed with a standard chow diet were used as controls, where only 18% of total calories are from fat and 58% from carbohydrates. The critical difference between the two fat-rich diets, except the amount of fat, is the amount of carbohydrates. Lack of carbohydrates in the ketogenic diet affects glycolysis, making gluconeogenesis the only source to maintain the body's glucose levels. Furthermore, the primary macronutrient of the ketogenic diet is fatty acids, which are catabolized by β-oxidation to acetyl-CoA, and then via the TCA cycle, both of which take place in mitochondria. Thus, studies with prolonged administration of ketogenic diet have often shown increased mitochondrial biogenesis. On the other hand, under a high-fat diet, mice usually gain weight due to the storage of much of the consumed fat in adipose tissue. Prolonged administration of high-fat diet has been shown to interact with mitochondrial dysfunction, especially in skeletal muscle (Jorgensen *et al.,* 2015), due to the resulting metabolic disturbances.

The effects of these fat-rich diets on mice were measured using different parameters, as described in the following sections;

5.2.1. Body weight

Mice exposed to either of the high-fat diets for a prolonged period gained excess weight when compared with chow-fed mice. AOX expression did not affect weight gain except for a slight but statistically significant difference on ketogenic diet, where AOX-expressing mice weighed less, on average, than their wild-type littermates between the ages of 16 and 34 weeks (figure 13). However, both genotypes exhibited a relatively wide variation in weight on the ketogenic diet, at every time point when measured. I hypothesized that this could possibly be due to behavioral interactions between males caged together affecting feeding and/or physical activity. Mice are, in general, territorial, and tend to form social hierarchies and even exhibit aggressive behavior towards their 'cage-mates' (Horii *et al.,* 2017). Such traits affect the behavior of mice, including eating and physical movement, which would in-turn affect the energy expenditure that could influence weight gain or loss. In order to investigate this further, I repeated the ketogenic diet experiment in a different facility where the mice were caged individually. In this smaller scale experiment, I observed much less variation in weight within the groups but, interestingly, the small difference between the genotypes was in the opposite direction to that observed in the first experiment. In the second trial, the AOX mice weighed slightly more than controls on ketogenic diet (figure 1C of paper (II)). Combined together, the slight weight differences exhibited by AOX mice on ketogenic diet were not systematic, despite being statistically significant in both experiments.

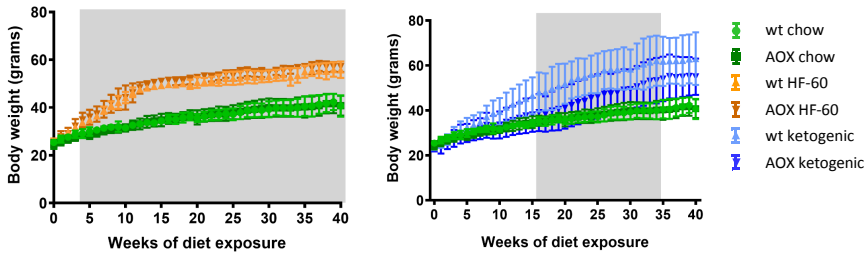

Figure 13: Body weight (means ± SD) of wild-type (wt) and AOX-expressing male mice (n ≥ 6 for all groups) fed with either standard chow (chow), high-fat (HF-60), or ketogenic diets, as indicated. Highlighted gray areas indicate statistical significance ($P < 0.05$), two-way ANOVA followed by Tukey's multiple comparisons analysis - (left) between diets but not genotypes, (right) between genotypes. Figure reprinted from (II) under CC by 4.0 license.

5.2.2. Body composition

In order to study the physiological response towards fat-rich diets in further detail, I measured the body composition of all mice using the DEXA imaging system, at the end of the diet experiment. As expected, mice fed with either of the fat-rich diets exhibited increased fat mass when compared to mice fed with chow diet (figure 2, II). In addition, the total fat percentage of mice fed with ketogenic diet was higher than that of mice fed with the HF-60 diet (figure 14), which was in accord with previous studies (Nilsson *et al.,* 2016; Ahola-Erkkilä *et al.,* 2010). Interestingly, the presence of the AOX transgene had a systematic effect on the lean mass of the mice, i.e. all AOX mice, irrespective of the diet, had less lean mass when compared to wild-type mice fed on the same diet. This could indicate a possible influence of AOX expression on the energy expenditure of mice, although further investigation is required to understand precisely how AOX expression affects the lean mass. Except for lean mass, AOX did not affect any other body-composition parameters measured; fat mass, fat %, bone mineral density, bone content and bone area (figure 2 of paper (II)).

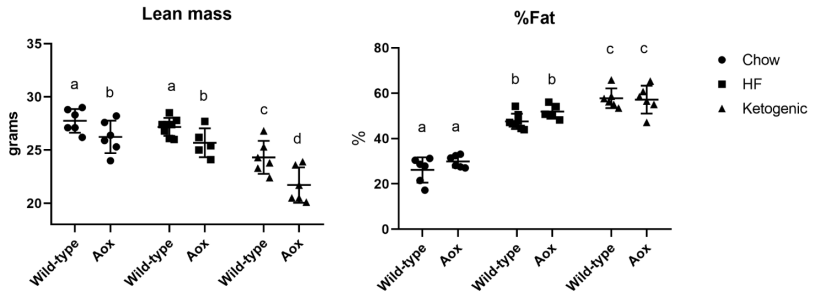

Figure 14: Dual-energy X-ray absorptiometry (DEXA) analysis of muscle mass (lean mass) and percentage of fat as indicated, on 48-week-old mice (n = 6 for all groups) of the indicated genotypes, fed on standard chow, high-fat (HF-60), or ketogenic diet as shown. Two-way ANOVA followed by Tukey's multiple comparison analysis, with lower-case letters denoting significantly different data groups in each panel. Figure reprinted from (II) under CC by 4.0 license.

5.2.3. Cardiac function

Previous studies have reported on cardiac dysfunction exhibited by mice exposed for a short period (4 weeks) to low carbohydrate, high fat (ketogenic-like) diets, proposed to be due to effects on energy metabolism from the altered amount of dietary fatty acids (Nilsson *et al.,* 2016). Fatty acids are an essential source of fuel for the myocardium, but fatty acid overload results in cardiac dysfunction (Nilsson *et al.,*

2016). This is proposed to be mainly due to the excess accumulation of metabolic intermediates affecting fatty acid oxidation, the TCA cycle and calcium signaling, which eventually impairs mitochondrial function. I set out to test (a) if prolonged exposure to ketogenic diet would induce a similar (or even more severe) cardiac phenotype and (b) if there is any interaction with AOX, which could be attributable, for example, to its enzymatic activation. To study this, I measured the cardiac ejection fraction in AOX mice and wild-type littermates using echocardiography, performed on 24 and 48-week old animals (16 and 40 weeks of ketogenic or standard chow diet exposure, respectively). At both time points, I observed a systematic though quantitatively modest difference with diet, where mice fed on ketogenic diet had a slightly lower ejection fraction compared to those fed on chow (figure 15).

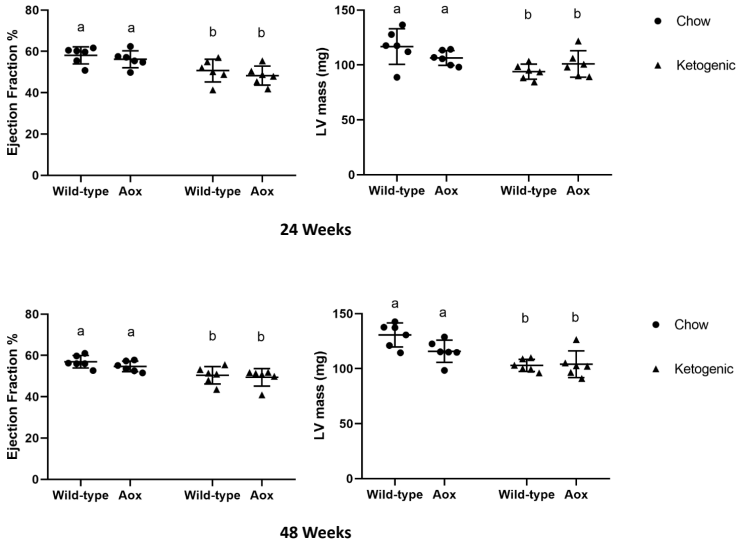

Figure 15: Echocardiographic assessment of the ejection fraction and left ventricular mass (LV mass) from 24- and 48-week-old mice (means ± SD, n = 6 for all groups) as shown. Difference in cardiac ejection fraction and LV mass was diet-dependent and not genotype-dependent. Two-way ANOVA, with lower-case letters denoting significantly different data classes in each panel. Figure reprinted from (II) under CC by 4.0 license.

However, AOX expression did not affect the cardiac phenotype of mice fed on ketogenic diet. The measured cardiac parameters also did not show the same degree of variation within groups, as I observed with total body weight. This implies that cardiac function is not directly affected by total body weight, but rather by the metabolic state of the myocardium as influenced by diet.

5.2.4. Gut microbiome

Changes in dietary composition has been shown to systematically alter gut microbial populations, which has been suggested to be correlated with changes in intestinal energy balance (Turnbaugh *et al.*, 2006; Wichmann *et al.,* 2013). To test for such an effect in our wild-type mice, and to assess whether AOX has any influence on the population of gut microbes, I studied the gut microbiome in collaboration with A.M. Lyyski, Dr. L. Paulin and Dr. P. Auvinen. Fecal samples were collected at the end of the study from the mice fed either with ketogenic (first experiment) or chow diet and were processed for DNA extraction, PCR and sequencing, using primers detailed in Materials and Methods (II). Samples from the HF-60 group were not collected since there was no significant difference in body weight between AOX and wild-type mice in this diet group. The pool of 16S rDNA sequences was then analyzed for differential abundance of microbial populations with respect to diet, body weight and genotype. In order to effectively study the effect of independent factors affecting the gut microbiome, the groups were separated; a) by diet alone, irrespective of genotype, b) based on weight, categorized into normal (median and below), over-weight (3rd quartile) and obese (4th quartile), and c) based on diet and genotype (figure 16). The results were as summarized below,

a) Comparing only the diets, chow *vs* ketogenic, the differences in microbial populations were significant across family, genus and taxonomic unit (OTU) classifications. This indicated a strong diet-dependent modification of the microbial population.
b) When compared between different weight categories, irrespective of genotype, the microbiome population was still different across all three classifications. Interestingly, there were clear differences between the normal weight group and both of the heavy weight groups (over-weight and obese) in the top 20 genera (figure 16B).
c) Between the genotypes (i.e. AOX *vs* wild-type), fed on ketogenic diet, there were no differences in the microbial populations at the level of families and genera but a few taxonomical units (OTU) were statistically significant. Considering only the genotype, irrespective of diets, there were a few significant differences at the genus and taxonomical unit (OTU) levels but the top 20 genera were not different (figure 16C).

A detailed list of all microbiome data is provided in supplementary tables S5 to S8 in (II).

In brief, AOX expression by itself only altered the population of a few microbial genera. Microbial populations were strongly correlated with diet and weight rather than genotype.

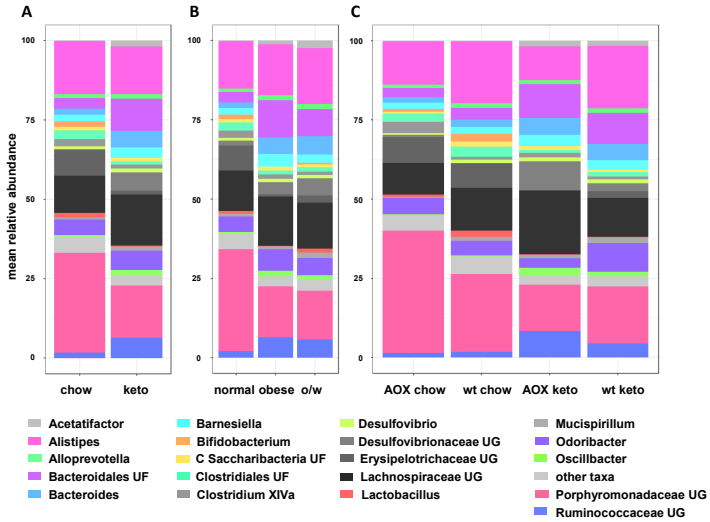

Figure 16: Distribution of top 20 gut microbial genera by abundance. (A) Comparing animals fed with chow versus ketogenic diet, (B) comparing different body weight groups by quartiles: normal weight (first two quartiles, <45.1 g, overweight (o/w, third quartile, 45.2 to 55.8 g) and obese (fourth quartile,> 55.8 g), (C) comparing animals by both genotype (wildtype, wt, or AOX-expressing) and diet. Taxa denoted by genus, or family: UF – unidentified family, UG – unidentified genus, C – candidate phylum. Figure reprinted from (II) under CC by 4.0 license.

In conclusion, I report in (II) that ubiquitously expressed AOX has only minor effects on the physiological changes induced by prolonged exposure to fat-rich diets. These findings can be interpreted in several different ways that are discussed in more detail in the next chapter. The most likely is that dietary stress induced by high-fat diets has no effect on mitochondrial complex III and/or IV, and therefore AOX remains unengaged. This has potential implications for the future use of AOX in therapy.

Based on the results from my first two studies, AOX mice do not exhibit any phenotypic difference from wildtype, whether under non-stressful conditions (I), nor even under the stress of extreme dietary modifications (II). These findings prompted me to combine AOX-expressing mice with other disease models that exhibit more severe forms of physiological disruption, including overt mitochondrial dysfunction. Firstly, I used a mouse model for inflammatory cardiomyopathy, where chronic infiltration of monocytes leads to cardiac failure. Secondly, I used a mouse model where mitochondrial cIV is removed by genetic manipulation in the cardiomyocytes, leading to cardiac failure and early lethality.

5.3 Effect of AOX expression in a mouse model for inflammatory cardiomyopathy

As discussed above (section 2.6), MCP1 overexpression in adult cardiomyocytes results in dose-dependent, lethal cardiac failure that has been suggested to involve ETC dysfunction and the consequent induction of excess mitochondrial ROS production in the respiratory chain. To test this idea, I combined Mcp1 mice with mice expressing AOX.

In order to exclude any strain-specific effects, I first backcrossed the Mcp1 mice (i.e. the mice overexpressing *Mcp1* specifically in adult cardiomyocytes), which were supplied originally on the FVB background, to the C57Bl6J/OlaHsd background for 8 generations, before setting up experimental crosses.

5.3.1. Survival phenotype

I observed that the Mcp1-C57Bl6J/OlaHsd mice exhibited early lethality at approximately 25 – 30 weeks of age (red line, figure 17), which was similar to mice homozygous for *Mcp1* overexpression in the FVB background (Kolattukudi *et al.,* 1998). The difference in survival also reflected the extent of cardiac dysfunction (figure 3B and 3C of paper (III)), analyzed by measuring the ejection fraction of mice by echocardiography. Interestingly, the cardiac ejection fraction of the Mcp1 mice was already compromised compared to wild-type littermates at 12 weeks of age and worsened as the mice aged. Note that only heterozygous Mcp1 mice were used for all my experiments, since they already manifest an early lethality phenotype. Although not studied, I assume that homozygous *Mcp1*-overexpressing mice in the C57Bl6/J background, would have suffered lethality at an earlier age than the heterozygous Mcp1 mice.

Although *Mcp1* is overexpressed only in the adult cardiomyocytes in the Mcp1 mice, there is a possibility that adaptations or maladaptations could occur in cell types other than cardiomyocytes, for example fibroblasts or macrophages, and these may also involve mitochondrial dysfunction. This could be an indirect result of cardiomyocyte loss, influencing the progression of contractile failure. In order to test this, I combined Mcp1 mice with ubiquitously AOX-expressing mice (AOX^{Rosa26}) as well as Cardio AOX mice, expressing AOX specifically in adult cardiomyocytes (figure 10). When crossed to mice expressing AOX constitutively, the timing of lethality of the Mcp1 mice did not

change (green line, figure 17). However, in combination with Cardio AOX, Mcp1 mice succumbed at a significantly earlier age, between 16-25 weeks (blue line, figure 17). Note that constitutive expression of Cre in adult cardiomyocytes also caused a lethal phenotype by itself (purple line, figure 17), but at a far later stage (after 35 weeks) and thus is judged not to have influenced the early lethality observed in Mcp1 + cardio AOX mice (blue line, figure 17) or any *Mcp1*-overexpressing mice. In order to maintain consistency in the read-outs, I used only male mice (n≥5 per group) for this analysis.

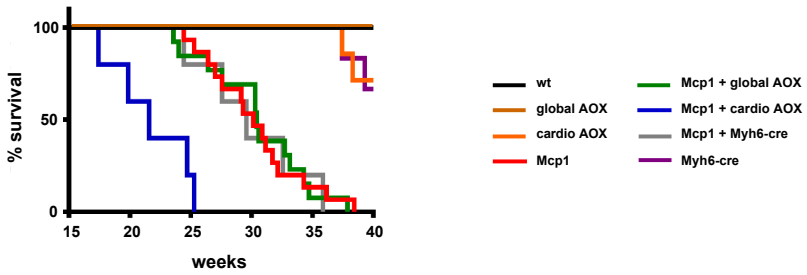

Figure 17: Effect of AOX expression on the survival of MCP1-overexpressing mice. Survival curves of mice of the indicated genotypes (wt – wild-type, Mcp1 – overexpressing Mcp1 in cardiomyocytes under the control of the Myh6 promoter; global AOX – expressing AOX constitutively; cardio AOX – expressing AOX specifically in cardiomyocytes, after activation of SNAPf-AOX by Myh6-cre, Myh6-cre – expressing only cre in adult cardiomyocytes, and combinations as shown, n ≥ 10 for all groups except those including Myh6-cre, where n ≥ 5). The survival curve for Mcp1 plus cardiomyocyte-specific AOX was significantly different from that of Mcp1 alone, or together with global AOX ($p < 0.0001$, Log-rank (Mantel-Cox) or Gehan-Breslow-Wilcoxon test). Figure reprinted from (III) under CC by 4.0 license.

5.3.2. Cardiac function

Echocardiographic analysis was done on males (n≥5 per group) at 4-weekly intervals from 12 weeks until 20 weeks of age. All mice undergoing the procedure were anesthetized using a constant supply of 4 % isoflurane gas for no more than 20 minutes in order to reduce any effect of isoflurane on the cardiac function. Ejection fraction (EF %), left ventricular diastolic volume (LV vol. diastolic) and left ventricular systolic volume (LV vol. systolic) were calculated from the images obtained and are represented as a measure of cardiac contractile function in the figures referred to below.

Assessment of cardiac function by echocardiography showed that the Mcp1 mice already suffered a moderate cardiac contractile dysfunction at 12 weeks of age (red squares, figure 18B), as mentioned above. The average ejection fraction of wild-type mice was 61 %, which is considered to be within the standard range for a healthy adult mouse (Lindsey *et al.,* 2018), whereas the ejection fraction of Mcp1 mice was

significantly lower, at 44 %. AOX expression, both ubiquitous and cardiomyocyte specific, modestly ameliorated the contractile dysfunction. The mean ejection fraction of Mcp1 mice with global (AOX^{Rosa26}) AOX expression was 53 % and with cardiomyocyte-specific (Cardio AOX) expression was 51 % (green and blue squares, respectively, figure 18B). Although not restored to the wild-type level, they were both significantly different from Mcp1 mice at 12 weeks.

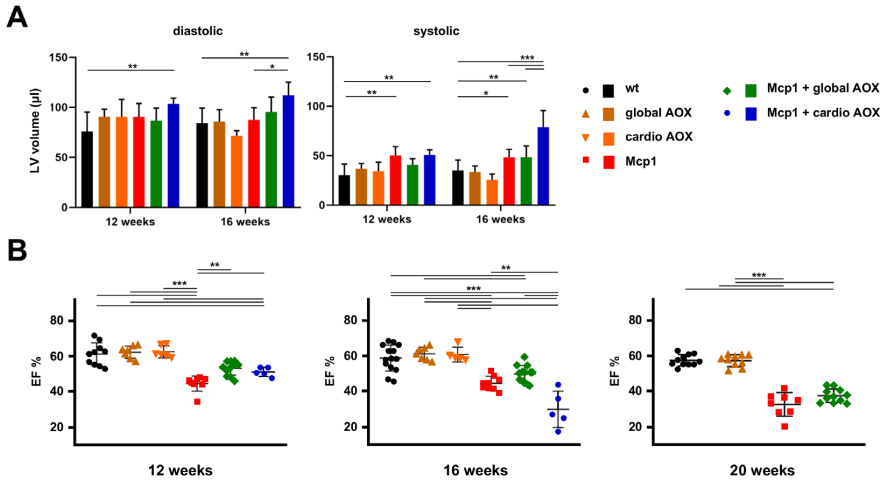

Figure 18: AOX expression preserves cardiac ejection fraction at early age. (A) Systolic and diastolic volume of the cardiac left ventricle (LV) of mice of the indicated genotypes, measured by ultrasound at 12 and 16 weeks, as indicated (means ± SD, n ≥ 5 for all groups). (B) Cardiac ejection fraction (EF %) computed for individual mice of the indicated genotypes and ages, means ± SD. Horizontal lines marked with asterisks indicate significant differences (one-way ANOVA within an age point, applying Tukey's post hoc HSD test; *, **, ***p < 0.05, 0.01, 0.001, respectively). Figure reprinted from (III) under CC by 4.0 license.

At 16 weeks of age, constitutive AOX expression no longer provided any benefit to Mcp1 mice, since the mean ejection fraction was similar to that of mice overexpressing *Mcp1* alone. However, at the same age, mice expressing cardiomyocyte-specific AOX had an exacerbated contractile dysfunction compared to the Mcp1 mice (figure 18B). The poor cardiac contractile function may be considered a reflection of the early lethality exhibited by Mcp1 + cardio AOX mice. Due to the low number of survivors at 20 weeks of age, this group was not included for echocardiographic measurement at that time point. At 20 weeks of age, both Mcp1 mice and Mcp1 + global AOX mice exhibited poor cardiac contractility compared to control mice, with mean ejection fraction (EF %) of 33 % and 38 %, respectively (figure 18B).

Mcp1 mice, at 12 weeks of age, had a significantly higher left ventricular systolic volume (red bar, figure 18A) when compared to wild-type mice, indicating that the low EF % was due to the poor contractility of the left ventricle. Mcp1 + cardio AOX mice, at this age, had a higher diastolic and systolic volume (blue bar, figure 18A), which was significantly different from wild-type mice but the ratio of diastolic to systolic volume was better than Mcp1 mice and thus gave a better EF %. At 16 weeks of age, all *Mcp1*-overexpressing mice, irrespective of AOX expression, had poor cardiac contractility as indicated by higher systolic volume (figure 18A). In addition, the left ventricular mass was not different between the groups, measured at 12 and 16 weeks of age (figure S2A, III).

5.3.3. Physical parameters

To test whether the cardiac contractile dysfunction, although only moderate at the early time points, would affect the physical performance of mice, I measured their endurance using a treadmill designed for rodents. This experiment was conducted later in the project and due to the lack of availability of cardio AOX mice they were not included in the experiment. The treadmill experiment performed at ages 12 and 16 weeks showed no clear difference between *Mcp1*-overexpressing mice and controls, irrespective of AOX expression (figure S2C of paper (III)). In addition, their body weights were also indistinguishable from those of controls (figure S2B of paper (III)).

5.3.4. Molecular parameters

In order to investigate the underlying molecular mechanism of the cardiac phenotype induced by *Mcp1* overexpression, and the impact of AOX expression thereon, I performed molecular analysis on the left ventricle of these mice. Since AOX expression, both global and adult cardiomyocyte specific, showed improvement in the cardiac function in Mcp1 mice at 12 weeks of age, I performed most of the molecular analysis at this time point.

a) Ultrastructural assessment

In a previous study, mitochondrial structural changes and disorganization of myofibrils in the cardiac tissue of the Mcp1 mouse model has been reported (Niu *et al.,* 2009). Assuming these observations were made when the mice had already developed a measurable cardiac phenotype and given the fact that Mcp1 mice acquired a moderate cardiac dysfunction in my study (figure 18) at a very young age, I wanted to check if there were any ultrastructural changes in Mcp1 mice at 12 weeks of age, and if AOX expression affected it. I collaborated with Dr. U. Gärtner from University of Giessen, who performed the electron microscopy imaging (detailed information on the embedding and sectioning is provided in (III)). In order to maintain uniformity, I collected a piece of tissue from the same region of the left ventricle of the various mice studied, 3 per group. Note, for this experiment, the groups included mice of both sexes.

From my analysis of the images, obtained from 2-3 different sections of left ventricular tissue, disoriented myofibrils were not visible in Mcp1 mice at this age (12 weeks). However, several dense structures containing mitochondria, putatively mitophagosomes or autophagosomes, were clearly visible in Mcp1 mice (figure 19A). There were almost none of these dense structures visible in Mcp1 + global AOX mice. A proper quantification of these dense structures or mitochondrial size/cristae count would ideally include the examination of several more regions, which would be labor intensive and time consuming, but might eventually yield additional insights. For this reason, I did not follow up this approach. In addition, at 12 weeks of age, both Mcp1 + global AOX and Mcp1 + cardio AOX mice exhibited similar cardiac function and so I did not anticipate a major difference between them at the ultrastructural level and thus omitted Mcp1 + cardio AOX mice from ultrastructural analysis.

b) Mitochondrial respiration analysis

To investigate whether the presence of putative mitophagosomes were a reflection of mitochondrial dysfunction, I measured the respiratory capacity of isolated mitochondria from the left ventricle of male mice (n≥3 per group) aged 12 and 16 weeks. I observed a clear decrease in cI- and cII-mediated respiration in heart mitochondria from Mcp1 mice compared with controls at 12 weeks of age (figure 19B). At this age, heart mitochondria from Mcp1 + global AOX mice did not show any significant improvement in cI-mediated respiration but did exhibit better preserved cII-

mediated respiration. Heart mitochondria from Mcp1 + cardio AOX mice at 12 weeks of age showed a similar trend in cII-mediated respiration compared with the Mcp1 mice, although this did not reach statistical significance.

Analysis of heart mitochondria from Mcp1 and Mcp1 + global AOX mice at 16 weeks of age exhibited a very similar pattern of mitochondrial respiration, whereas cI-mediated respiration was significantly lower in both these groups compared with wild-type mice. However, at this age, the cII-mediated respiration was still better preserved in Mcp1 + global AOX mice when compared with Mcp1 mice (figure 19B).

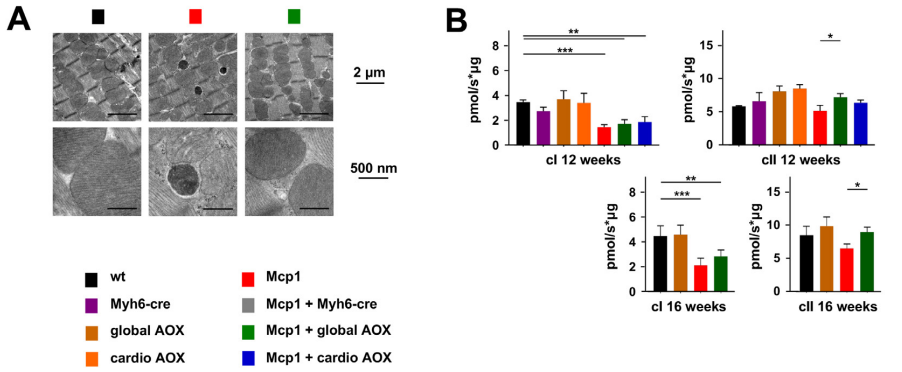

Figure 19: Effect of AOX on mitochondrial structure and respiration. (A) Transmission electron micrographs of cardiac left ventricle from 12-week old animals of the indicated genotypes and treatments. Scale bars as indicated: lower images represent higher magnification of portions of those shown in the top line. The dark inclusions in close proximity to mitochondria, seen in cardiomyocytes from the Mcp1-overexpressing mice, are interpreted as secondary lysosomes. >12 such sections were analysed from mice of each genotype (2–3 sections from each of 2 blocks from 3 individuals). Multiple such inclusions were seen in the sections from Mcp1 mice, but not from controls or from mice expressing global AOX. Note also the less densely packed cristae in mitochondria from the Mcp1-overexressing mice, which was evident in all sections analysed. (B) Respirometry of mitochondrial suspensions from heart tissue of mice of the indicated genotypes, driven by cI- (pyruvate, glutamate and malate in the presence of ADP) or cII-linked (succinate in the presence of rotenone) substrates as shown. Figure reprinted from (III) under CC by 4.0 license.

c) Protein expression analysis

To test whether the compromised mitochondrial respiration reflects a loss of mitochondrial OXPHOS complexes, I studied the protein expression levels of representative subunits of each OXPHOS complex, using the commercially available OXPHOS antibody cocktail, and other mitochondrial markers using tissue lysates from the left ventricle of 12-week old male mice (n=5 per group). Western blots showed that several subunits, notably of cI and cIII, were mildly decreased in all groups of *Mcp1*-overexpressing mice, irrespective of AOX expression, when

compared to wild-type (figure 5C of paper (III)). However, quantification of these bands by densitometry found that these differences were not statistically significant in most cases (figure S3A, III) except for subunit ATP5A of cV, which was significantly lower in Mcp1 + global AOX and Mcp1 + cardio AOX when compared to wild-type controls (figure S3A of paper (III)).

In addition, I did not observe any significant difference in the level of the mitochondrial outer-membrane protein, porin, in all *Mcp1*-overexpressing mice when compared to wild-type (figure 5C and S3A of paper (III)). This implies that there is no severe loss of mitochondria in the left ventricle of Mcp1 mice at 12 weeks of age.

Interestingly, the levels of GAPDH, a glycolytic enzyme, were significantly higher in all *Mcp1*-overexpressing mice when compared to wild-type (figure 5C and S3A of paper (III)), indicating a possible increase in the capacity of the glycolytic pathway in these mice.

Western blot analysis of the left ventricle of 16 week old mice showed a similar trend for the respiratory chain subunits and for GAPDH (figure S3B of paper (III)) between all *Mcp1*-overexpressing mice and controls.

d) RNA expression analysis

To further investigate the changes in gene expression, I performed RT-qPCR analysis on the left ventricle of 12-week old mice (males, n=5 per group). My analysis provided evidence of various kinds of stress signaling and consequent tissue remodeling (figure 20), as follows:

I. mRNA for the immunomodulatory cytokine IL10 was increased, consistent with an inflammatory state
II. markers for mitochondrial stress, Fgf21 and Gdf15 were elevated, strongly indicating mitochondrial dysfunction
III. a switch towards a fetal-like gene expression pattern was detected, where beta myosin heavy chain (*Myh7*) and *Gata4* mRNAs were upregulated and that for alpha myosin heavy chain (*Myh6*) downregulated, consistent with the initiation of cardiac remodeling.

In addition, contradicting my initial hypothesis that oxidative stress observed in Mcp1 mice could emanate from mitochondria due to respiratory dysfunction, RNA for Sod2, a mitochondrial ROS detoxifying enzyme, was downregulated. When combined with AOX, whether global or cardio, the altered expression levels of all of these markers was not significantly different from that in the hearts of Mcp1 mice without AOX (figure 20).

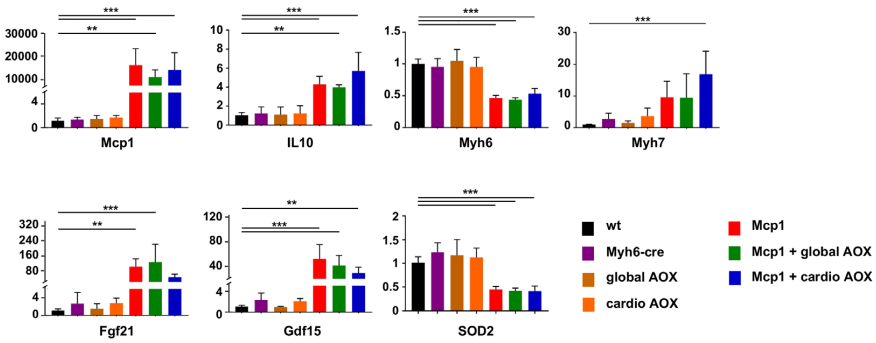

Figure 20: Effect on mRNA expression resulting from overexpression of *Mcp1* and AOX. RT-qPCR analysis of levels of the indicated RNAs in cardiac left ventricle of 12-week old mice of the genotypes shown, in each case normalized to the value for wild-type (means ± SD, n = 5 for each genotype). Horizontal lines marked with asterisks indicate significant differences between wild-type and other groups (one-way ANOVA with Tukey post hoc HSD test; **, ***p < 0.01, 0.001, respectively). Figure reprinted from (III) under CC by 4.0 license.

e) Reduced Q pool measurement

Results from all the experiments mentioned above indicate a clear cardiac phenotype induced by *Mcp1*-overexpression already at 12 weeks of age. Interestingly, the cardiac function and mitochondrial cII-mediated respiration of mice overexpressing both *Mcp1* and AOX were significantly different from mice overexpressing *Mcp1* only. These data suggest that the physiological and molecular differences observed in Mcp1 + global AOX and Mcp1 + cardio AOX mice, in comparison to Mcp1 mice at 12 weeks, were due to the activation of AOX. However, this activation, i.e. participation of AOX in respiratory electron flow, requires certain specific conditions in the mitochondria, in particular the accumulation of the CoQ electron carrier in the reduced form (ubiquinol) above a certain threshold, which is approximately a ratio of 0.4 to the oxidized form (Dry *et al.,* 1989, Dogan *et al.,* 2018).

To test if the compromised respiratory capacity observed in Mcp1 mice favored conditions that were sufficient for AOX activation, I studied the CoQ levels in the left

ventricle of 12-week old mice, in collaboration with Dr. G. Brea-Calvo, who performed the quinone measurements. The ratio of the reduced to the oxidized form of CoQ_9, which is the most abundant quinone in mice, was higher than in wild-type mice but did not reach the optimal level for AOX activation, i.e. 0.4 or above (figure S3C of paper (III)). However, the reduced form of CoQ_{10} significantly accumulated in Mcp1 compared to wild-type mice. Surprisingly, global AOX expression did not decrease the proportion of reduced CoQ_{10} in Mcp1 mice, but cardio AOX did, almost to the levels of wild-type mice (figure 5D of paper (III)).

f) Global metabolomic analysis

To investigate the impact of the above-mentioned changes upon global metabolism, I collaborated with the metabolomics core facility in the University of California, Los Angeles (UCLA) to perform a metabolomic flux analysis on 12-week old mice of the different genotypes. Three mice per group, mixed sexes, were administered $^{13}C_6$ glucose intraperitoneally before sacrificing by cervical dislocation and harvesting the left ventricle. The control groups were administered $^{12}C_6$ glucose before sacrifice and tissue harvest. Administration of glucose and tissue harvesting were done by myself, whereas metabolomic flux analysis was performed on the tissue extracts by the UCLA metabolomics unit. From Principal Component Analysis (PCA) of the labeled metabolites, it was clear that Mcp1 mice grouped separately from the control mice (green points, figure 6 of paper (III)). Mcp1 + global AOX mice clustered along with Mcp1 mice (red points, figure 6 of paper (III)) but Mcp1 + cardio AOX mice formed a separate group from the rest (blue points, figure 6 of paper (III)). The clear difference between Mcp1 + cardio AOX mice and Mcp1 + global AOX mice at the metabolomic level correlates with the rapid progression of cardiac contractile dysfunction in Mcp1 + cardio AOX mice at 16 weeks of age and early lethality when compared to Mcp1 + global AOX mice.

Taken together, these results support previously published data pointing towards adverse cardiac remodeling induced by *Mcp1* overexpression, with AOX expression providing only a transient protection against this process. However, cardiomyocyte-specific AOX expression proved to be detrimental to the Mcp1 mice. Possible reasons for these apparently contradictory findings are discussed in chapter 6.

5.4 Effect of AOX expression in a mouse cardiomyopathy model with mitochondrial complex IV dysfunction

To study the impact of AOX expression in a phenotypically more severe cardiomyopathy model where the mitochondrial respiratory system is directly affected, I used $Cox10^{fl/fl}$ mice (Diaz *et al.,* 2005), where exon 6 of the *Cox10* gene is floxed. COX10 is essential for the biosynthesis of heme a, the active core of mitochondrial cIV. Therefore, lack of the enzyme should prevent the biosynthesis of active cIV, thus blocking respiratory electron flow at the final step. A previous study (Dassa *et al.*, 2009) reported that COX deficiency induced by *COX10* knockdown in human fibroblasts could be complemented by *Ciona* AOX expression. To test if this would work in heart *in vivo*, i.e. at the whole organism level, I used genetic crosses to combine the $SNAP\text{-}AOX^{Rosa26}$ mice with $Cox10^{fl/fl}$ and the adult cardiomyocyte-specific Cre driver used in the MCP1 experiments described above, *Myh6-Cre*. A detailed list of the crossing scheme and progeny is provided in table S5 of paper (III).

To test if *Cox10* KO in the adult cardiomyocytes would cause a phenotype in mice, I made the crosses described below:

$$Cox10^{(fl/wt)} \text{ X } Cox10^{(fl/wt)}; tg^{(Myh6\text{-}Cre/wt)}$$

and

$$Cox10^{(fl/fl)} \text{ X } Cox10^{(fl/wt)}; tg^{(Myh6\text{-}Cre/wt)}$$

From my initial assessment, *Cox10* KO in adult-cardiomyocytes caused early lethality (pink line, figure 21A) in mice where the maximum survival was 21 days post-natally, i.e. before weaning.

To test if AOX expression in these mice would affect the phenotype, I made crosses to generate *Cox10* KO mice also expressing AOX, as described below:

$$Cox10^{(fl/fl)} \text{ X } Cox10^{(fl/wt)}; Aox^{(+/wt)}; tg^{(Myh6\text{-}Cre/wt)}$$

In the above mentioned cross, $Aox^{(+/wt)}$ describes heterozygous $SNAP\text{-}AOX^{Rosa26}$ mice. Mice positive for AOX expression and lacking COX10 in adult-cardiomyocytes did not show any difference in survival or phenotype (turquoise green, figure 21A) when compared to *Cox10* KO mice. This is in contrast to previous findings on cell models.

Surprisingly, from my qualitative assessments of embryos and newborn pups, no *Cox10* KO mice, irrespective of AOX expression, showed any distinguishable morphology or developmental delay compared to the controls. This indicates that the total loss of COX10 does not affect development, but results in a sudden and rapid onset of lethality in mice once born.

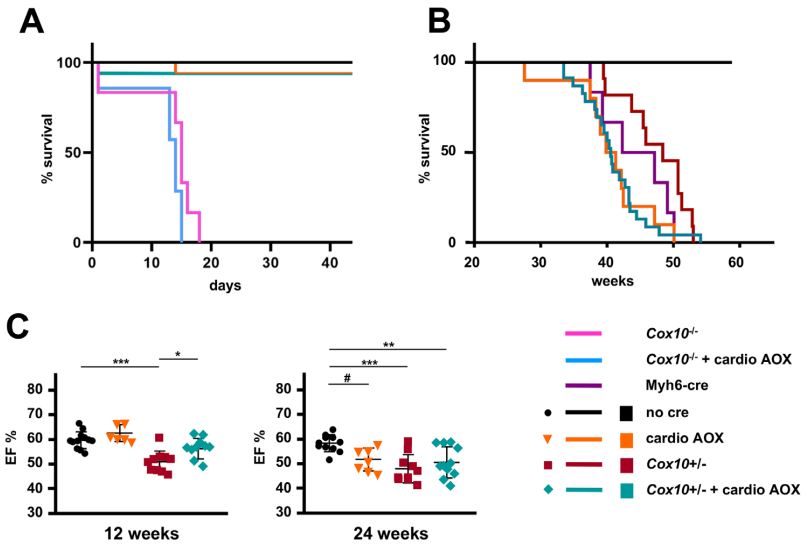

Figure 21: AOX did not have a major effect on the phenotype induced by Cox10 knockout in cardiomyocytes. (A,B) Survival curves of mice of the indicated genotypes: $Cox10^{-/-}$ – cardiomyocyte-specific knockout of Cox10, i.e. mice were $Cox10^{fl/fl}$ plus Myh6-$cre^{+/-}$; $Cox10^{-/-}$ + cardio AOX – cardiomyocyte-specific knockout of Cox10 plus activation of SNAPf-AOX by Myh6-cre (both heterozygous); Myh6-cre – Myh6-$cre^{+/-}$ only, no cre – control mice lacking Myh6-cre, cardio AOX – cardiomyocyte-specific activation of SNAPf-AOX by Myh6-cre, both hemizygous; $Cox10^{+/-}$ – cardiomyocyte-specific heterozygous knockout of Cox10, i.e. mice were $Cox10^{+/fl}$ and Myh6-$cre^{+/-}$; $Cox10^{+/-}$ + cardio AOX – cardiomyocyte-specific heterozygous knockout of Cox10, i.e. mice were $Cox10^{+/fl}$ and heterozygous for both Myh6-cre and SNAPf-AOX. n ≥ 6 for all groups. (C) Cardiac ejection fraction (EF %) computed for individual mice of the indicated genotypes and ages, means ± SD, by echocardiography. Horizontal lines marked with asterisks indicate significant differences (one-way ANOVA within an age point, applying Tukey's post hoc HSD test; *, **, ***$p < 0.05, 0.01, 0.001$, respectively). Figure reprinted from (III) CC by 4.0 license.

On the other hand, heterozygous knockout of *Cox10* in adult cardiomyocytes did not cause a severe phenotype, such as seen in the homozygous knockout mice. These mice seemed indistinguishable from control mice, and did not show any behavioral phenotype. However, they did suffer a mild but statistically significant cardiac contractile dysfunction at 12 weeks of age (figure 21C). Mice expressing AOX in the *Cox10* heterozygous knockout background manifested slightly better cardiac function, represented by cardiac ejection fraction, than the heterozygous *Cox10* knockout mice (figure 21C).

Long-term evaluation of these mice was not possible as the chronic expression of Cre in cardiomyocytes by itself was cardiotoxic, as has been reported previously (Pugach *et al.,* 2015), resulting in cardiac dysfunction and lethality in all mice expressing *Myh6-Cre* (figure 21B) with a mean survival of about 45 weeks. The effect of Cre expression on cardiac function was already visible at 24 weeks of age and so we discounted any difference observed in cardiac ejection fraction from this time point on.

Since the effect of Cre expression was observed only from age 24 weeks, it is unlikely that the early lethality phenotype observed in *Cox10* KO mice was due to Cre expression. Instead, I propose that the the early lethality phenotype was caused solely by the lack of COX10 in the adult-cardiomyocytes, although an interaction between the two genetic manipulations in combination cannot be excluded.

In conclusion, from this study I report that;

a) cardiomyocyte-specific knockout of *Cox10* causes early lethality in mice.

b) heterozygous knockout of *Cox10* does not cause a severe phenotype in mice, although a mild cardiac contractile dysfunction is observed at 12 weeks of age.

c) AOX expression was neither beneficial nor detrimental in *Cox10*-deficient mice.

6. Discussion

Since the ancient time of endosymbiosis, mitochondria have evolved into an integral part of the eukaryotic cell contributing to and coordinating cellular homeostasis *via* its multiple functions. Due to the tightly interconnected metabolic pathways operating in mitochondria, i.e. the products of one pathway being the substrate or co-regulators of others, fluctuations in one pathway often induce a negative (or positive) feedback on others. This can result in a disturbed metabolic homeostasis. Such dysfunction has been shown to be particularly detrimental for cells that are heavily dependent on mitochondria for energy, e.g. cardiomyocytes (reviewed by Lopaschuk *et al.,* 2010; Lesnefsky *et al.,* 2016; Hoppel *et al.,* 2017). Under physiological conditions, mitochondrial function in the cardiomyocytes is maintained to match the energy demand by regulating mitochondrial biogenesis and dynamics. For example, disruption of the fission/fusion machinery has been shown to be detrimental to the cell (Chen *et al.,* 2011, reviewed by Ong *et al.,* 2013, Piquereau *et al.,* 2013 and Vasquez-Trincado *et al.,* 2015). In chronic conditions of mitochondrial dysfunction, accumulation of these stresses increases the possibility of cell death and tissue damage (reviewed by Rosca *et al.*, 2014).

Defects in the OXPHOS system not only compromise net ATP produced by mitochondria but can also impair flux in metabolic pathways, cause excess production of ROS and dysregulate cell signaling, thereby affecting cellular function at multiple levels. For example, a defective ETC could result in the release of cytochrome *c* into the cytosol, triggering apoptosis (Liu *et al.,* 1996, reviewed by Cai *et al.,* 1998). Basal amounts of ROS are required for cellular function (Owusu-Ansah *et al.,* 2009, Tormos *et al.,* 2011). However, when accumulated in larger quantities, they produce detrimental effects by targeting other molecules and by signaling the induction of autophagy (reviewed by Zhang *et al.*, 2007; Schieber *et al.,* 2014).

The cell-type specificity of these defects, plus the variable heteroplasmic load of defective mitochondria, are some of the major factors responsible for the wide variation in age of onset and severity of clinical symptoms in mitochondrial disorders (Khan *et al.,* 2015). The complexity of mitochondrial diseases and the overlapping nature of clinical presentations has made early diagnosis and treatment highly problematic. With advances in molecular tools and techniques in the past decades, several research models have been generated to investigate the underlying

molecular mechanism of complex mitochondrial diseases (reviewed by Wallace, 2001; 2002; Rudolph *et al.,* 2016).

In this doctoral thesis project, I used such a model where *Ciona* AOX was genetically engineered for expression in mice. This has allowed me to study the impact of OXPHOS dysfunction under dietary stress and in animal models of heart failure.

6.1. Impact of AOX expression in mice

Despite its presence in phyla composed of slow-moving and sessile organisms, among the metazoans, the reason for the evolutionary loss of AOX in vertebrates and insects is not understood. Changes in environmental conditions, for example, a decrease in atmospheric sulfide levels (Weaver, 2019), or gene loss events in an environment where AOX provided no reproductive or survival advantage (McDonald *et al.,* 2009) have been previously postulated to account for this evolutionary loss. In addition, transgenic flies expressing AOX showed a modest developmental delay, as well as weight loss in young adult flies, indicating a possible interference by AOX in the efficiency of catabolism (Fernandez-Ayala *et al.,* 2009). Such an effect, although minor, could have a cumulative and detrimental impact with age. Although AOX does not interfere with the standard ETC under conditions that are favorable for its enzymatic activity, it will result in less ATP production when compared to the standard pathway, provided a portion – even a small one – of the respiratory electron flow from cI is diverted into it. Such a diversion would be detrimental for cells with high energy demand, e.g. cardiomyocytes. Such a phenomenon might underlie the loss of AOX in higher, motile animals during evolution. However, the potential benefits of AOX-mediated respiration in diseases where the cytochrome pathway is defective has inspired its investigation as a therapeutic option.

Safe and stable expression of transgenic AOX in mice was first reported by El-Khoury et al., (2013). However, the use of lentiviral transduction resulted in multiple integrations of the AOX coding sequence. Although the founder mice and first offspring showed strong and stable expression of AOX, the gene expression levels and patterns became irregular in succeeding generations (personal communication from prof. Pierre Rustin and Dr. El-Khoury), making it impossible, on a practical level, to maintain the mouse line and combine it with other disease models. Thus, a genetically tractable mouse with a single integration of the AOX coding sequence was later generated to make efficient use of AOX mice (I). The characterization of this

model was the starting point for the work described in this thesis. I went on to characterize, in addition, a second model, in which the AOX transgene was conditionally activatable by the removal of a floxed cassette carrying the SNAP coding sequence (section 2.8 and (III)). This second model was mostly studied in combination with the Myh6-cre driver, activating AOX expression in adult cardiomyocytes. The activation of AOX expression specifically in the heart (figure 10), serves as a validation for the use of the second model in combination with mice expressing Cre in diverse tissue-specific patterns, so as to restrict AOX expression accordingly.

Transgenic AOX mouse models, both ubiquitous and cardiac expressing (I) and with expression specifically in adult cardiomyocytes (III), did not show any detrimental phenotype under normal physiological conditions. Multiple lines of evidence from my observations support this conclusion, as described below.

a) If AOX was enzymatically active, the OXPHOS pathway should be affected thereby affecting metabolic homeostasis in diverse ways. However, metabolite analysis of heart (figure S2H of paper (I)) and muscle tissue (figure 22) showed no difference between wildtype and transgenic AOX mice. It is a very relevant finding since several studies have shown evidence for metabolic disturbances, especially involving lipid and carbohydrate metabolism, due to mitochondrial respiratory defects (Hansson *et al.,* 2004, Deepa *et al.,* 2018, Rajendran *et al.,* 2019). Although this measurement was done only once and on young mice (Aox^{Rosa26} – males, 8-weeks-old and SNAP-AOX^{Rosa26} – males and females, 12-weeks-old), the results indicate a lack of impact of AOX on the overall metabolism of mice in this age range. In addition, in a different study conducted by Rajendran *et al.* (2019), AOX expression was shown not to alter the metabolite levels in the heart, liver and kidneys of 150-day-old mice. This is also reflected in other parameters measured, including total body weight, fat content, muscle mass, bone composition and blood metabolites of mice at various measured time points (figure 13, 14, 15 and 22). Taken together, these results show that AOX does not affect the metabolic homeostasis in young adult mice.

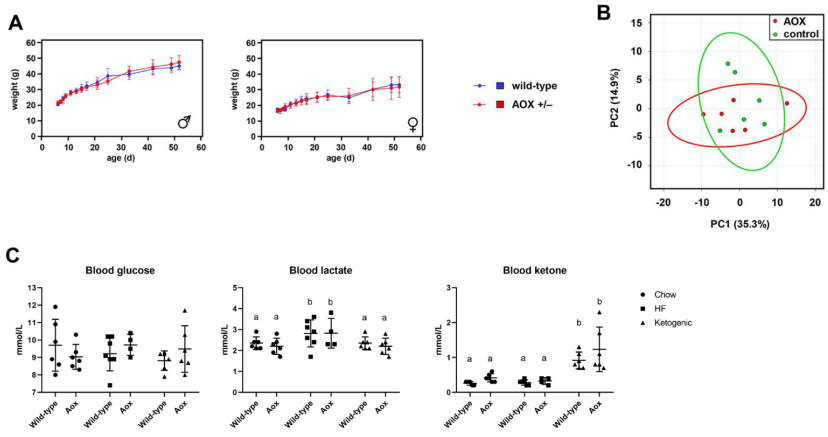

Figure 22: AOX expression does not affect the normal physiology of mice. (A) Total body weight (mean ±s.d.) of hemizygous AOX^{Rosa26} (AOX +/-) and wild-type mice of the sexes and time (weeks of age) indicated, n≥8 for each sex and genotype analyzed. (B) Principal component analysis of metabolome data from skeletal muscle of hemizygous AOX^{Rosa26} (red circles) and wild-type littermate control mice (green circles; n=6 for both groups. (C) Glucose, lactate and ketone-body concentrations measured from 48-week-old mouse tail-vein blood (n≥4) of the indicated genotypes, fed on standard chow, high fat (HF) or ketogenic diet as indicated. Statistical analysis was performed using Student's t-test for (A) and Two-way ANOVA for (C), revealed no difference between genotypes. Figure reprinted from (I) and (II) under CC by 4.0 license.

b) Branching the ETC by the introduction of AOX should result in less ATP production due to the decreased contribution of electron flow from the two proton-pumping complexes, cIII and cIV. This should have a more noticeable impact on tissues with higher energy demand, like the heart. The cardiac ejection fraction showed no difference between wild-type mice and transgenic AOX mice under normal physiological conditions (figure 11, 15 and 18). The implication is that AOX does not contribute substantially to electron flow under these conditions.

c) The rates of respiration of isolated mitochondria from different tissues were nearly identical between wild-type and transgenic AOX mice, unless treated with a cIII inhibitor, antimycin A or cIV inhibitors, such as cyanide or azide, for which AOX conferred robust resistance in all tissues except adult brain (figure 11 and 19). If AOX was constitutively active enzymatically, the maximum coupled respiration rate of isolated mitochondria should have been significantly different in tissues from the transgenic mice. The finding of unchanged respiration *in vitro* was also supported by a lack of difference in the expression levels of subunits of the endogenous respiratory complexes in transgenic mice, based on the idea that compromised functional activity of cIII

and cIV might be expected to have had a negative (or positive) feedback on the expression levels of their subunits (figure 9; figure 5C of paper (III)). However, I only measured the expression of one subunit representing each OXPHOS complex. The observation should therefore be considered as indicative rather than conclusive. A more comprehensive study could be undertaken to settle the issue.

d) Additionally, AOX expression by itself did not cause lethality or any other gross phenotype in mice during the observed time period (figure 17). Furthermore, the extensive phenotyping performed by GMC showed no major differences between wild-type and transgenic AOX mice.

These various observations indicate that the overall impact of AOX expression is phenotypically undetectable at the whole-organism level, under normal physiological conditions. Thus, AOX can be considered to be functionally inactive in mice under non-stressed and moderately stressed conditions, unless interfered with by cytochrome-targeted toxins, such as antimycin A or cyanide. Even under moderate stress, conferred, for example, by treadmill running (I) or fat-rich diets (II), (discussed further in the next section), I was unable to demonstrate any convincing phenotypic deviation from wild-type. This inference also supports previous observations in human cell-culture models, fruit flies and lentivirally transduced mice (Hakkart *et al.,* 2006; Fernandez-Ayala *et al.,* 2009; El-Khoury *et al.,* 2013). However, all of the measurements in mice, excluding those related to the heart, but including the extensive phenotyping by the GMC, were not repeated. It is also worth noting that the GMC phenotyping tests were conducted on young mice, and at a single age point. A more extensive future study could reveal accumulated effects of AOX expression over time, where minor variations could eventually be revealed. To resolve this question, a longitudinal measurement of at least the major parameters needs to be implemented over the lifetime of the animal. Note, however, that such an experimental set-up might be ethically challenging, considering the 3R principle for animal experiments. The 3R principle, representing replacement, reduction and refinement (Russel *et al.,* 1959) guides researchers in planning and conducting animal experiments. Its major focus, as it says, is to replace animals with other study models; to avoid excess use of animals; and to treat them as humanely as possible. Additionally, such a longitudinal measurement may also not be particularly informative, unless AOX is to be developed as a therapy to treat chronic diseases

that result from the cumulative effects of minor defects over time, involving either persistent stress or natural aging.

6.1.1. Effect of long-term exposure to fat-rich diets

Long-term exposure of mice to fat-rich diets, both HF-60 and ketogenic, resulted in body weight gain, increased fat mass, reduced bone mineral density and increased bone area. AOX-expressing mice showed a reduced body weight gain compared to the wild-type mice under ketogenic diet, however, the difference reversed when they were caged individually, as discussed below. Additionally, AOX expression also had a minor effect on the lean mass of the mice, in a diet-independent manner, and moderately altered the gut microbiota of both control- and ketogenic diet-fed mice. Except for these parameters, AOX expression did not affect any other parameter measured, including cardiac ejection fraction measured on mice fed with ketogenic diet.

Long-term exposure of mice to high-fat diets induces a condition of chronic stress resulting in excessive weight gain, hyperglycemia, insulin resistance and altered cardiac parameters (Calligaris *et al.,* 2013), leading to overt cardiac dysfunction (Che *et al.,* 2018). Since mitochondria play a major role in the metabolism of carbon macronutrients, i.e. carbohydrates and fatty acids, the metabolic syndrome induced by long-term exposure to high-fat diets has been shown to produce specific effects on mitochondrial function and to result in increased mitochondrial H_2O_2 production (Anderson *et al.,* 2019; review by Putti *et al.,* 2015). Additionally, several independent studies have reported on the detrimental effect of high-fat diets on mitochondrial function (Sparks *et al.,* 2005, Cormier *et al.,* 2019, Jha *et al.,* 2019, Xu *et al.,* 2019). On the contrary, previous studies have also reported on the beneficial effects of ketogenic diet on a patient with Alpers–Huttenlocher syndrome (Santra *et al.,* 2004) and a mouse model for mutated mitochondrial helicase TWINKLE (Deletor mouse; Ahola *et al.,* 2010). However, efforts of using modified atkins diet to treat patients with mitochondrial myopathy (Ahola *et al.,* 2016) proved to be detrimental, since the diet-induced ketosis in patients, resulting in progressive muscle damage due to the already impaired mitochondrial respiratory chain activity (Ahola *et al.,* 2016). Such conditions might be predicted to result in the engagement of AOX if, for example, a defective or overloaded ETC was part of the mechanism producing these effects. However, from my observations (II), fat-rich diet-induced phenotypes were almost

identical between wild-type mice and transgenic AOX mice. Small differences in body weight between AOX and wild-type mice under ketogenic diet were observed in an initial experiment, where transgenic AOX mice weighed slightly less compared to wild-type mice, possibly indicating an effect possibly attributable to AOX activation. This difference is similar to the observation in *Drosophila* (Fernandez-Ayala et al. 2009), where AOX expression resulted in a slight decrease in the body weight of young flies, except that, in this case, the flies were maintained on a standard laboratory diet. As in flies, the observed weight differences in mice could reflect an alteration in overall catabolism, resulting from at least a partial activation of AOX. This implication is also suggested by the systematic decrease in lean mass, measured at the end of the study, associated with AOX expression in all diet groups tested (figure 14).

The huge variation in body weight within the diet groups disappeared in a follow-up experiment, in which the mice were individually caged. Moreover, the difference between the genotype groups in mean weight was in the opposite direction than in the first experiment, with transgenic AOX mice now slightly heavier than control mice. These observations suggest that differences in social interaction among mice can influence other relevant aspects of their behavior, including food consumption and activity, ultimately affecting their energy expenditure. My observation is consistent with previous reports where environmental factors such as, caging conditions, noise levels, animal handling have been shown to cause stress and abnormal behavior in rodents (Brown & Grunberg, 1996, Neely *et al.,* 2018, reviewed by Sundberg & Schofield, 2018). If the small difference in weight gain between the genotype groups in the second diet experiment were indeed due to the activity of AOX, a causal relationship may be hypothesized between AOX activation and diet composition (or physical activity). However, *in vivo* measurement of AOX activity is not yet possible, and assays *in vitro* would be uninformative, since the exact metabolic conditions during exercise *in vivo* are not straightforward to simulate. AOX from other organisms can be activated by organic acids, including pyruvate (Millar *et al.,* 1993), although this has not been established for the metazoan enzyme. Thus, the effects of diet on AOX activation remain to be studied.

It should be noted that the activity of AOX can only complement defects of cIII or cIV, under conditions where ubiquinone in the reduced form has accumulated beyond the capacity of the cytochrome pathway to metabolize it (Dry *et al.,* 1989, Dogan *et al.,* 2018). In steady-state conditions metabolic rate should match energy demand: but

chronic exposure to fat-rich diets may affect this metabolic balance due to increased availability of substrates. In such situations, substrate uptake may exceed the rate of catabolism, leading to accumulation of metabolic intermediates, including NADH and $FADH_2$, which would not have formed under steady-state levels. Such an overload could directly affect reduction of cI and/or ubiquinol, with excess reduction leading to electron leak (reverse electron transfer) via cI, which has been proposed to be a possible mechanism for mitochondrial H_2O_2 production, initially as a superoxide (Anderson *et al.,* 2019). In the same study, expression of mitochondrially targeted human catalase and administration of a small-peptide antioxidant, which localizes to the mitochondrial inner membrane, prevented diet-induced insulin insensitivity in mice. These results indicate a critical role of superoxide production in mitochondria, under high-fat-fed conditions, in the development of the phenotype. Assuming a similar condition was induced by chronic exposure of mice to the even more extreme ketogenic diet, AOX would have been enzymatically active, preventing the over-reduction of ubiquinol, thereby limiting excess ROS production and consequent phenotypes. But the quantitatively minor difference between AOX transgenic and control mice reared on fat-rich diets suggests either the dietary stress was not sufficient to constantly maintain ubiquinol in an over-reduced state or that any AOX-mediated energy deprivation may have been compensated by increased food intake. Since both the ketogenic diet, which is in paste form, and the HF-60 diet, which disintegrates due to high fat content, was quite difficult to be measured once added to the cage, food consumption by each individual mouse was not accurately measurable in this study. A proper way to study this would require controlled feeding and regular measurement of metabolic and physiological parameters.

6.2. Partial rescue of *Mcp1*-induced phenotype by AOX

The Mcp1 mouse model is engineered to constitutively express MCP1 under the adult-cardiomyocyte-specific *Myh6* promoter (Kolattukudy *et al.,* 1998). The constitutive expression of MCP1 results in cardiac failure as a consequence of chronic inflammation. Previous studies on Mcp1 mice, showing evidence for oxidative stress-induced cell death, accompanied by mitochondrial structural damage (Niu & Kolattukudi*,* 2009, Younce & Kolattukudi, 2010). Although ROS production in the inflammatory process is normally considered to be due to the activity of NADPH oxidase (Zeng *et al.,* 2019), an involvement of the mitochondrial ETC cannot be excluded. Moreover, the observation that hyperoxia is able to block the development

of the inflammatory phenotype in Mcp1 mice (reported in the first portion of paper (III), to which I did not contribute data) provided an additional rationale for testing the ability of AOX to rescue the pathology.

However, AOX provided only a transient rescue of the *Mcp1*-induced phenotype, which was lost as the mice aged. Furthermore, adult cardiomyocyte-specific expression of AOX exacerbated the phenotype in mice after 16 weeks of age. The accumulation of reduced ubiquinol, CoQ_{10}, in Mcp1 mice (figure 5D of paper (III)) does indicate blockade of electron flow downstream of CoQ, which constitutes a favorable condition for AOX activation. The AOX-mediated mitigation of excess ROS production at cIII, and/or the prevention of metabolic stalling due to ETC inhibition, could be possible reasons for the ability of AOX to decrease the extent of cardiac dysfunction in young mice (12-16 weeks of age) overexpressing both *Mcp1* and AOX. It should also be noted that the mitochondrial ETC is considered a key target of damage by excess ROS, as well as a possible source thereof. AOX should afford little or no protection against damage resulting from ROS produced elsewhere, e.g. due to NADPH oxidase, which is consistent with my observations. In a different study, preventing excess production of mitochondrial ROS, by introducing AOX was shown to exacerbate the phenotype of a mouse model with skeletal muscle-specific COX15 knockout (Dogan *et al.,* 2018). Unlike skeletal muscle cells, cardiomyocytes do not regenerate postnatally at a cellular level. Nevertheless, redox-sensitive signaling might be critical for initiating adaptive mechanisms in cardiomyocytes under conditions of chronic hypoxia (reviewed by Guzy and Schumacker, 2006; Santos *et al.,* 2011). This might explain why AOX was unable to sustain the initial beneficial effects in older Mcp1 mice and, when expressed only in adult cardiomyocytes, actually led to a worsening of the phenotype.

6.2.1. Pathology of Mcp1 mice

Although *Mcp1* expression has been shown to be beneficial in conditions of ischemic insult (Morimoto *et al.,* 2006), its constitutive expression has proven detrimental in mice (Kolattukudi *et al.,* 1998). This suggests a biphasic role of *Mcp1*, where its acute expression aids in tissue repair and prevents scar formation following an injury or infection, but prolonged expression eventually leads to tissue damage. MCP1 is a cytokine that is secreted by and can act directly or indirectly on several cell types, including immune cells and neighboring cells (reviewed by Deshmane *et al.,* 2009,

Stow *et al.,* 2009 and Conductier *et al.,* 2010), thus having a complex role in tissue repair and remodeling. The overexpression of *Mcp1* in adult cardiomyocytes is therefore expected to affect other cell types, including neighboring cardiomyocytes, endothelial cells, fibroblasts, resident immune cells and infiltrating monocytes. Although my study was not aimed at exploring the detailed effects of MCP1 on different cell-types, the differences are likely be critical for the progression of cardiac failure in Mcp1 mice. This is because of the inherent plasticity of resident cardiac cells. Apart from their specific roles in aiding cardiac function, they also undergo changes under conditions of tissue damage or injury to adapt and complement the loss of other cell types, especially cardiomyocytes (reviewed by Gray *et al.,* 2018). In general terms, this could be one of the reasons behind the observed difference in the effects of global and cardiac-specific AOX expression in response to MCP1 insult. In mice expressing global AOX, all the cells, including endothelial cells, fibroblasts and immune cells, express AOX, which could have limited excess mitochondrial ROS production if the mitochondrial cytochrome pathway became damaged or overloaded, and thus provided protection against ROS damage within mitochondria. In contrast, in cardiac AOX mice, AOX expression is restricted to adult-cardiomyocytes. As a result, ROS damage occurring in other cell types would not be mitigated by AOX, whilst AOX activation in cardiomyocytes might result in decreased ATP production, exacerbating the pathological phenotype.

6.2.2. Evidence for cardiac remodeling

MCP1-induced adverse cardiac remodeling was confirmed by several observations, especially, by the switch in the expression levels of myosin heavy chain isoforms. An increase in the level of beta myosin heavy chain (*Myh7*) mRNA, which is expressed at a high level during fetal development, and a concomitant decrease in the mRNA for the adult-specific, alpha myosin heavy chain Myh6 (figure 20), indicates activation of the fetal-gene program, which has been observed previously in failing hearts (Allard *et al.,* 1994; reviewed by Taegtmeyer *et al.,* 2010). This was further supported by an increase in the expression level of GAPDH (figure 5C of paper (III)), compared to the controls, consistent with a shift towards increased glycolysis, a decrease in mitochondrial respiratory capacity (figure 19B), loss of cardiac contractile function (figure 18) and a clear shift in the global metabolome assessed by principal component analysis (figure 6 of paper (III)). Although the average lifespan of Mcp1 mice was 35 weeks, all of these changes were already observable in early adulthood

(12 weeks of age). The molecular changes, plus the accompanying decrease in cardiac performance (figure 3 of paper (III)), are early signs of the pathological condition, and I hypothesize that the cumulative effect of metabolic disturbances and altered gene expression eventually results in cardiac failure. Global AOX expression in Mcp1 mice had only a small impact on these molecular parameters, indicating that mitochondrial involvement in the phenotype is not the result of any induced defect in mitochondrial metabolism, at least not one specifically affecting cIII and/or cIV, but is instead part of a global metabolic switch.

6.2.3. Oxygen metabolism

Subjecting Mcp1 mice to hyperoxic conditions, which was performed by my collaborators in Germany, mitigated cardiac contractile dysfunction and ultrastructural damage (figure 1 of paper (III)), suggesting that *Mcp1*-overexpression and/or the resulting infiltration of immune cells induces a hypoxic-like condition. In turn, this suggests the possibility that MCP1 acts by stabilizing HIF-1α, triggering HIF1-mediated metabolic reprogramming, which includes the downregulation of mitochondrial respiration (Papandreou *et al.,* 2006, Kim *et al.,* 2006). This hypothesis is supported by the decreased respiration of isolated mitochondria from Mcp1 mouse heart (figure 19). Note, however, that, if this were limited by flux through cIII and cIV, AOX expression would be expected to restore it. However, respiratory limitation might be upstream of the cytochrome chain, involving an overall downregulation of the ETC and related metabolic pathways. This could be further tested by using an alternative NADH-ubiquinone oxidoreductase, e.g. *Saccharomyces cerevisiae* Ndi1. Like AOX, Ndi1 is a single subunit protein that is localized on the inner mitochondrial membrane and participates in the ETC without proton pumping, i.e. in other respects it functions similar to the mammalian cI by transferring electrons from NADH to ubiquinol (de Vries *et al.,* 1988). In a recent study, preischemic administration of Ndi1 to Langendorff-perfused rat hearts decreased superoxide production, preserved ATP levels and mitochondrial integrity, and diminished the infarct size following ischemia-reperfusion (I/R; Perry *et al.,* 2011). In addition, preischemic administration of Ndi1 also decreased the infarct size in an *in-vivo* model for I/R injury (Mentzer *et al.,* 2014).

Given that *Mcp1* overexpression does induce excess ROS production in cardiomyocytes (Niu *et al.,* 2009), the counteracting effect of hyperoxic treatment on cardiac function would, taken in isolation, suggest a possible involvement of cIV in

the molecular mechanism, since cIV is the major oxygen-consuming enzyme of the cell. Although *Mcp1* overexpression did not dramatically affect that of Cox1 (a subunit of cIV), it might have indirect effects on cIV activity. For example, Mcp1 mice exhibit elevated levels of iNOS (Niu *et al.,* 2009), suggesting a possible regulation of cIV mediated by nitric oxide (Cleeter *et al.,* 1994, Brown *et al.,* 1994, reviewed by Erusalimsky *et al.,* 2007). Another major site of ROS production is cI, where it is associated with reverse electron flow. *Mcp1* overexpression also results in increased levels of TNFα and IL-1β (Niu *et al.,* 2009), which could adversely affect the activity of cI and ATP production (Lopez-Armada *et al.,* 2006, Mariappan *et al.,* 2010). For example, in a study where TNFα was administered to rats, it resulted in LV dysfunction (Mariappan *et al.,* 2010). The molecular changes involved decreased activity of the ETC complexes, especially cI, excess production of mitochondrial superoxide, and a decrease in ATP levels and MnSOD activity (Mariappan *et al.,* 2010).

Taken together, *Mcp1* overexpression may therefore have a broader effect on the mitochondrial ETC, thus negating any beneficial effects of AOX, which can only complement a blockade in the cytochrome pathway.

6.2.4. Possible impact of AOX on macrophage polarization

The polarization of monocytes into either pro-inflammatory (M1) or anti-inflammatory (M2) macrophages is regulated by the primary metabolic source of energy production within the cell, i.e. glycolysis or OXPHOS, respectively (reviewed by Galvan-Pena *et al.*, 2014). Macrophages are activated by specific signals and vary in their functions. M1 macrophages are activated either by bacterial infections or administration of bacterial-derived products like lipopolysaccharides (LPS), whereas M2 macrophages are activated by parasitic infections and their related signals. Under conditions of tissue damage, an initial burst of M1 macrophages is followed by a switch to M2 type, to promote tissue repair, once the immediate danger has passed. The switch in the phenotype of macrophages has been suggested to be a consequence of alterations in ROS production, mitochondrial respiration and related metabolic pathways (reviewed by O'Neil *et al.*, 2016). In support of this concept, AOX has been shown to mitigate LPS-induced lethality in mice, by limiting succinate accumulation and consequent ROS production resulting from reverse electron flow *via* cI (Mills *et al.,* 2016), which has been proposed to alter the expression levels of inflammatory genes.

Assuming a similar condition occurs in the MCP1-induced inflammatory response, global AOX expression should affect macrophage polarization in a similarly beneficial manner, whereas cardiomyocyte-specific AOX expression could not induce such a phenotypic change in macrophages. However, to clearly understand the impact of AOX expression in the polarization of macrophages, and determine the conditions that would influence an AOX-mediated phenotypic switch therein, a macrophage-specific AOX expression model would be necessary.

6.3. Lack of rescue of Cox10 KO mouse model by AOX

Unlike previous observations where AOX prevented lethal effects of cIV dysfunction in human cell cultures and *Drosophila* models (Dassa *et al.,* 2009, Fernandez-Ayala *et al.,* 2009, Kemppainen *et al.,* 2014), AOX was unable to rescue the lethal phenotype of cIV loss due to adult cardiomyocyte-specific COX10 KO in mice (figure 21). As discussed above, active AOX is expected to complement defective cIII and/or cIV but at the cost of net ATP production. My observations indicate that restoring metabolic homeostasis may be more important than the overall level of mitochondrial ATP production in cultured cells or in smaller organisms such as fruit flies, but not in a mammalian organ like the heart which is heavily dependent on mitochondrial ATP production. Thus AOX was able to mitigate the severe phenotype resulting from knockdown of cIV or a cIV-biosynthetic gene in cells and flies, without causing severe adverse effects. However, this was not the case in the mouse, where proper cardiac function cannot be sustained if too great a decrease in ATP production occurs.

There are several possible reasons to explain why adult cardiomyocyte-specific COX10 KO mice survived for up to two-weeks post-natally, but then succumbed.

- Lactate produced *via* glycolysis is the major source of energy in cardiomyocytes during fetal development and is supplemented by fatty acid oxidation only after birth, when the cardiomyocytes are exposed to an oxygen-rich environment (Bartelds *et al.,* 2000). Thus during fetal development, loss of cIV should not have a major impact on cardiac development and function, despite having an active ETC. However, loss of cIV will adversely affect cardiac function once the switch to aerobic respiration occurs, and mitochondria become important as the main seat of ATP production.
- COX10 KO is mediated by *Cre-loxP* activity, and KO in adult cardiomyocytes is achieved by driving *Cre* expression from an adult-cardiomyocyte specific

promoter, *Myh6*. In rodents, the expression of the adult-type (alpha) myosin heavy chain (*Myh6*) varies during fetal development, but is considered minimal from embryonic day 10.5 until birth. In contrast, the fetal (beta) isoform (*Myh7*) is maximally expressed throughout embryonic development but decreases to a minimal level after birth, when *Myh6* attains maximum expression (Lyons *et al.,* 1990). Therefore, the low activity of the *Myh6* promoter during development might not be sufficient to knockout both copies of COX10 in all cardiomyocytes until birth.

- COX10 is an enzyme and its half-life may be long enough to sustain activity for an extended period of time subsequent to knockout of the gene. In such a case, loss of COX10 expression immediately after birth might not have a severe impact for many days, because of the presence of sufficient amounts of previously synthesized COX10 polypeptide (or its heme product). Ideally, this should be detectable by western blotting, but was not done in this study. This is supported by the observation from mice with heterozygous COX10 KO, which did not exhibit a deleterious phenotype, other than a mild decrease in cardiac contractile function. Additionally, the degradation of COX10 might happen only gradually, which could result in a gradual loss of cIV and thus not severely impacting the survival of the pups for a number of days after birth.

7. Conclusions and future prospects

The work presented in this thesis explores the impact of mitochondrial respiratory defects in two mouse models of cardiomyopathy with different etiology. In the first model, *Mcp1* overexpression in adult cardiomyocytes decreases mitochondrial respiratory capacity as a consequence of inflammation-mediated cellular stress, albeit by an unknown mechanism. In the second model, ETC dysfunction within the cytochrome pathway is induced in adult cardiomyocytes by excision of the gene for COX10, an enzyme essential for biogenesis of the prosthetic group in cIV. These mouse models can be considered complementary, since mitochondrial impairment in the two cases is the respective consequence of indirect and direct insults, providing a broad perspective on ETC dysfunction. By expressing AOX in these disease models, I was able to further understand the importance of ATP production and redox balance in the pathogenesis of cardiomyopathy. In addition, this study implicitly investigated the therapeutic potential of AOX for diseases involving mitochondrial respiratory defects.

AOX has been lost during the course of evolution in mammals. Nevertheless, it has biochemical properties and biological functions that protect its natural hosts from stress conditions that closely replicate human disease. This raised the question of whether a therapeutic use of AOX could be beneficial, provided it does not evoke detrimental side effects that counteract putatively beneficial consequences. A better understanding of the bioenergetic consequences of xenotopic AOX expression e.g. on regular physiology and stress-response mechanisms was thus a prerequisite for its use. This was tested using a model organism approach by xenotopic expression in the mouse. Recently several model organisms with transgenic AOX expression were generated, and were exposed to different stresses affecting mitochondrial function. Aox^{Rosa26} mice, described in (I), constitute one such model. In my first study (I), I characterized the Aox^{Rosa26} mouse model under non-stressed and moderately stressed conditions. From my observations, I conclude that *Ciona* AOX can be safely expressed in mice and does not alter normal physiology under non-stress conditions. Yet, it provides resistance to a lethal dose of cyanide, i.e. a potent inhibitor of cIV of the ETC. I have reasoned that the lack of change in the physiology of Aox^{Rosa26} mice, when compared to wild-type mice, is due to the enzymatic inactivity of AOX under standard physiological conditions. This is crucial information, considering the potential therapeutic use of AOX, supporting the proposition that it may be

administered safely. However, as discussed above, a more thorough longitudinal analysis of all relevant parameters, would be essential for testing the long-term effects of AOX administration.

In my second study (II), I have addressed the issue raised above, by exposing Aox^{Rosa26} mice to dietary stress for a 40 week period. Against my expectation, I conclude that AOX expression has only minor effects on the phenotype induced by chronic exposure to fat-rich diets. The lack of a severe effect of AOX in mice exposed to fat-rich diets provides further evidence for its enzymatic inactivity under conditions that may not directly affect the ETC. Despite evidence from elsewhere that fat-rich diets may compromise mitochondrial function, I found no consistent evidence for a significant negative interaction between AOX expression and nutritional stress of this type. Alternatively, since AOX affected the lean mass in mice in a diet-independent manner, although not significantly different from the wild-type mice, it argues for a possible impact of AOX on overall catabolism in mice. This could be further investigated using a different experimental set up, where AOX mice are subjected to a calorically restricted diet. These mice would then be tested to see if an altered energy metabolism is induced, thereby severely affecting the muscle mass and/or the activity of the mice.

Validation of the Aox^{Rosa26} mouse model in studies (I) and (II) laid the foundation for its combination with the above-mentioned cardiomyopathy models. From my third study (III), I conclude the following;

(i) AOX expression can be restricted to adult-cardiomyocytes, and does not induce any adverse phenotype on its own.
(ii) In conditions of inflammatory cardiomyopathy, AOX expression is able to provide only a transiently beneficial effect in young mice.
(iii) Cardiomyocyte-specific AOX expression exacerbates the harmful cardiac phenotype of *Mcp1* overexpression.
(iv) AOX expression does not prevent the lethal phenotype of COX10 KO in adult cardiomyocytes in mice.

In this study, AOX did not confer protection against the detrimental effects of excessive inflammation in the heart but, in a different study, it was protective against a LPS-induced lethal phenotype (Mills *et al.,* 2016). Although the cause of lethality under both conditions is assumed to be excessive inflammation, the induced metabolic conditions affected the impact of AOX differently. Additionally, the adverse

effect of cardiomyocyte-specific AOX expression on *Mcp1* overexpression mice raises the possible role of AOX in macrophage maturation. The impact of AOX on the maturation of infiltrating macrophages can be tested by utilizing bone-marrow transplantation technique. Briefly, the bone marrow of the Mcp1 mice (host) can be depleted by irradiation, followed by engrafting bone marrow cells from Aox^{Rosa26} mice (donor). The resulting chimeric mice will have MCP1 over-expression in the adult cardiomyocytes and AOX expression in the bone marrow-derived cells, and studying the specific effect of AOX on macrophage polarization and thereby its impact on the *Mcp1*-induced phenotype would also be informative. A potential challenge in this system would be the time of irradiation. The typical age for irradiating mice is above 10 weeks after birth and a complete replenishment of the bone marrow derived cells would take about 10 weeks post transplantation. Since the Mcp1 mice develop a cardiac phenotype at an early age, detectable at 12 weeks of age, the bone-marrow transplantation might not be effective in preventing the development of the cardiac phenotype. However, this experiment could still provide valuable insights on the impact of macrophage polarization in the progression of cardiac contractile failure, provided that AOX can indeed be demonstrated to affect macrophage maturation. For a comprehensive review on bone-marrow transplantation technique and its limitations with respect to studies on cardiovascular diseases, see Aparicio-Vergara et al., (2010). Alternatively, AOX expressed under a macrophage-specific *Cre* driver will also be resourceful to study the effect of AOX expression in macrophage maturation.

We are just starting to understand the impact of AOX expression in mammals and several recent studies have shown differential beneficial effects of AOX in respective disease conditions. In order to better understand the potential of AOX as a therapeutic option, further studies are required to elucidate the regulatory and stress response mechanisms in different organs that may be affected by the catalytic AOX engagement thereby affecting specific pathological conditions.

8. Acknowledgements

This thesis work was carried out at the Doctoral Programme in Biomedicine (DPBM), Faculty of Medicine. Majority of the research work was conducted in the facilities of Biomedicum, Helsinki, Stem cells and Metabolism research program (STEMM), Viikki campus, Helsinki, Institute of Biotechnology and a part of the work was conducted in the facility of Arvo building, Tampere, Faculty of Medicine and Health Technology, University of Tampere. I wish to express my gratitude to Orion Research Foundation, The Maud Kuistila Memorial Foundation and The Finnish Foundation for Cardiovascular Research (Sydäntutkimussäätiö) for supporting a part of my research work through their grants. I thank Troy Faithfull, MSc, for revising the language of this thesis and thank Anna Valius, MSc, Kira Holmström, PhD and Tea Tuomela, BSc, for translating the abstract to Finnish.

I thank the thesis committee members, Professor Katriina Aalto-Setälä and Professor Klaus-Dieter Schlüter for their valuable support, guidance and motivation during my PhD.

I thank the external reviewers Jaakko Pohjoismäki, PhD and Professor Roberta A. Gottlieb, for reviewing my thesis and for providing valuable comments. I thank Professor Hannu Sariola for accepting to be the custos and thank Professor Anthony Moore for accepting to be the opponent.

I would like to convey my profound gratitude to Professor Howard T. Jacobs for providing me the opportunity to do research in his lab. I very much appreciate the independence you provided me in the lab and for all the valuable discussions we had during these years, both scientific and on personal development. As a scientist, you amuse me with your depth of knowledge on many fields of science, your curiosity to learn more and your careful, yet bold, way of approaching a scientific question. As a mentor, you set an example for many young researchers, including me, and inspire us to become one.

I would like to convey my uttermost gratitude to Marten Szibor, MD, for his guidance, encouragement and advice throughout my project. I have been extremely fortunate to have a supervisor who has provided constant guidance with great patience and immense care, even during the most hectic times. Your positive attitude and confidence in me has encouraged me significantly during the challenging phases of

the project. I highly value your critical evaluation of my work and consistent expectation of quality research, which has molded me into a better scientist. I feel grateful for the support, supervision, and friendship you have provided me all these years and feel honored to have worked with a great mentor.

I feel lucky to have worked alongside an engaging, supportive, and cheerful colleagues at Professor Howard T. Jacobs' lab. I thank Maarit Partanen, BSc, and Antti Muranen, MSc, for all the technical assistance and for creating a friendly atmosphere in the lab. I thank Tea Tuomela, BSc, and Eveliina Teeri, BE, for their wonderful support in the lab during my visits to Tampere. I thank Eric Dufour, PhD, for the unconditional guidance and teaching throughout these years, and especially for those excellent coffees and never-ending croissants. I wish to express my appreciation to Giuseppe Cannino, PhD, Çağri Yalgin, PhD, Ana Andjelković, PhD, Jack George, MSc, Jose Gonzalez de Cozar, MSc, and Sina Saari, PhD, for their friendly support in the lab. I thank Troy Faithful, MSc, for providing massive moral support during the stressful times, kindness and sense of humor. Your willingness to always help is an extraordinary trait. I thank Kira Holmström, PhD, for all the technical and moral support, guidance and valuable discussions on the projects. I thank Luca Giordano, PhD, and Udy Bar Yosef, PhD, for keeping up the enthusiasm in the lab, which has often cheered me up. I thank Kaisa Immonen, MSc, and Anna Valius, MSc, for their incredible support with administrative matters and moral support.

Science is a group effort, I thank all my collaborators for their contribution to the projects. Speaking of group effort, I feel very grateful to have been introduced to the supportive and enthusiastic scientific community in Helsinki and Tampere. I especially thank the research groups of Professor Anu S. Wartiovaara, and Brendan J. Battersby, PhD and Associate Professor Henna Tyynismaa, for the support and guidance during my PhD. I would like to further extend my gratitude to Professor Anu S. Wartiovaara for adopting me into the lab during my final years of the thesis work and I must thank all her group members for their support during that period. I especially thank Liliya Euro, PhD, Nahid Akhtar Khan, PhD, Catalina Vasilescu, MSc, Olesia Ignatenko, MSc, Anastasiia Marmyleva, MSc, Markus Innilä and Babette Hollmann for their vast support. I would like to express my deep appreciation to Brendan J. Battersby, PhD, for all the curious discussions, guidance and mentoring over these years. I admire your passion for science and the selfless willingness to guide fellow researchers. I thank Christopher Carroll, PhD, and Uwe Richter, PhD, for

their support and guidance, which was substantial especially during the initial days of my PhD. I thank Vinod Kumar, PhD, for teaching me the basics of Immunostaining.

I am very grateful to all my friends for their support and care throughout these years. I especially thank Jayasimman, for all the wise advice and for taking care of me like a big brother, Darshan, for always inspiring me with his charm and cheerfulness, Luis, for the brotherly care, sarcastic motivations and probably the worst sangria ever made on this planet, Nahid, for the wisdom, moral support and more importantly for the delicious foods, Troy and Kira, for the wonderful friendship and astonishing support, Maarit, Antti and Babette, for the mind-boggling coffee time conversations and Divya, for constantly motivating me with your character.

I thank my parents, Madhumathi Parthasarathy and Dhandapani Raji, for their unconditional love and constant encouragement to pursue my ambition. Last but not least, I thank my dear wife, Poojitha Bukka, for the love, care and especially for adding extra-large portions of spice to my life.

Praveen Kumar Dhandapani

Helsinki, April 2020

9. References

Abdulhag UN, Soiferman D, Schueler-Furman O, Miller C, Shaag A, Elpeleg O, Edvardson S, Saada A. Mitochondrial complex IV deficiency, caused by mutated COX6B1, is associated with encephalomyopathy, hydrocephalus and cardiomyopathy. Eur. J. Hum. Genet. 2015, 23(2): 159-164.

Acharya A, Baek ST, Huang G, Eskiocak B, Goetsch S, Sung CY, Banfi S, Sauer MF, Olsen GS, Duffield JS, Olson EN, Tallquist MD. The bHLH transcription factor Tcf21 is required for lineage-specific EMT of cardiac fibroblast progenitors. Development 2012, 139(12): 2139-2149.

Adams PL, Turnbull DM. Disorders of the electron transport chain. J. Inherit. Metab. Dis. 1996, 19(4): 463-469.

Ahola S, Auranen M, Isohanni P, Niemisalo S, Urho N, Buzkova J, Velagapudi V, Lundbom N, Hakkarainen A, Muurinen T, Piirilä P, Pietiläinen KH, Suomalainen A. Modified Atkins diet induces subacute selective ragged-red-fiber lysis in mitochondrial myopathy patients. EMBO Mol. Med. 2016, 8(11): 1234-1247.

Ahola-Erkkila S, Carroll CJ, Peltola-Mjosund K, Tulkki V, Mattila I, Seppanen-Laakso T, Oresic M, Tyynismaa H, Suomalainen A. Ketogenic diet slows down mitochondrial myopathy progression in mice. Hum Mol Genet. 2010, 19: 1974-1984.

Allard MF, Schonekess BO, Henning SL, English DR, Lopaschuk GD. Contribution of oxidative metabolism and glycolysis to ATP production in hypertrophied hearts. Am. J. Physiol. 1994, 267: H742-H750.

Anderson EJ, Lustig ME, Boyle KE, Woodlief TL, Kane DA, Lin CT, Price JW 3rd, Kang L, Rabinovitch PS, Szeto HH, Houmard JA, Cortright RN, Wasserman DH, Neufer PD. Mitochondrial H2O2 emission and cellular redox state link excess fat intake to insulin resistance in both rodents and humans. J. Clin. Invest. 2009, 119(3): 573-581.

Andreu AL, Checcarelli N, Iwata S, Shanske S, DiMauro S. A missense mutation in the mitochondrial cytochrome b gene in a revisited case with histiocytoid cardiomyopathy. Pediatr. Res. 2000, 48(3): 311-314.

Antico Arciuch VG, Elguero ME, Poderoso JJ, Carreras MC. Mitochondrial regulation of cell cycle and proliferation. Antioxid. Redox. Signal. 2012, 16(10): 1150-1180.

Antonicka H, Leary SC, Guercin GH, Agar JN, Horvath R, Kennaway NG, Harding CO, Jaksch M, Shoubridge EA. Mutations in COX10 result in a defect in mitochondrial heme A biosynthesis and account for multiple, early-onset clinical phenotypes associated with isolated COX deficiency. Hum. Mol. Genet. 2003, 12(20): 2693-2702.

Antonicka H, Mattman A, Carlson CG, Glerum DM, Hoffbuhr KC, Leary SC, Kennaway NG, Shoubridge EA. Mutations in COX15 produce a defect in the mitochondrial heme biosynthetic pathway, causing early-onset fatal hypertrophic cardiomyopathy. Am. J. Hum. Genet. 2003, 72(1): 101-114.

Aoki T, Fukumoto Y, Sugimura K, Oikawa M, Satoh K, Nakano M, Nakayama M, Shimokawa H. Prognostic impact of myocardial interstitial fibrosis in non-ischemic heart failure. - Comparison between preserved and reduced ejection fraction heart failure. Circ. J. 2011, 75(11): 2605-2613.

Aparicio-Vergara M, Shiri-Sverdlov R, de Haan G, Hofker MH. Bone marrow transplantation in mice as a tool for studying the role of hematopoietic cells in metabolic and cardiovascular diseases. Atherosclerosis 2010, 213(2): 335-344.

Arakelyan A, Petrkova J, Hermanova Z, Boyajyan A, Lukl J, Petrek M. Serum levels of the mcp-1 chemokine in patients with ischemic stroke and myocardial infarction. Mediators Inflamm. 2005, 2005(3): 175-179.

Albury MS, Dudley P, Watts FZ, Moore AL. argeting the plant alternative oxidase protein to Schizosaccharomyces pombe mitochondria confers cyanide-insensitive respiration. J. Biol. Chem. 1996, 271(29): 17062-17066.

Altmann R. The elemental organisms and their relationships to the cells. Leipzig, 1890, p. 125. Iink: German Text Archive http://www.deutschestextarchiv.de/altmann_elementarorganismen_1890/141

Banerjee I, Fuseler JW, Price RL, Borg TK, Baudino TA. Determination of cell types and numbers during cardiac development in the neonatal and adult rat and mouse. Am. J. Physiol. Heart Circ. Physiol. 2007, 293(3): H1883-H1891.

Bartelds B, Knoester H, Smid GB, Takens J, Visser GH, Pennings L, Leij FRVD, Beaufort-Krol GCM, ijlstra WG, Heymans HSA, Kuipers JRG. Perinatal changes in myocardial metabolism in lambs. Circulation 2000, 102: 926–931.

Barth E, Stammler G, Speiser B, Schaper J. Ultrastructural quantitation of mitochondria and myofilaments in cardiac muscle from 10 different animal species including man. J. Mol. Cell Cardiol. 1992, 24: 669-681.

Bates MG, Nesbitt V, Kirk R, He L, Blakely EL, Alston CL, Brodlie M, Hasan A, Taylor RW, McFarland R. Mitochondrial respiratory chain disease in children undergoing cardiac transplantation: a prospective study. Int. J. Cardiol. 2012, 155(2): 305-306.

Bayrhuber M, Meins T, Habeck M *et. al.*Structure of the human voltage-dependent ion channel. PNAS 2008, 105: 15370-15375.

Becker RO, Chapin S, Sherry R. Regeneration of the ventricular myocardium in amphibians. Nature 1974, 248(5444): 145-147.

Benda C. Uber die Spermatogenese Arch, Anal. Physiol. 1898, 393–398.

Bentinger M, Tekle M, Dallner G. Coenzyme Q – Biosynthesis and functions. Biochem. and Biophys. Res. Comm. 2010, 396: 74–79

Berg JM, Tymoczko JL, Stryer L. The Respiratory Chain Consists of Four Complexes: Three Proton Pumps and a Physical Link to the Citric Acid Cycle. Biochemistry. 5th edition. New York: W H Freeman; 2002. Section 18.3, Available from: https://www.ncbi.nlm.nih.gov/books/NBK22505/

Berthold DA, Stenmark P. Membrane-bound diiron carboxylate proteins. Annu. Rev. Plant Biol. 2003, 54: 497-517.

Botting KJ, Wang KC, Padhee M, McMillen IC, Summers-Pearce B, Rattanatray L, Cutri N, Posterino GS, Brooks DA, Morrison JL. Early origins of heart disease: low birth weight and determinants of cardiomyocyte endowment. Clin. Exp. Pharmacol. Physiol. 2012, 39(9): 814-823.

Brand MD. The sites and topology of mitochondrial superoxide production. Exp. Gerontol. 2010, 45(7-8): 466 - 472.

Brand MD, Goncalves RL, Orr AL, Vargas L, Gerencser AA, Borch Jensen M, Wang YT, Melov S, Turk CN, Matzen JT, Dardov VJ, Petrassi HM, Meeusen SL, Perevoshchikova IV, Jasper H, Brookes PS, Ainscow EK. Suppressors of Superoxide-H2O2 Production at Site IQ of Mitochondrial Complex I Protect against Stem Cell Hyperplasia and Ischemia-Reperfusion Injury. Cell Metab. 2016, 24(4): 582 - 592.

Brecht M, Richardson M, Taranath A, Grist S, Thorburn D, Bratkovic D. Leigh Syndrome caused by the mt-ND5 m.13513G>A mutation: a case presenting with wpw-like conduction defect, cardiomyopathy, hypertension and hyponatraemia. JIMD Rep. 2015, 19: 95-100.

Brown GC, Cooper CE. Nanomolar concentrations of nitric oxide reversibly inhibit synaptosomal respiration by competing with oxygen at cytochrome oxidase. FEBS letters 1994, 356(2-3): 295-298.

Brown KJ, Grunberg NE. Effects of environmental conditions on food consumption in female and male rats. Physiol. Behav. 1996, 60(1): 293-297.

Brunel-Guitton C, Levtova A2, Sasarman F. Mitochondrial Diseases and Cardiomyopathies. Can. J. Cardiol. 2015, 31(11): 1360-1376.

Bugiani M, Lamantea E, Invernizzi F, Moroni I, Bizzi A, Zeviani M, Uziel G. Effects of riboflavin in children with complex II deficiency. Brain and Development 2006, 576-581.

Cai J, Yang J, Jones DP. Mitochondrial control of apoptosis: the role of cytochrome c. Biochim. Biophys. Acta. 1998, 1366(1-2): 139-149.

Cape JL, Bowman MK, Kramer DM. A semiquinone intermediate generated at the Qo site of the cytochrome bc1 complex: importance for the Q-cycle and superoxide production. Proc. Natl. Acad. Sci. U S A. 2007, 104(19): 7887 - 7892.

Carroll J, Fearnley IM, Skehel M, Shannon RJ, Hirst J, Walker JE. Bovine complex I is a complex of 45 different subunits. JBC 2006, 281: 32724-32727.

Calligaris SD, Lecanda M, Solis F, Ezquer M, Gutiérrez J, Brandan E, Leiva A, Sobrevia L, Conget P. Mice long-term high-fat diet feeding recapitulates human cardiovascular alterations: an animal model to study the early phases of diabetic cardiomyopathy. PLoS One 2013, 8(4): e60931.

Catteruccia M, Sauchelli D, Della Marca G, Primiano G, Cuccagna C, Bernardo D, Leo M, Camporeale A, Sanna T, Cianfoni A, Servidei S. "Myo-cardiomyopathy" is commonly associated with the A8344G "MERRF" mutation. J. Neurol. 2015, 262(3): 701-710.

Chandel NS. Mitochondria as signalling organelles. BMC Biol. 2014, 12:34.

Chandel NS. Evolution of mitochondria as signalling organelles. Cell Metab. 2015, 22(2): 204-206.

Che Y, Wang ZP, Yuan Y, Zhang N, Jin YG, Wan CX, Tang QZ. Role of autophagy in a model of obesity: A long-term high fat diet induces cardiac dysfunction. Mol. Med. Rep. 2018, 18(3): 3251-3261.

Cherry AD, Piantadosi CA. Regulation of mitochondrial biogenesis and its intersection with inflammatory responses. Antioxid. Redox Signal. 2015, 22(12): 965-976

Chen Q, Camara AK, Stowe DF, Hoppel CL, Lesnefsky EJ. Modulation of electron transport protects cardiac mitochondria and decreases myocardial injury during ischemia and reperfusion. Am. J. Physiol. Cell Physiol. 2007, 292(1): C137-147.

Chen L, Knowlton AA. Mitochondria and heart failure: new insights into an energetic problem. Minerva Cardioangiol. 2010, 58(2): 213-229.

Chen Y, Liu Y, Dorn GW. Mitochondrial fusion is essential for organelle function and cardiac homeostasis. Circ. Res. 2011, 109(12): 1327-1331.

Cheng Z, Ristow M. Mitochondria and metabolic homeostasis. Antioxid. Redox Signal. 2013, 19(3): 240-242.

Chiong M, Wang ZV, Pedrozo Z, Cao DJ, Troncoso R, Ibacache M, Criollo A, Nemchenko A, Hill JA, Lavandero S. Cardiomyocyte death: mechanisms and translational implications. Cell Death Dis. 2011, 2: e244.

Clapham DE. Calcium signaling. Cell 2007, 131(6): 1047-1058.

Cleeter MWJ, Cooper JM, Darley-Usmar VM, Moncada S, Schapira AHV. Reversible inhibition of cytochrome c oxidase, the terminal enzyme of the mitochondrial respiratory chain, by nitric oxide: Implications for neurodegenerative diseases. FEBS letters 1994, 345(1): 50-54.

Coenen MJ, van den Heuvel LP, Ugalde C, Ten Brinke M, Nijtmans LG, Trijbels FJ, Beblo S, Maier EM, Muntau AC, Smeitink JA. Cytochrome c oxidase biogenesis in a patient with a mutation in COX10 gene. Ann. Neurol. 2004, 56(4): 560-564.

Cogliati S, Enriquez JA and Scorrano L. Mitochondrial cristae: where beauy meets functionality. Trends Biochem. Sci. 2016, 41: 3.

Conductier G, Blondeau N, Guyon A, Nahon JL, Rovère C. The role of monocyte chemoattractant protein MCP1/CCL2 in neuroinflammatory diseases. J. Neuroimmunol. 2010, 224(1-2): 93-100.

Conway MA, Allis J, Ouwerkerk R, Niioka T, Rajagopalan B, Radda GK. Detection of low phosphocreatine to ATP ratio in failing hypertrophied human myocardium by 31P magnetic resonance spectroscopy. Lancet 1991, 338(8773): 973-6.

Cormier RPJ, Champigny CM, Simard CJ, St-Coeur PD, Pichaud N. Dynamic mitochondrial responses to a high-fat diet in Drosophila melanogaster. Sci. Rep. 2019, 9(1): 4531.

Dassa EP, Dufour E, Goncalves S, Paupe V, Hakkart GA, Jacobs HT, Rustin P. Expression of alternative oxidase complements cytochrome c oxidase deficiency in human cells. EMBO Mol. Med. 2009, 1(1): 30-36.

de Vries S, Grivell LA. Purification and characterization of a rotenone-insensitive NADH:Q6 oxidoreductase from mitochondria of Saccharomyces cerevisiae. Eur. J. Biochem. 1988, 176(2): 377-384.

Deepa SS, Pharaoh G, Kinter M, Diaz V, Fok WC, Riddle K, Pulliam D, Hill S, Fischer KE, Soto V, Georgescu C, Wren JD, Viscomi C, Richardson A, Van Remmen H. Lifelong reduction in complex IV induces tissue-specific metabolic effects but does not reduce lifespan or healthspan in mice. Aging Cell. 2018, 17(4): e12769.

Deshmane SL, Kremlev S, Amini S, Sawaya BE. Monocyte chemoattractant preotein-1 (MCP-1): An overview. J. Interferon Cytokine Res. 2009, 29(6): 313-326.

Dhall A, Self W. Cerium oxide nanoparticles: a brief review of their synthesis methods and biomedical applications. Antioxidants (Basel) 2018, 7(8): 97.

Diaz F, Thomas CK, Garcia S, Hernandez D, Moraes CT. Mice lacking COX10 in skeletal muscle recapitulate the phenotype of progressive mitochondrial myopathies associated with cytochrome c oxidase deficiency. Hum. Mol. Genet. 2005, 14(18): 2737- 2748.

Diaz F, Garcia S, Hernandez D, Regev A, Rebelo A, Oca-Cossia J, Moraes CT. Pathophysiology and fate of hepatocytes in a mouse model of mitochondrial hepatopathies. Gut 2009, 57(2): 232-242.

Dimmock DP, Lawlor MW. Presentation of diagnostic evaluation of mitochondrial disease. Pediatr. Clin. North Am. 2017, 64(1): 161-171.

Dogan SA, Cerutti R, Benincá C, Brea-Calvo G, Jacobs HT, Zeviani M, Szibor M, Viscomi C. Perturbed Redox Signaling Exacerbates a Mitochondrial Myopathy. Cell Metab. 2018, 28(5): 764-775.

Dominy JE, Puigserver P. Mitochondrial biogenesis through activation of nuclear signaling proteins. Cold Spring Harb. Perspect. Biol. 2013, 5(7). pii: a015008.

Dry IB, Moore AL, Day DA, Wiskich JT. Regulation of alternative pathway activity in plant mitochondria: nonlinear relationship between electron flux and the redox poise of the quinone pool. Arch. Biochem. Biophys. 1989, 273(1): 148-157.

El Alaoui-Talibi Z, Landormy S, Loireau A, Moravec J. Fatty acid oxidation and mechanical performance of volume-overloaded rat hearts. Am. J. Physiol. 1992, 262: H1068-H1074.

El-Hattab AW, Adesina AM, Jones J, Scaglia F. MELAS syndrome: Clinical manifestations, pathogenesis, and treatment options. Mol. Genet. Metab. 2015, 116(1-2): 4-12.

El-Hattab AW, Zarante AM, Almannai M, Scaglia F. Therapies for mitochondrial diseases and current clinical trials. Mol. Genet. Metab. 2017, 122(3): 1-9.

El-Khoury R, Dufour E, Rak M, Ramanantsoa N, Grandchamp N, Csaba Z, Duvillié B, Bénit P, Gallego J, Gressens P, Sarkis C, Jacobs HT, Rustin P. Alternative oxidase expression in the mouse enables bypassing cytochrome c oxidase blockade and limits mitochondrial ROS overproduction. PLoS Genet. 2013, 9(1): e1003182.

Erusalimsky JD, Moncada S. Nitric oxide and mitochondrial signaling: from physiology to pathophysiology. Arterioscler. Thromb. Vasc. Biol. 2007, 27(12): 2524-2531.

Esposti MD. Inhibitors of NADH–ubiquinone reductase: an overview. Biochem. Biophys. Acta 1997, 1364: 222-235.

Fabra MA, Navas P, Calvo GB. Coenzyme Q biosynthesis and its role in the respiratory chain structure. Biochem. Biophys. Acta 2016, 1857: 1073-1078.

Fernandez-Ayala DJ, Sanz A, Vartiainen S, Kemppainen KK, Babusiak M, Mustalahti E, Costa R, Tuomela T, Zeviani M, Chung J, O'Dell KM, Rustin P, Jacobs HT. Expression of the Ciona intestinalis alternative oxidase (AOX) in Drosophila complements defects in mitochondrial oxidative phosphorylation. Cell Metab. 2009, 9(5): 449-460.

Fillmore N, Mori J, Lopaschuk GD. Mitochondrial fatty acid oxidation alterations in heart failure, ischaemic heart disease and diabetic cardiomyopathy. Br. J. Pharmacol. 2014, 171(8): 2080-2090.

Fridovich I. Superoxide radical and superoxide dismutases. Annu. Rev. Biochem. 1995, 64: 97-112.

Galván-Peña S, O'Neill LA. Metabolic reprograming in macrophage polarization. Front. Immunol. 2014, 5: 420.

Gimenes AC, Bravo DM, Napolis LM, Mello MT, Oliveira ASB, Neder JA, Nery LE. Effect of L-carnitine on exercise performance in patients with mitochondrial myopathy. Braz. J. Med. Biol. Res. 2015, 48(4): 354-362.

Giordano FJ. Oxygen, oxidative stress, hypoxia, and heart failure. J. Clin. Invest. 2005, 115(3): 500-508.

Giorgi C, Agnoletto C, Bononi A, Bonora M, De Marchi E, Marchi S, Missiroli S, Patergnani S, Poletti F, Rimessi A, Suski JM, Wieckowski MR, Pinton P. Mitochondrial calcium homeostasis as potential target for mitochondrial medicine. Mitochondrion 2012, 12(1): 77-85.

Gray GA, Toor IS, Castellan R, Crisan M, Meloni M. Resident cells of the myocardium: more than spectators in cardiac injury, repair and regeneration. Curr. Opin. Physiol. 2018, 1: 46-51.

Glerum DM, Tzagoloff A. Isolation of a human cDNA for hemeA.farnesyltransferase by functional complementation of a yeast cox10 mutant. PNAS 1994, 91(18): 8452-8456.

Gorman GS, Schaefer AM, Ng Y, Gomez N, Blakely EL, Alston CL, Feeney C, Horvath R, Yu-Wai-Man P, Chinnery PF, Taylor RW, Turnbull DM, McFarland R. Prevalence of nuclear and mitochondrial DNA mutations related to adult mitochondrial disease. Ann. Neurol. 2015, 77(5): 753-759.

Gottlieb RA, Burleson KO, Kloner RA, Babior BM, Engler RL. Reperfusion injury induces apoptosis in rabbit cardiomyocytes. J. Clin. Invest. 1994, 94(4): 1621-1628.

Gray MW, Burger G and Lang BF. Mitochondrial evolution. Science 1999, 283 5407: 1476-1481.

Green DR, Reed JC. Mitochondria and apoptosis. Science 1998, 281(5381): 1309-1312.

Guénebaut V, Vincentelli R, Mills D, Weiss H, Leonard KR. Three-dimensional structure of NADH-dehydrogenase from Neurospora crassa by electron microscopy and conical tilt reconstruction. J. Mol. Biol. 1997, 265(4): 409 - 418.

Guzy RD, Schumacker PT. Oxygen sensing by mitochondria at complex III: the paradox of increased reactive oxygen species during hypoxia. Exp. Physiol. 2006, 91(5): 807-819.

Hakkaart GAJ, Dassa EP, Jacobs HT, Rustin P. Allotopic expression of a mitochondrial alternative oxidase confers cyanide resistance to human cell respiration. EMBO Rep. 2006, 7(3): 341-345.

Hakonen AH, Goffart S, Marjavaara S, Paetau A, Cooper H, Mattila K, Lampinen M, Sajantila A, Lönnqvist T, Spelbrink JN, Suomalainen A. Infantile-onset spinocerebellar ataxia and mitochondrial recessive ataxia syndrome are associated with neuronal complex I defect and mtDNA depletion. Hum. Mol. Genet. 2008, 17(23): 3822-3835.

Handy DE, Loscalzo J. Redox regulation of mitochondrial function. Antioxid. Redox. Signal. 2012, 16(11): 1323-1367.

Hansson A, Hance N, Dufour E, Rantanen A, Hultenby K, Clayton DA, Wibom R, Larsson NG. A switch in metabolism precedes increased mitochondrial biogenesis in respiratory chain-deficient mouse hearts. Proc. Natl. Acad. Sci. U S A. 2004, 101(9): 3136-3141.

Hägerhäll C. Succinate: quinone oxidoreductases variations on a conserved theme. Biochem. Biophys. Acta 1997, 1320: 107-141.

Hirst J, Carroll J, Fearnley IM, Shannon RJ, Walker JE. The nuclear encoded subunits of complex I from bovine heart mitochondria. Biochem. Biophys. Acta 2003, 1604: 135-150.

Horii Y, Nagasawa T, Sakakibara H, Takahashi A, Tanave A, Matsumoto Y, Nagayama H, Yoshimi K, Yasuda MT, Shimoi K, Koide T. Hierarchy in the home cage affects behaviour and gene expression in group-housed C57BL/6 male mice. Sci. Rep. 2017, 7(1): 6991.

Holloszy JO. Biochemical adaptations in muscle. Effects of exercise on mitochondrial oxygen uptake and respiratory enzyme activity in skeletal muscle. J. Biol. Chem. 1967, 242: 2278-2282.

Holmgren D, Wåhlander H, Eriksson BO, Oldfors A, Holme E, Tulinius M. Cardiomyopathy in children with mitochondrial disease; clinical course and cardiological findings. Eur. Heart J. 2003, 24(3): 280-288.

Hoppel CL, Lesnefsky EJ, Chen Q, Tandler B. Mitochondrial Dysfunction in Cardiovascular Aging. Adv. Exp. Med. Biol. 2017, 982: 451-464.

Howell NJ, Tennant DA. The role of HIFs in ischemia-reperfusion injury. Hypoxia (Auckl) 2014, 2: 107-115.

Huang C, Andres AM, Ratliff EP, Hernandez G, Lee P, Gottlieb RA. Preconditioning involves selective mitophagy mediated by Parkin and p62/SQSTM1. PLoS One. 2011, 6(6): e20975.

Inamdar AA, Inamdar AC. Heart Failure: Diagnosis, Management and Utilization. J. Clin. Med. 2016, 5(7). pii: E62.

Ingwall JS, Weiss RG. Is the failing heart energy starved? On using chemical energy to support cardiac function. Circ. Res. 2004, 95(2): 135-145.

Jha D, Mitra Mazumder P. High fat diet administration leads to the mitochondrial dysfunction and selectively alters the expression of class 1 GLUT protein in mice. Mol. Biol. Rep. 2019, 46(2): 1727-1736.

Jeppensen TD, Schwartz M, Olsen DB, Wibrand F, Krag T, Duno M, Hauerslev S, Vissing J. Aerobic training is safe and improves exercise capacity in patients with mitochondrial myopathy. Brain 2006, 129: 3402-3412.

Jiang Y, Beller DI, Frendl, G, Graves DT. Monocyte chemoattractant protein-1 regulates adhesion molecule expression and cytokine production in human monocytes. J. Immunol. 1992, 148(8): 2423-2428.

Jornayvaz FR, Shulman GI. Regulation of mitochondrial biogenesis. Essays Biochem. 2010, 47: 69-84.

Joshi CN, Greenberg CR, Mhanni AA, Salman MS. Ketogenic diet in Alpers-Huttenlocher syndrome. Pediatr. Neurol. 2009, 40:314–6

Kaikita K, Hayasaki T, Okuma T, Kuziel WA, Ogawa H, Takeya M. Targeted deletion of CC chemokine receptor 2 attenuates left ventricular remodeling after experimental myocardial infarction. Am. J. Pathol. 2004, 165(2): 439-47.

Kavantzas NG, Lazaris AC, Agapitos EV, Nanas J, Davaris PS. Histological assessment of apoptotic cell death in cardiomyopathies. Pathology. 2000, 32(3): 176-180.

Kemppainen KK, Rinne J, Sriram A, Lakanmaa M, Zeb A, Tuomela T, Popplestone A, Singh S, Sanz A, Rustin P, Jacobs HT. Expression of alternative oxidase in Drosophila ameliorates diverse phenotypes due to cytochrome oxidase deficiency. Hum. Mol. Genet. 2014, 23(8): 2078 - 2093.

Keller BB, Liu LJ, Tinney JP, Tobita K. Cardiovascular developmental insights from embryos. Ann. N Y Acad. Sci. 2007, 1101: 377-3388.

Keppler A, Kindermann M, Gendreizig S, Pick H, Vogel H, Johnsson K. Labeling of fusion proteins of O6-alkylguanine-DNA alkyltransferase with small molecules in vivo and in vitro. Methods 2004, 32(4): 437-444.

Khan NA, Govindaraj P, Meena AK, Thangaraj K. Mitochondrial disorders: Challenges in diagnosis & treatment. Indian J. Med. Res. 2015, 141(1): 13–26.

Kim JW, Tchernyshyov I, Semenza GL, Dang CV. HIF-1-mediated expression of pyruvate dehydrogenase kinase: a metabolic switch required for cellular adaptation to hypoxia. Cell Metab. 2006, 3(3): 177-185.

Kolattukudy PE, Quach T, Bergese S, Breckenridge S, Hensley J, Altschuld R, Gordillo G, Klenotic S, Orosz C, Parker-Thornburg J. Myocarditis induced by targeted expression of the MCP-1 gene in murine cardiac muscle. Am. J. Pathol. 1998, 152(1): 101-111.

Krebs HA, Henseleit K. Untersuchungen uber die Harnstoffbildung im Tierkörper. Hoppe-Seyler´s Zeitschrift für physiologische Chemie 1932, 210(1-2): 33–66. DOI: https://doi.org/10.1515/bchm2.1932.210.1-2.33

Krebs HA. Rate control of the tricarboxylic cycle. Advances in Enzyme Regulation 1970, 8: 335-353.

Kroemer G, Reed JC. Mitochondrial control of cell death. Nat. Med. 2000, 6: 513-519.

Lackner LL. Shaping the dynamic mitochondrial network. BMC Biology 2014, 12: 35.

Lenaz G, Genova ML. Structure and organization of mitochondrial respiratory complexes: A new understanding of an old subject. Antioxid. Redox Signal 2010, 12: 961–1008.

Lesnefsky EJ, Chen Q, Hoppel CL. Mitochondrial metabolism in aging heart. Circ. Res. 2016, 118(10): 1593-1611.

Lewis MR, Lewis WH. Mitochondria in tissue culture. Science 1914, 39: 330-333.

Lindsey ML, Kassiri Z, Virag JAI, de Castro Brás LE, Scherrer-Crosbie M. Guidelines for measuring cardiac physiology in mice. Am. J. Physiol. Heart Circ. Physiol. 2018, 314(4): H733-H752.

Liron T, Raphael B, Hiram-Bab S, Bab IA, Gabet Y. Bone loss in C57BL/6J-OlaHsd mice, a substrain of C57BL/6J carrying mutated alpha-synuclein and multimerin-1 genes. J. Cell. Physiol. 2018, 233(1): 371-377.

Liu Q, Docherty JC, Rendell JCT, Clanachan AS, Lopaschuk GD. High levels of fatty acids delay the recovery of intracellular pH and cardiac efficiency in post-ischemic hearts by inhibiting glucose oxidation. J. Am. Coll. Cardiol. 2002, 39(4): 718-725.

Liu X., Kim C.N., Yang J., Jemmerson R., Wang X. Induction of apoptotic program in cell-free extracts: requirement for dATP and cytochrome c. Cell. 1996, 86: 147-157.

Llopis J, McCaffery JM, Miyawaki A, Farquhar MG, Tsien RY. Measurement of cytosolic, mitochondrial, and Golgi pH in single living cells with green fluorescent proteins. Proc. Natl. Acad. Sci. U S A 1998, 95(12): 6803–6808.

Lodish H, Berk A, Zipursky SL, et al. Molecular Cell Biology. 4th edition. New York: W. H. Freeman; 2000. Section 9.7, Organelle DNAs. Available from: https://www.ncbi.nlm.nih.gov/books/NBK21574/

Lopaschuk GD, Ussher JR, Folmes CD, Jaswal JS, Stanley WC. Myocardial fatty acid metabolism in health and disease. Physiol. Rev. 2010, 90: 207–258.

Lopez MF, Kristal BS, Chernokalskaya E, Lazarev A, Shestopalov AI, Bogdanova A, Robinson M. High-throughput profiling of the mitochondrial proteome using affinity fractionation and automation. Electrophoresis 2000, 21(16): 3427-3440.

López-Armada MJ, Caramés B, Martín MA, Cillero-Pastor B, Lires-Dean M, Fuentes-Boquete I, Arenas J, Blanco FJ. Mitochondrial activity is modulated by TNFalpha and IL-1beta in normal human chondrocyte cells. Osteoarthritis Cartilage. 2006, 14(10): 1011-1022.

Low FN. Mitochondrial structure. J. Biophysic. Biochem. Cytol. 1956, 2 4.

Lyons GE, Schiaffino S, Sassoon D, Barton P, Buckingham M. Developmental regulation of myosin gene expression in mouse cardiac muscle. J. Cell. Biol. 1990, 111(6 Pt 1): 2427-2436.

Mariappan N, Elks CM, Fink B, Francis J. TNF-induced mitochondrial damage: a link between mitochondrial complex I activity and left ventricular dysfunction. Free Radic. Biol. Med. 2009, 46(4): 462-470.

Margulis L. Symbiosis in cell evolution. Freeman, San Francisco, 1981. (Accessed via openlibrary.org).

Martin LJ. Mitochondrial and Cell Death Mechanisms in Neurodegenerative Diseases. Pharmaceuticals (Basel). 2010, 3(4): 839-915.

Maxwell DP, Wang Y, McIntosh L. The alternative oxidase lowers mitochondrial reactive oxygen production in pant cells. Proc. Natl. Acad. Sci. USA 1999, 96(14): 8271-8276.

McDonald AE, Vanlerberghe GC, Staples JF. Alternative oxidase in animals: unique characteristics and taxonomic distribution. J. Exp. Biol. 2009, 212(Pt 16): 2627-2634.

McDonald AE, Gospodaryov DV. Alternative NAD(P)H dehydrogenase and alternative oxidase: Proposed physiological roles in animals. Mitochondrion 2019, 45: 7-17.

McDonald A, Vanlerberghe G. Branched mitochondrial electron transport in the Animalia: presence of alternative oxidase in several animal phyla. IUBMB Life. 2004, 56(6): 333-341.

Mentzer RM Jr, Wider J, Perry CN, Gottlieb RA. Reduction of infarct size by the therapeutic protein TAT-Ndi1 in vivo. J. Cardiovasc. Pharmacol. Ther. 2014, 19(3): 315-320.

Meyers DE, Basha HI, Koenig MK. Mitochondrial cardiomyopathy. Pathophysiology, diagnosis and management. Tex. Heart Inst. J. 2013, 40(4): 385-394.

Millar A.H., Wiskich J.T., Whelan J., Day D.A. Organic acid activation of the alternative oxidase of plant mitochondria. FEBS Lett. 1993, 329: 259–262.

Mills EL, Kelly B, Logan A, Costa ASH, Varma M, Bryant CE, Tourlomousis P, Däbritz JHM, Gottlieb E, Latorre I, Corr SC, McManus G, Ryan D, Jacobs HT, Szibor M, Xavier RJ, Braun T, Frezza C, Murphy MP, O'Neill LA. Succinate Dehydrogenase Supports Metabolic Repurposing of Mitochondria to Drive Inflammatory Macrophages. Cell 2016, 167(2): 457-470.

Mitchell P. Coupling of phosphorylation to electron and hydrogen transfer by a chemi-osmotic type of mechanism. Nature 1961, 191: 144-148.

Moller IM, Berczi A, van der Plas LHW, Lambers H. Measurement of the activity and capacity of the alternative pathway in intact plant tissues: identification of problems and possible solutions. Physiol. Plant 1988, 72: 642–649.

Moore AL, Umbach AL, Siedow JN. Structure-function relationships of the alternative oxidase of plant mitochondria: a model of the active site. J. Bioenerg. Biomembr. 1995, 27(4): 367-377.

Moore-Morris T, Guimarães-Camboa N, Yutzey KE, Pucéat M, Evans SM. Cardiac fibroblasts: from development to heart failure. J. Mol. Med. (Berl). 2015, 93(8): 823-830.

Morimoto H, Takahashi M, Izawa A, Ise H, Hongo M, Kolattukudy PE, Ikeda U. Cardiac overexpression of monocyte chemoattractant protein-1 in transgenic mice prevents cardiac dysfunction and remodeling after myocardial infarction. Circ. Res. 2006, 99(8): 891-899.

Morimoto H, Hirose M, Takahashi M, Kawaguchi M, Ise H, Kolattukudy PE, Yamada M, Ikeda U. MCP-1 induces cardioprotection against ischaemia/reperfusion injury: role of reactive oxygen species. Cardiovascular Research 2008, 78(3): 554-562.

Murakami T, Reiter LT, Lupski JR. Genomic structure of the human heme A:farnesyltransferase (*COX10*) gene. Genomics 1997, 42: 161-164.

Murphy MP. How mitochondria produce reactive oxygen species. Biochem. J. 2009, 417(1): 1 - 13.

Nakayama H, Chen X, Baines CP, Klevitsky R, Zhang X, Zhang H, Jaleel N, Chua BH, Hewett TE, Robbins J, Houser SR, Molkentin JD. Ca2+- and mitochondrial-dependent cardiomyocyte necrosis as a primary mediator of heart failure. J. Clin. Invest. 2007, 117(9): 2431-2444.

Narula J, Pandey P, Arbustini E, Haider N, Narula N, Kolodgie FD, Dal Bello B, Semigran MJ, Bielsa-Masdeu A, Dec GW, Israels S, Ballester M, Virmani R, Saxena S, Kharbanda S. Apoptosis in heart failure: release of cytochrome c from mitochondria and activation of caspase-3 in human cardiomyopathy. Proc. Natl. Acad. Sci. U S A., 1999, 96(14): 8144 - 8149.

Neary MT, Ng KE, Ludtmann MHR, Hall AR, Piotrowska I, Ong SB, Hausenloy DJ, Mohun TJ, Abramov AY, Breckenridge RA. Hypoxia signaling controls postnatal changes in cardiac mitochondrial morphology and function. J. Mol. Cell Cardiol. 2014, 74: 340-352.

Neely C, Lane C, Torres J, Flinn J. The Effect of Gentle Handling on Depressive-Like Behavior in Adult Male Mice: Considerations for Human and Rodent Interactions in the Laboratory. Behav. Neurol. 2018, 2018: 2976014.

Nelson, D.L. and Cox, M.M. Lehninger Principles of Biochemistry. 2017, 7th Edition, W.H. Freeman, New York.

Neubauer S. The failing heart--an engine out of fuel. N. Engl. J. Med. 2007, 356(11): 1140-1151.

Neubauer S, Horn M, Cramer M, Harre K, Newell JB, Peters W, Pabst T, Ertl G, Hahn D, Ingwall JS, Kochsiek K. Myocardial phosphocreatine-to-ATP ratio is a predictor of mortality in patients with dilated cardiomyopathy. Circulation 1997, 96(7): 2190-2196.

Neupert W and Herrmann J. Translocation of proteins into mitochondria. Annu. Rev. Biochem. 2007, 76: 723-749.

Neupert W. Protein import into mitochondria. Annu. Rev. Biochem. 1997, 66: 863 – 917.

Neustadt J, Pieczenik SR. Medication-induced mitochondrial damage and disease. Mol. Nutr. Food Res. 2008, 52(7): 780 - 788.

Nicholls DG, Ferguson SJ. Bioenergetics 2. Academic Press; 2014.

Nicholson GA, Magdelaine C, Zhu D, Grew S, Ryan MM, Sturtz F, Vallat JM, Ouvrier RA. Severe early-onset axonal neuropathy with homozygous and compound heterozygous MFN2 mutations. Neurology. 2008, 70(19): 1678-1681.

Nilsson J, Ericsson M, Joibari MM, Anderson F, Carlsson L, Nilsson SK, Sjödin A, Burén J. A low-carbohydrate high-fat diet decreases lean mass and impairs cardiac function in pair-fed female C57BL/6J mice. Nutr. Metab. (Lond). 2016, 13: 79.

Nisoli E, Carruba MO. Nitric oxide and mitochondrial biogenesis. J. Cell Sci. 2006, 119(Pt 14): 2855-2862.

Niu J, Azfer A, Rogers LM, Wang X, Kolattukudy PE. Cardioprotective effects of cerium oxide nanoparticles in a transgenic murine model of cardiomyopathy. Cardiovasc Res. 2007, 73(3): 549-59.

Niu J, Kolattukudy PE. Role of MCP-1 in cardiovascular disease: molecular mechanisms and clinical implications. Clinical Science 2009, 117: 95-109.

Niyazov DM, Kahler SG, Fyre RE. Primary mitochondrial disease and secondary mitochondrial dysfunction: importance of distinction for diagnosis and treatment. Mol. Syndromol. 2016, 7: 122-137.

Nobrega MP, Nobrega FG, Tzagoloff A. *COX10* codes for a protein homologous to the ORF1 product of *Paracoccus denitrificans* and is required for the synthesis of yeast cytochrome oxidase. J. Biol. Chem. 1990, 265(24): 14220-14226.

Nosek J, Tomáska L, Fukuhara H, Suyama Y, Kovác L. Linear mitochondrial genomes: 30 years down the line. Trends Genet. 1998, 14(5): 184-188.

Olivetti G, Cigola E, Maestri R, Corradi D, Lagrasta C, Gambert SR, Anversa P. Aging, cardiac hypertrophy and ischemic cardiomyopathy do not affect the proportion of mononucleated and multinucleated myocytes in the human heart. J. Mol. Cell. Cardiol. 1996, 28(7): 1463-1477.

O'Neill, L.A., and Pearce, E.J. Immunometabolism governs dendritic cell and macrophage function. J. Exp. Med. 2016, 213: 15–23.

Ong SB, Hall AR, Hausenloy DJ. Mitochondrial dynamics in cardiovascular health and disease. Antioxid. Redox Signal. 2013, 19(4): 400-414.

Otto DA, Onko JA. Activation of mitochondrial fatty acid oxidation by calcium. J. Biol. Chem. 1977, 253(3): 789-799.

Ow YP, Green DR, Hao Z, Mak TW. Cytochrome c: functions beyond respiration. Nat. Rev. Mol. Cell. Biol. 2008, 9(7): 532 - 542.

Owusu-Ansah E, Banerjee U. Reactive oxygen species prime Drosophila haematopoietic progenitors for differentiation. Nature 2009, 461(7263): 537-541.

Palade GE. The Fine Structure of mitochondria. Anat. Rec. 1952, 114: 427.

Palmer JW, Tandler B, Hoppel CL. Biochemical properties of subsarcolemmal and interfibrillar mitochondria isolated from rat cardiac muscle. J. Biol. Chem. 1977, 252(23): 8731-8739.

Papandreou I, Cairns RA, Fontana L, Lim AL, Denko NC. HIF-1 mediates adaptation to hypoxia by actively downregulating mitochondrial oxygen consumption. Cell Metab. 2006, 3(3): 187-197.

Parikh S, Karaa A, Goldstein A, Bertini ES, Chinnery PF, Christodoulou J, Cohen BH, Davis RL, Falk MJ, Fratter C, Horvath R, Koenig MK, Mancuso M, McCormack S, McCormick EM, McFarland R, Nesbitt V, Schiff M, Steele H, Stockler S, Sue C, Tarnopolsky M, Thorburn DR, Vockley J, Rahman S. Diagnosis of 'possible' mitochondrial disease: an existential crisis. J. Med. Gen. 2019, 56: 123-130.

Parikh S, Goldstein A, Koenig MK, Scaglia F, Enna GM, Saneto R, Anselm I, Collins A, Cohen BH, Debrosse SD, Dimmock D, Falk MJ, Ganesh J, Greene C, Gropman AL, Haas R, Kahler SG, Kamholz J, Kendall F, Korson MS, Mattman A, Milone M, Niyazov D, Pearl PL, Reimschisel T, Salvarinova-Zivkovic R, Sims K, Tarnopolsky M, Tsao CY, Hove JV, Walsh L, Wolfe LA. Practice patterns of mitochondrial disease physicians in North America. Part 1: Diagnostic and clinical challenges. Mitochondrion 2014, 14: 26-33.

Kuznetsov AV, Hermann M, Saks V, Hengster P, Margreiter R. The cell-type specificity of mitochondrial dynamics. Int. J. Biochem. Cell. Biol., 2009, 41(10): 1928-1939.

Parikh S, Saneto R, Falk MJ, Anselm I, Cohen BH, Haas R. A modern approach to the treatment of mitochondrial diseases. Curr. Treat. Options Neurol. 2009, 11(6): 414-430.

Paupe V, Prudent J. New insights into the role of mitochondrial calcium homeostasis in cell migration. Biochem. Biophys. Res. Commun. 2018, 500(1): 75-86.

Pelicano H, Xu RH, Du M, Feng L, Sasaki R, Carew JS, Hu Y, Ramdas L, Hu L, Keating MJ, Zhang W, Plunkett W, Huang P. Mitochondrial respiration defects in cancer cells cause activation of Akt survival pathway through a redox-mediated mechanism. J. Cell Biol. 2006, 175(6): 913-923.

Pena-Oliver Y, Sanchez-Roige S, Stephens DN, Ripley TL. Alpha-synuclein deletion decreases motor impulsivity but does not affect risky decision making in a mouse Gambling Task. Psychopharmacology (Berl). 2014, 231(12): 2493 - 2506.

Perry CN, Huang C, Liu W, Magee N, Carreira RS, Gottlieb RA. Xenotransplantation of mitochondrial electron transfer enzyme, Ndi1, in myocardial reperfusion injury. PLoS One. 2011, 6(2): e16288.

Piper HM, Sezer O, Schleyer M, Schwartz P, Hütter JF, Spieckermann PG. Development of ischemia-induced damage in defined mitochondrial subpopulations. J. Mol. Cell Cardiol. 1985, 17(9): 885-896.

Piquereau J, Caffin F, Novotova M, Lemaire C, Veksler V, Garnier A, Ventura-Clapier R, Joubert F. Mitochondrial dynamics in the adult cardiomyocytes: which roles for a highly specialized cell? Front. Physiol. 2013, 4:102.

Pohjoismäki JL, Boettger T, Liu Z, Goffart S, Szibor M, Braun T. Oxidative stress during mitochondrial biogenesis compromises mtDNA integrity in growing hearts and induces a global DNA repair response. Nucleic Acids Res. 2012, 40(14): 6595-6607.

Pohjoismäki JL, Goffart S. The role of mitochondria in cardiac development and protection. Free Radic. Biol. Med. 2017, 106: 345-354.

Pohjoismäki JL, Krüger M, Al-Furoukh N, Lagerstedt A, Karhunen PJ, Braun T. Postnatal cardiomyocyte growth and mitochondrial reorganization cause multiple changes in the proteome of human cardiomyocytes. Mol. Biosyst. 2013, 9(6): 1210-1219.

Porrello ER, Mahmoud AI, Simpson E, Hill JA, Richardson JA, Olson EN, Sadek HA. Transient regenerative potential of the neonatal mouse heart. Science. 2011, 331(6020): 1078-1080.

Pugach EK, Richmond PA, Azofeifa JG, Dowell RD, Leinwand LA. Prolonged Cre expression driven by the α-myosin heavy chain promoter can be cardiotoxic. J. Mol. Cell Cardiol. 2015, 86: 54-61.

Putti R, Sica R, Migliaccio V, Lionetti L. Diet impact on mitochondrial bioenergetics and dynamics. Front. Physiol. 2015, 6:109.

Radermacher M, Ruiz T, Clason T, Benjamin S, Brandt U, Zickermann V. The three-dimensional structure of complex I from Yarrowia lipolytica: a highly dynamic enzyme. J. Struct. Biol. 2006, 154(3): 269 - 279.

Rajendran J, Purhonen J, Tegelberg S, Smolander OP, Mörgelin M, Rozman J, Gailus-Durner V, Fuchs H, Hrabe de Angelis M, Auvinen P, Mervaala E, Jacobs HT, Szibor M, Fellman V, Kallijärvi J. Alternative oxidase-mediated respiration prevents lethal mitochondrial cardiomyopathy. EMBO Mol. Med. 2019, 11(1).

Reheman A, Tasneem S, Ni H, Hayward CP. Mice with deleted multimerin 1 and alpha-synuclein genes have impaired platelet adhesion and impaired thrombus formation that is corrected by multimerin 1. Thromb. Res. 2010, 125(5): e177-183.

Riley LG, Cooper S, Hickey P, Rudinger-Thirion J, McKenzie M, Compton A, Lim SC, Thorburn D, Ryan MT, Giegé R, Bahlo M, Christodoulou J. Mutation of the mitochondrial tyrosyl-tRNA synthetase gene, YARS2, causes myopathy, lactic acidosis, and sideroblastic anemia--MLASA syndrome. Am. J. Hum. Genet. 2010, 87(1) :52-59.

Ritterhoff J, Tian R. Metabolism in cardiomyopathy: every substrate matters. Cardiovasc. Res. 2017, 113(4): 411-421.

Robin ED, Wong R. Mitochondrial DNA molecules and virtual number of mitochondrial cells in mammalian cells. J. Cell. Physiol. 1998, 136: 507-513.

Rosca MG, Hoppel CL. Mitochondrial dysfunction in heart failure. Heart Fail. Rev. 2013, doi: 10.1007/s10741-012-9340-0.

Rosca MG, Tandler B, Hoppel CL. Mitochondrial in cardiac hypertrophy and heart failure. J. Mol. Cell Cardiol. 2013, 55: 31-41.

Rudolph G, Dimitriadis K, Buchner B, Heck S, Al-Tamami J, Seidensticker F, Rummey C, Leinonen M, Meier T, Klopstock T. Effects of idebenone on color vision in patients with Leber Hereditary Optic Neuropathy. J. Neuro-Opthalmol. 2013, 33: 30-36.

Russell WMS, Burch RL. The principles of humane experimental technique. Wheathampstead (UK): Universities Federation for Animal Welfare. 1959. (as reprinted 1992). Link to the digital version: http://altweb.jhsph.edu/pubs/books/humane_exp/het-toc.

Ruzzenente B, Rotig A, Metodiev MD. Mouse models for mitochondrial diseases. Hum. Mol. Gen. 2016, 25(2): 115-122.

Saari S, Garcia GS, Bremer K, Chioda MM, Andjelković A, Debes PV, Nikinmaa M, Szibor M, Dufour E, Rustin P, Oliveira MT, Jacobs HT. Alternative respiratory chain enzymes: Therapeutic potential and possible pitfalls. Biochim. Biophys. Acta. Mol. Basis. Dis. 2019, 1865(4): 854-866.

Santra S, Gilkerson RW, Davidson M, Schon EA. Ketogenic treatment reduces deleted mitochondrial DNAs in cultured human cells. Ann. Neurol. 2004, 56(5): 662-669.

Santos CX, Anilkumar N, Zhang M, Brewer AC, Shah AM. Redox signaling in cardiac myocytes. Free Radic. Biol. Med. 2011, 50(7): 777-793.

Siedow JN, Umbach AL, Moore AL. The active site of the cyanide-resistant oxidase from plant mitochondria contains a binuclear iron center. FEBS Lett. 1995, 362(1): 10-14.

Scaglia F, Towbin JA, Craigen WJ, Belmont JW, Smith EO, Neish SR, Ware SM, Hunter JV, Fernbach SD, Vladutiu GD, Wong LJ, Vogel H. Clinical spectrum, morbidity, and mortality in 113 pediatric patients with mitochondrial disease. Pediatrics. 2004, 114(4): 925-931.

Schieber M, Chandel NS. ROS function in redox signaling and oxidative stress. Curr. Biol. 2014, 24(10): R453-462.

Schluz H. Beta oxidation of fatty acids. Biochem. Biophys. Acta 1991, 1081: 109-120.

Segers VFM, Brutsaert DL, De Keulenaer GW. Cardiac Remodeling: Endothelial Cells Have More to Say Than Just NO. Front. Physiol. 2018, 9: 382.

Shimizu S, Narita M, Tsujimoto Y. Bcl-2 family proteins regulate the release of apoptogenic cytochrome c by the mitochondrial channel VDAC. Nature. 1999, 399(6735): 483-487.

Smith DR, Hua J, Lee RW. Evolution of linear mitochondrial DNA in three known lineages of Polytomella. Curr. Genet. 2010, 56(5): 427-438.

Soonpaa MH, Kim KK, Pajak L, Franklin M, Field LJ. Cardiomyocyte DNA synthesis and binucleation during murine development. Am. J. Physiol. 1996, 271: H2183-H2189.

Sparks LM, Xie H, Koza RA, Mynatt R, Hulver MW, Bray GA, Smith SR. A high-fat diet coordinately downregulates genes required for mitochondrial oxidative phosphorylation in skeletal muscle. Diabetes 2005, 54(7): 1926-1933.

Specht CG, Schoepfer R. Deletion of multimerin-1 in alpha-synuclein-deficient mice. Genomics 2004, 83(6): 1176 - 1178.

Stanley WC, Recchia FA, Lopaschuk GD. Myocardial substrate metabolism in normal and failing heart. Physiol. Rev. 2005, 85(3): 1093-1129.

Stewart AG, Laming EM, Sobti M, Stock D. Rotary ATPases – Dynamic molecular mechanisms. Current Opinion in Structural Biology 2014, 25: 40–48.

Stow JL, Low PC, Offenhäuser C, Sangermani D. Cytokine secretion in macrophages and other cells: pathways and mediators. Immunobiology. 2009, 214(7): 601-612.

Suliman HB, Piantadosi CA. Mitochondrial biogenesis: regulation by endogenous gases during inflammation and organ stress. Curr. Pharm. Des. 2014, 20(35): 5653-5662.

Sundberg JP, Schofield PN. Living inside the box: environmental effects on mouse models of human disease. Dis. Model. Mech. 2018, 11(10). pii: dmm035360.

Sung FL, Zhu TY, Au-Yeung KKW, Siow YL, Karmin SO. Enhanced MCP-1 expression during ischemia/reperfusion injury is mediated by oxidative stress and NF-κB. Kidney International 2002, 62(4): 1160-1170.

Suomalainen A. Therapy for mitochondrial disorders: Little proof, high research activity and some promise. Seminars in Fetal & Neonatal Medicine 2011, 16: 236-240

Poulton J, Chiaratti MR, Meirelles FV, Kennedy S, Wells D, Holt IJ. Transmission of mitochondrial dna diseases and ways to prevent them. Plos Genetics 2010, 6: pii: e1001066.

Taegtmeyer H, Sen S, Vela D. Return to the fetal gene program. Ann. N. Y. Acad. Sci. 2010, 1188: 191-198.

Tarnopolsky MA, Roy BD, MacDonald JR. A randomized, controlled trial of creatine monohydrate in patients with mitochondrial cytopathies. Muscle Nerve 1997, 20(12): 1502-1509.

Thorn MB. Malonate inhibition of succinic dehydrogenase. Biochem. J. 1953, 53(1): i.2–ix.1.

Tieu BC, Lee C, Sun H, Lejeune W, Recinos A 3rd, Ju X, Spratt H, Guo DC, Milewicz D, Tilton RG, Brasier AR. An adventitial IL-6/MCP1 amplification loop accelerates macrophage-

mediated vascular inflammation leading to aortic dissection in mice. J. Clin. Invest. 2009, 119(12): 3637-3651.

Tormos KV, Anso E, Hamanaka RB, Eisenbart J, Joseph J, Kalyanaraman B, Chandel NS. Mitochondrial complex III ROS regulate adipocyte differentiation. Cell Metab. 2011, 14(4): 537-544.

Trachootham D, Lu W, Ogasawara MA, Nilsa RD, Huang P. Redox regulation of cell survival. Antioxid. Redox Signal. 2008, 10(8): 1343-1374.

Treberg JR, Quinlan CL, Brand MD. Evidence for two sites of superoxide production by mitochondrial NADH-ubiquinone oxidoreductase (complex I). J. Biol. Chem. 2011, 286(31): 27103 - 27110.

Turnbaugh PJ, Ley RE, Mahowald MA, Magrini V, Mardis ER, Gordon JI. An obesity-associated gut microbiome with increased capacity for energy harvest. Nature 2006, 444(7122): 1027-1031.

Vásquez-Trincado C, García-Carvajal I, Pennanen C, Parra V, Hill JA, Rothermel BA, Lavandero S. Mitochondrial dynamics, mitophagy and cardiovascular disease. J. Physiol. 2015, 594(3): 509-525.

Vanlerberghe GC. Alternative oxidase: a mitochondrial respiratory pathway to maintain metabolic and signaling homeostasis during abiotic and biotic stress in plants. Int. J. Mol. Sci. 2013, 14(4): 6805-6847.

Vandecasteele G, Szabadkai G, Rizzuto R. Mitochondrial calcium homeostasis: mechanisms and molecules. IUBMB Life. 2001, 52(3-5): 213-219.

Valente M, Calabrese F, Thiene G, Angelini A, Basso C, Nava A, Rossi L. In vivo evidence of apoptosis in arrhythmogenic right ventricular cardiomyopathy. Am. J. Pathol. 1998, 152(2): 479-484.

Wagner AM, Krab K, Wagner MJ, Moore AL. Regulation of thermogenesis in flowering Araceae: the role of the alternative oxidase. Biochim. Biophys. Acta. 2008, 1777(7-8): 993-1000.

Wallace DC. Mouse models for mitochondrial disease. Am. J. Med. Genet. 2001, 106(1): 71-93.

Wallace DC. Animal models for mitochondrial disease. Methods Mol. Biol. 2002, 197: 3-54.

Wan B, LaNoue KF, Cheung JY, Scaduto RC. Regulation of citric acid cycle by calcium. J. Biol. Chem. 1989, 264(23): 13430-13439.

Wang Z, Wang Y, Hegg EL. Regulation of the heme A biosynthetic pathway: differential regulation of heme A synthase and heme O synthase in Saccharomyces cerevisiae. J. Biol. Chem. 2009, 284: 839-847.

Watt IN, Montgomery MG, Runswick MJ, Leslie AGW, Walker JE. Bioenergetic cost of making an adenosine triphosphate molecule in animal mitochondria. Proc. Natl. Acad. Sci. USA 2010, 107(39): 16823-16827.

WHO report on the prevalence of cardiovascular diseases, web link source: https://www.who.int/news-room/fact-sheets/detail/cardiovascular-diseases-(cvds).

Weatermann B. Mitochondria fusion and fission in cell life and death. Nat. Rev. Mol. Cell Biol. 2010, 11: 872 – 884.

Weaver RJ. Hypothesized evolutionary consequences of the alternative oxidase (AOX) in animal mitochondria. Integr. Comp. Biol. 2019, pii: icz015.

Wenz T. Regulation of mitochondrial biogenesis and PGC-1a under cellular stress. Mitochondrion 2013, 13: 134-142.

West AP, Brodsky IE, Rahner C, Woo DK, Erdjument-Bromage H, Tempst P, Walsh MC, Choi Y, Shadel GS, Ghosh S. TLR signalling augments macrophage bactericidal activity through mitochondrial ROS. Nature. 2011, 472(7344): 476-480.

Wichmann A, Allahyar A, Greiner TU, Plovier H, Lundén GÖ, Larsson T, Drucker DJ, Delzenne NM, Cani PD, Bäckhed F. Microbial modulation of energy availability in the colon regulates intestinal transit. Cell Host Microbe. 2013, 14(5): 582-590.

Wittig JG, Münsterberg A. The Early Stages of Heart Development: Insights from Chicken Embryos. J. Cardiovasc. Dev. Dis. 2016, 3(2). pii: E12.

Xu D, Jiang Z, Sun Z, Wang L, Zhao G, Hassan HM, Fan S, Zhou W, Han S, Zhang L, Wang T. Mitochondrial dysfunction and inhibition of myoblast differentiation in mice with high-fat-diet-induced pre-diabetes. J. Cell Physiol. 2019, 234(5): 7510-7523.

Ylikallio E, Suomalainen A. Mechanisms of mitochondrial diseases. Annals of Medicine 2012, 44: 41-59.

Yoshida K, Shibata M, Terashima I, Noguchi K. Simultaneous determination of in vivo plastoquinone and ubiquinone redox states by HPLC-based analysis. Plant Cell Physiol. 2010, 51(5): 836-841.

Younce CW, Kolattukudi PE. MCP-1 causes cardiomyoblast death via autophagy resulting from ER stress caused by oxidative stress generated by inducing a novel zinc-finger protein, MCPIP. J. Biochem. 2010, 426: 43-53.

Zeviani M, Moraes CT, DiMauro S, Nakase H, Bonilla E, Schon EA, Rowland LP. Deletions of mitochondrial DNA in Kearns-Sayre syndrome. Neurology. 1998, 51(6): 1525-1533.

Zhang DX, Gutterman DD. Mitochondrial reactive oxygen species-mediated signaling in endothelial cells. J. Physiol. Am. J. Physiol. Heart Circ. Physiol. 2007, 292(5): H2023-2031.

Zhao RZ, Jiang S, Zhang L, Yu ZB. Mitochondrial electron transport chain, ROS generation and uncoupling (Review). Int. J. Mol. Med. 2019, 44(1): 3 - 15.

Zeng MY, Miralda I, Armstrong CL, Uriarte SM, Bagaitkar J. The roles of NADPH oxidase in modulating neutrophil effector responses. Mol. Oral Microbiol. 2019, 34(2): 27-38.

Zhou L, Azfer A, Niu J, Graham S, Choudhury M, Adamski FM, Younce C, Binkley PF, Kolattukudy PE. Monocyte chemoattractant protein-1 induces a novel transcription factor that causes cardiac myocyte apoptosis and ventricular dysfunction. Circ. Res. 2006, 98(9): 1177-1185.

Zhou P, Pu WT. Recounting cardiac cellular composition. Circ. Res. 2016, 118(3): 368-370.

Zhou B, Tian R. Mitochondrial dysfunction in pathophysiology of heart failure. J. Clin. Invest. 2018, 128(9): 3716–3726.

ISBN 978-951-51-5998-4 (PRINT)
ISBN 978-951-51-5999-1 (ONLINE)
ISSN 2342-3161 (PRINT)
ISSN 2342-317X (ONLINE)
http://ethesis.helsinki.fi

HELSINKI 2020